

5-2007

Optimal Placement of Metal Foils in Ultrasonic Consolidation Process

Raji Rexavier

Clemson University, rrexavi@clemson.edu

Follow this and additional works at: https://tigerprints.clemson.edu/all_theses



Part of the [Engineering Mechanics Commons](#)

Recommended Citation

Rexavier, Raji, "Optimal Placement of Metal Foils in Ultrasonic Consolidation Process" (2007). *All Theses*. 136.
https://tigerprints.clemson.edu/all_theses/136

This Thesis is brought to you for free and open access by the Theses at TigerPrints. It has been accepted for inclusion in All Theses by an authorized administrator of TigerPrints. For more information, please contact kokeefe@clemson.edu.

OPTIMAL PLACEMENT OF METAL FOILS IN ULTRASONIC
CONSOLIDATION PROCESS

A Thesis
Presented to
the Graduate School of
Clemson University

In Partial Fulfillment
of the Requirements for the Degree
Master of Science
Mechanical Engineering

by
Raji Rexavier
May 2007

Accepted by
Georges M Fadel, Committee Chair
Joshua D Summers
Gregory Mocko

ABSTRACT

Ultrasonic Consolidation is a combination of additive and subtractive manufacturing processes resulting in considerable material waste. This waste is a function of the geometry of the part being manufactured and of the relative placement of the layer with respect to the metal bands. Thus the waste may be minimized by careful choice of the layer angle and offset from the original position.

Previous work done in this field had developed an automated algorithm which optimally places and orients the individual slices of the STL file of the artifact being manufactured. However, the problem was solved on a 2-D scale and the 3-D nature of the part was not considered for the development of the algorithm. The earlier algorithm employed approximation on the input data to minimize the computational expense. This resulted in convergence of the optimizer to sub-optimal solutions. Further, as the final part is made of anisotropic material the relative angles and overlap between subsequent layers also plays an important role in the final part strength. Finally, it is noted that the build time required for the ultrasonic consolidation process is a function of the number of bands required to form each slice.

Considering these limitations and opportunities, this thesis presents an algorithm which optimally orients and places the part layers with respect to aluminum bands in order to minimize the waste formed and the build time required. The algorithm has the capability of increasing the part strength by forming crisscross and brick structures using the metal foils. This research work also improves on the previous algorithm by extending the functionality of the algorithm by building in capability to handle multiple loops within the same slice and non convex slice data. Further, the research studies the choice of optimizer that needs to be employed for different types of input data.

DEDICATION

I dedicate this work to my family and friends without whose support this work would have been impossible.

ACKNOWLEDGMENTS

I would like to express my profound thanks to my advisor Dr. Georges M Fadel for the guidance and support extended to me throughout the research work. The discussions I had with Dr. Fadel had been intellectually motivating and has helped me develop a critical approach to problems. I am grateful for his advice on the different aspects of research, from the initial phases of the project to the final documentation work

I would also like to thank the other members of my committee, Dr. Joshua Summers and Dr. Gregory Mocko for motivating me to push my limits to achieve better results in this research work. I gratefully acknowledge the suggestions and ideas offered which has helped in the successful completion of this research work

I sincerely thank Mr. Manuel M Schwager and Mr. Julien Galli for establishing the groundwork for this research. I also appreciate the time taken by them to answer my queries related to the work.

Last but not the least; I would like to express my sincere gratitude to all CREDO/AID members and my friends for having the faith in me and the supporting me and encouraging me during the hard times of the project.

TABLE OF CONTENTS

	Page
TITLE PAGE	i
ABSTRACT	iii
DEDICATION	v
ACKNOWLEDGMENTS	vii
LIST OF FIGURES	xiii
LIST OF EQUATIONS	xvii
CHAPTER	
1 INTRODUCTION	1
1.1 Rapid Manufacturing	4
1.1.1 Fused Deposition Modeling (FDM)	5
1.1.2 Selective Laser Sintering (SLS)	6
1.1.3 Laser Engineering Net Shaping (LENS)	7
1.1.4 Electron Beam Melting (EBM)	8
1.1.5 Ultrasonic Consolidation (UC)	9
1.1.5.1 Dependency of Waste Area on θ and δ	14
1.1.5.2 Strength	16
1.1.5.3 Build Time	17
1.2 Advantages of Rapid Manufacturing Methods	19
1.3 Closure	23
2 LITERATURE REVIEW	25
2.1 Research in Rapid Manufacturing/Prototyping	25
2.1.1 Accuracy	26
2.1.2 Repeatability	28
2.1.3 Surface finish	28
2.1.4 Part strength	30
2.1.5 Performance	31
2.2 Review of Research in Ultrasonic Consolidation	33
2.2.1 New application development	34
2.2.2 New material development	35
2.2.3 Process Refinements	36

Table of Contents (Continued)	Page
2.2.3.1 <i>Build Time</i>	36
2.2.3.2 <i>Strength</i>	36
2.2.3.3 <i>Waste</i>	37
2.3 Problem Description And Objective	37
2.4 Existing Algorithm	38
2.4.1 <i>Multi Loop Slices</i>	41
2.4.2 <i>Concave Data</i>	43
2.5 Closure	44
3 RESEARCH ISSUES AND FORMULATION	47
3.1 Research Issues	47
3.2 Mathematical Formulation	49
3.3 Closure	51
4 RESEARCH PROCEDURE AND STEPS	53
4.1 Band area calculation	54
4.2 Ability to handle multiple loops in the same slice	57
4.3 Ability to handle non convex objects	60
4.4 Constraint handling	61
4.4.1 <i>Angular Constraint</i>	62
4.4.2 <i>Translational Constraint</i>	63
4.5 Reduced computational complexity	64
4.5.1 <i>Intersection calculation</i>	65
4.5.2 <i>Elimination of internal loops</i>	67
4.6 Ability to Reduce Build Time Required	69
4.7 Modified File Structure for Efficient Processing	71
4.8 Global Coordinate System	74
4.9 Search Bounds	76
4.9.1 <i>Slice data with no axis of symmetry</i>	76
4.9.2 <i>Slice data with Multiple axes of symmetry</i>	77
4.10 Closure	79
5 IMPLEMENTATION	81
5.1 Program Architecture	81
5.2 Preprocessor	83
5.3 Objective Function	84
5.4 Constraint Evaluator	86
5.5 Search Space Sampler	87
5.6 Closure	92
6 RESULTS	95
6.1 Test Case Metrics and Test Shapes	95

Table of Contents (Continued)	Page
6.2 Validation of algorithm.....	96
6.3 Choice of Optimizer.....	99
6.4 Benchmarking.....	104
6.5 Closure	105
7 CONCLUSIONS AND FUTURE WORK	107
7.1 Conclusion	107
7.2 Future Work.....	108
REFERENCES	111

LIST OF FIGURES

Figure	Page
1.1 Fused Deposition Modeling ^[13]	5
1.2 Selective Laser Sintering ^[14]	6
1.3 Laser Engineered Net Shaping ^[17]	8
1.4 Electron Beam Melting ^[21]	9
1.5 Different steps of the Ultrasonic Consolidation process.....	10
1.6 Sonotrode	11
1.7 Clamping waste.....	11
1.8 Ultrasonic Consolidation Process	12
1.9 Ultrasonic Consolidation bond formation ^[23]	13
1.10 Part slice, aluminum bands and waste area.....	14
1.11 Coordinate System of the Ultrasonic Consolidation Process	15
1.12 Comparison of waste area.....	16
1.13 Reduction of part strength with increasing aspect ratio ^[25]	16
1.14 Compromise between build time/part strength and waste ^[25]	18
1.15 Bionic structure ^[27]	20
1.16 Feasible domains in Conventional and Rapid manufacturing	21
1.17 Concurrent Engineering and time saving ^[4]	22
2.1 Overhang in layered manufacturing.....	27
2.2 z-axis error ^[40]	27

List of Figures (Continued)

	Page
2.3 Stair Step Effect	29
2.4 Rapid Manufacturing research issues	33
2.5 Optimization of UC process for waste reduction ^[78]	40
2.6 Addition of waste due to use of approximation ^[78]	42
2.7 Comparison of waste area without and with approximation	43
2.8 Conversion of concave data into convex data.....	44
4.1 Problem solution approach and flowchart	54
4.2 Calculation of band area required	56
4.3 Calculation of waste area	57
4.4 Brain Gear	58
4.5 Brain gear slices	59
4.6 Ability to handle multiple loops	60
4.7 Ability to handle non convex objects.....	60
4.8 Optimization for part strength.....	61
4.9 Angle constraint.....	62
4.10 Aluminum bands in crisscross structure ^[22]	63
4.11 Translation constraint.....	64
4.12 Aluminum foils in brick structure ^[22]	64
4.13 Modified intersection point calculation	67
4.14 Modified algorithm for eliminating internal loops	68
4.15 Elimination of internal loops	69

List of Figures (Continued)

	Page
4.16 NoB Reduction.....	71
4.17 Existing File Structure	72
4.18 Proposed File Structure.....	74
4.19 Global Coordinate System	75
4.20 Validation of search bounds.....	77
4.21 Waste area for slice data with multiple axes of symmetry	78
4.22 Waste area for slice data with one axis of symmetry.....	78
5.1 Program Architecture.....	82
5.2 Preprocessor flowchart.....	84
5.3 Objective function flowchart	86
5.4 Constraint evaluator flowchart.....	87
5.5 Sample slice data.....	88
5.6 Waste area as a function of θ and δ	88
5.7 Starting point selection by sampling.....	89
5.8 Need for robust sampling.....	90
5.9 Comparison of Sampling Methods	91
5.10 Sampling flowchart.....	92
6.1 Test shapes for validation	96
6.2 Optimization results of test cases.....	97
6.3 Formation of crisscross and overlap structure	98
6.4 STL file of club	100

List of Figures (Continued)

	Page
6.5 Waste area history using Simplex algorithm	102
6.6 Waste area history using NSGA II algorithm	102
6.7 Waste area history using NSGA II algorithm-1000 generations	103
6.8 Comparison of existing and new algorithm	104
7.1 Choice of z-axis	109

LIST OF EQUATIONS

Equation	Page
3.1 Problem Formulation	50
4.1 Angular Constraints	62
4.2 Translation Constraint.....	63
4.3 Calculation of intersection point.....	66
4.4 Modified Problem formulation	80
6.1 Mathematical formulation of all in one optimization	101

CHAPTER 1

INTRODUCTION

Engineering design is a multi step process which converts the user-defined needs or requirements into a product which satisfies all the design constraints and criteria^[1]. The product has to fulfill all the functional requirements and meet the criteria identified prior to and during the design of the product. It is evident that the design process can become a very complex task to perform even for the design of relatively simple products. The design complexity increases exponentially depending on the functional complexity of the product and the number of internal or external interactions of the product^[2].

This chapter introduces the reader to the field of Rapid Manufacturing (RM). The importance of prototyping and time compression techniques in the design process is discussed. A brief overview of different types of rapid manufacturing processes available is presented. The working principles of three of these processes are explained. The chapter concludes with a discussion of the advantages of using a rapid manufacturing method in the design process.

Designers resort to various tools and methods to meet the design requirements^[1]. The intention is to get a ‘satisficing’ design meeting most, if not all, of the functional requirements^[3]. Prototyping is one such method that has been employed to test various aspects of the design before the product goes for final

production run. This pre-production testing is necessary to correct any errors in the design by helping the designer to visualize the product better and test some of the intended functionality. This also avoids costly manufacturing retooling in case of design changes later in the process. Given the short time for developing new products, designers often opt for rapid prototyping for the testing phase^[4].

Design trials are an expensive and wasteful activity as far as the objective of the design process is concerned. However, as discussed earlier, this step cannot be avoided. Prototyped parts which exhibit physical properties similar to the final product can be used for direct testing of functional integrity. However, most of the prototyping processes involve a circuitous route to form the part mockup and involve tooling to a certain extent. Furthermore, even though the shape of the design intent is captured during the prototyping process, the mechanical properties of the prototyped part will not match those of the final product. This is attributed to the layered or additive manufacturing methods used by the rapid prototyping systems vis-à-vis to the conventional manufacturing systems, which use a subtractive (e.g. milling, drilling and shaping) or forced formation process (e.g. extrusion, forming and pressing). A newer technology, Rapid Manufacturing, developed over the last few years^[5], has helped designers to directly manufacture the final part without any tooling requirement. Furthermore, the ability of these processes to use metals has helped to manufacture prototypes which have comparable mechanical properties to those of a finished product.

Rapid manufacturing is a multidisciplinary field in which properties of specific materials are exploited by the use of specialized processes. These generate products which can be used as end products rather than as mockups of the final part^[6, 7]. This approach has helped in reducing the time taken for product realization, especially in the prototyping and tooling phases^[4].

The use of computers in the design process has further enabled the easy portability of design data between the different phases of the design process. It has furthermore facilitated the integration between the manufacturing and the design processes^[4]. Once the design intent has been captured in a CAD format, the data can be manipulated easily to communicate with practically any type of rapid manufacturing machine. The de facto standard adopted by the industry for exchange of design intent data with rapid manufacturing machines is the STL file format which results from the tessellation of the product surface into triangles. Even though the STL file format has been shown to be an inefficient representation of contour data due to the restrictions imposed on the manipulation of contour points and increased data file size, STL continues to be the choice of the industry^[8]. Furthermore, most of the commercial CAD software available has built in translators which export the native file format into the tessellated STL format.

The next section introduces the various Rapid Manufacturing methods developed and their working principles.

1.1 Rapid Manufacturing

Rapid manufacturing can be defined as “the use of computer aided design (CAD) – based automated additive manufacturing process to construct parts that are used directly as finished products or components”^[5]. Based on the phase of the raw material used rapid manufacturing methods can be classified into three main categories^[4, 9].

1. Liquid Based:
 - a. Stereolithography
 - b. Solid Ground Curing
 - c. Fused Deposition Modeling
 - d. Shape Deposition Manufacturing
2. Powder Based:
 - a. Selective Laser Sintering (Polymers, Ceramics and Metal)
 - b. Laser Engineering Net Shaping
 - c. Electron Beam Melting
3. Solid Sheet Based:
 - a. Laminated Object Manufacture
 - b. Paper Lamination Technology
 - c. Ultrasonic Consolidation

In the following section, a few of these processes are discussed briefly. For a detailed study of the various processes the reader may refer to various literatures available ^[4, 5, 10].

1.1.1 Fused Deposition Modeling (FDM)

FDM is a rapid prototyping technology that was developed in the late 1980s and commercialized by Stratasys Inc during the 1990s. This is an additive process which lays a plastic filament in the shape of the product being manufactured. A thread of uniform cross section (1/16" diameter)^[11] is fed from a coil to the printing head where it is heated to 0.5°C above its melting temperature. The melted plastic solidifies as soon as it leaves the printing nozzle, usually within 0.1 seconds. The printing head is computer controlled to move in a path that forms the geometric profile of the product being manufactured^[12]. The product build quality is ensured by controlling the extrusion rate and the nozzle speed. For overhanging parts, support structures are also built along with the main part. The support material is usually built of water soluble material so that it can be easily removed once the part building is completed. The schematic of the FDM process is shown in Figure 1.1

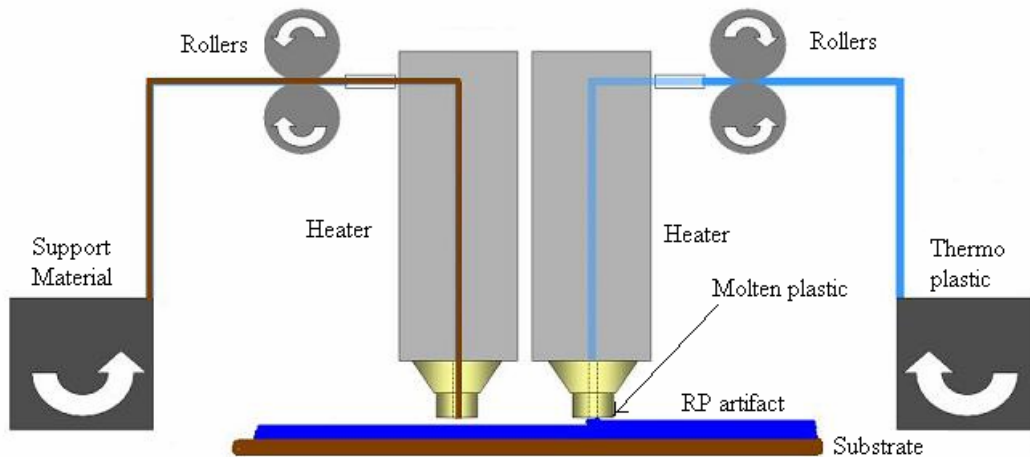


Figure 1.1 Fused Deposition Modeling^[13]

1.1.2 Selective Laser Sintering (SLS)

SLS is a powder based layered rapid manufacturing process. SLS was patented in 1989 and commercialized in 1992^[4]. The method works by indexing the work table on which a polymer base powder is laid. A laser selectively scans the powder on the worktable, which sinters the powder to form a solid polymer. Once a layer is completely scanned by the laser head, the work table indexes downwards by 100 μm and an additional layer of powder is laid. The portions of the previous layer which were not sintered act as the support structure in case of overhangs in the current layer. This process is continued to build the complete 3-D part. To avoid stresses during the sintering process, the powder is preheated by an infrared heater to a temperature close to the sintering temperature^[5]. Figure 1.2 shows a schematic of the SLS process.

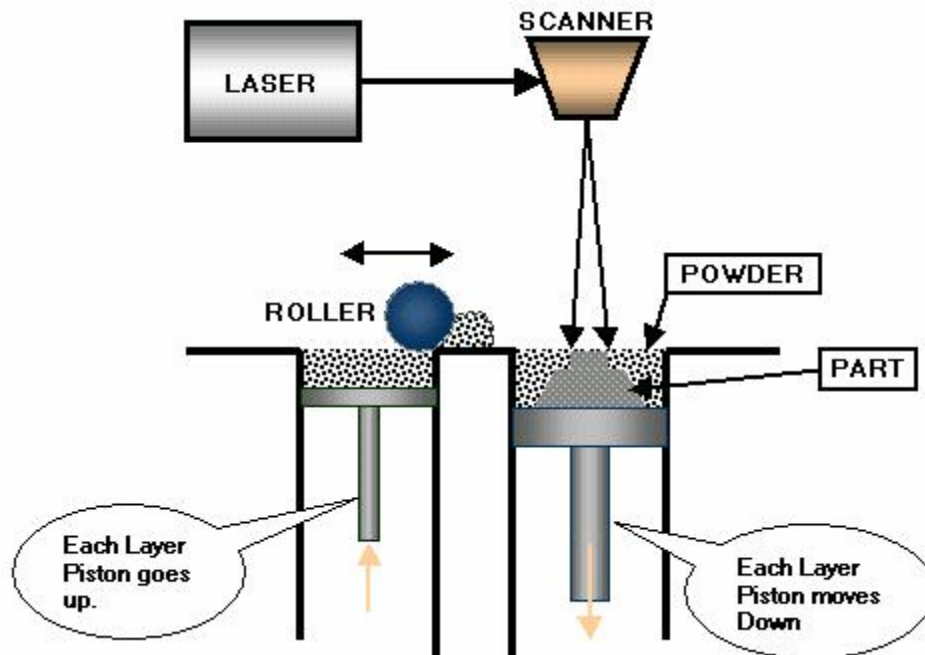


Figure 1.2 Selective Laser Sintering^[14]

1.1.3 Laser Engineering Net Shaping (LENS)

The Laser Engineering Net Shaping or LENS process, was developed by Sandia National Laboratories and commercialized by Optomec^[4]. LENS can be considered as a variation of the SLS process. The LENS process uses a CO₂ laser beam to sinter metal powder which is continuously fed into a laser induced plasma pool or into the laser beam.

The laser head unit is guided to move in a path based on the geometry of the part being manufactured. The laser beam is focused using lenses to a very narrow spot, increasing the wattage intensity to a value high enough to melt metal. The high intensity laser beam melts the top layer of the metal and forms a molten pool into which the powder is injected. The operating environment is made inert to prevent oxidation of the high temperature metal formed during the process. Based on the path followed by the laser head, a layer of the artifact is formed. Once the scanning of a layer is completed, the table is indexed and the process is repeated. The non sintered metal powder acts as the support structure for the subsequent layers^[15].

The method can be used to form different types of metals like stainless steel alloys, nickel-based super alloys, tool steel alloys, titanium alloy and some other special metal alloys^[16]. A schematic of the LENS process is shown in Figure 1.3.

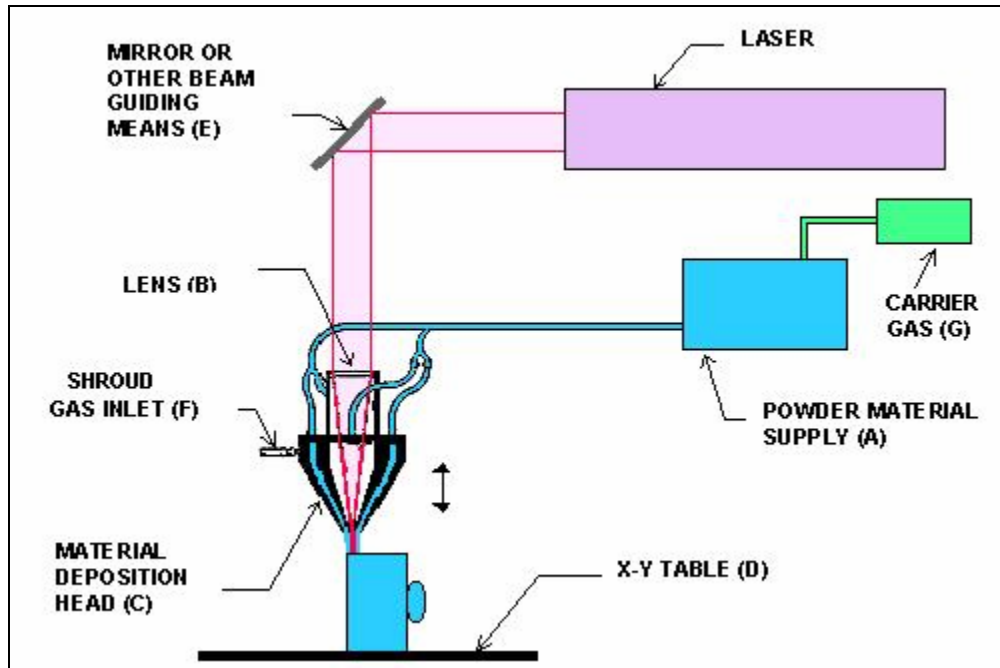


Figure 1.3 Laser Engineered Net Shaping^[17]

1.1.4 Electron Beam Melting (EBM)

Electron Beam Melting or EBM was commercialized by Arcam in 2001^[18]. EBM is a variation of the SLS technology. The main difference between SLS and EBM is the energy source used for the melting of the metal powder. While SLS uses a high power laser beam to form the artifact, EBM uses an electron beam for melting the metal^[19]. Also, since the energy source is an electron beam, the beam has to be focused to a concentrated point with the help of focusing coils. The focusing coils act as electrical lenses in place of the optical lens used in laser based processes.

The bonds between layers are achieved by melting of the metal and do not require any filler material. Due to this reason the part attains its full mechanical strength

even without secondary thermal treatment^[20]. The formation is done in an inert atmosphere which prevents the formation of metal oxides when the metal is in the melted condition. This process is an ideal candidate for the manufacture of performance components. The process is capable of handling different types of metals including stainless steel and titanium alloys. A schematic of the EBM process is shown in Figure 1.4

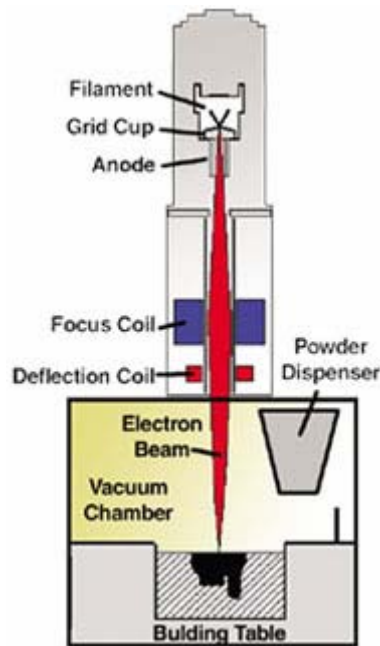


Figure 1.4 Electron Beam Melting^[21]

1.1.5 Ultrasonic Consolidation (UC)

Ultrasonic Consolidation was patented by Solidica®, in 2000. The Ultrasonic Consolidation process is a layered manufacturing technology. It combines additive and subtractive manufacturing methods. Ultrasonic Consolidation uses thin metal foils as raw material for the formation process. The process requires addition of material to build the part envelope and later removal of material from

areas where it is not needed to form the details of the part being manufactured. A milling head is used for the material removal process.

The complete process steps involved in the production of an artifact is shown in Figure 1.5

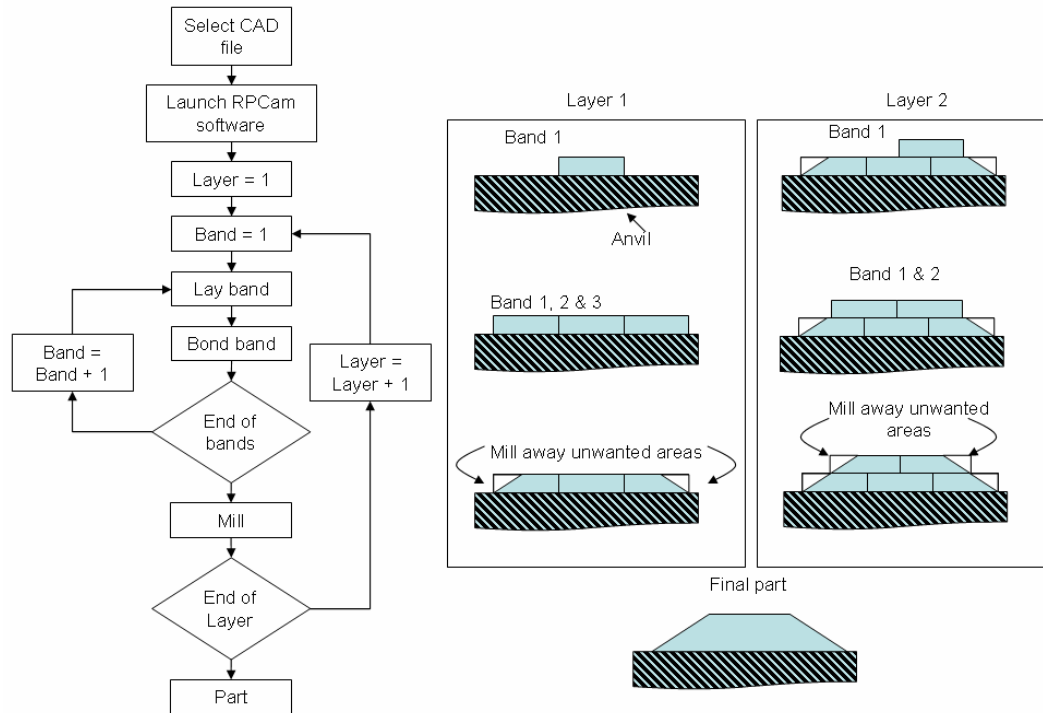


Figure 1.5 Different steps of the Ultrasonic Consolidation process

The commonly used raw material for this process is aluminum foil which is 0.9375 inch wide and 0.0006 inch thick. The aluminum foils are laid on the sacrificial anvil and clamped by the sonotrode which is shown in Figure 1.6.

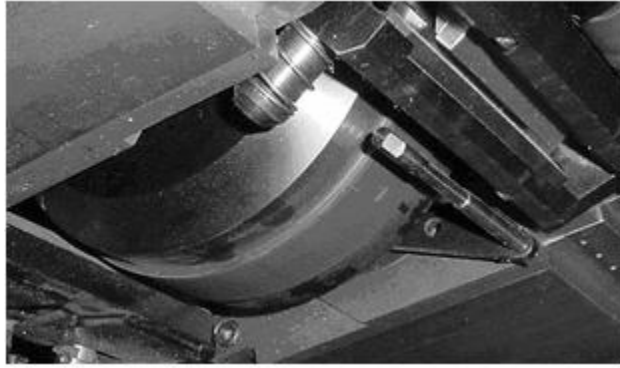


Figure 1.6 Sonotrode

For the clamping step the machine requires an additional five inches of aluminum foil on each side of every band placed. This additional clamping allowance is shown in Figure 1.7.

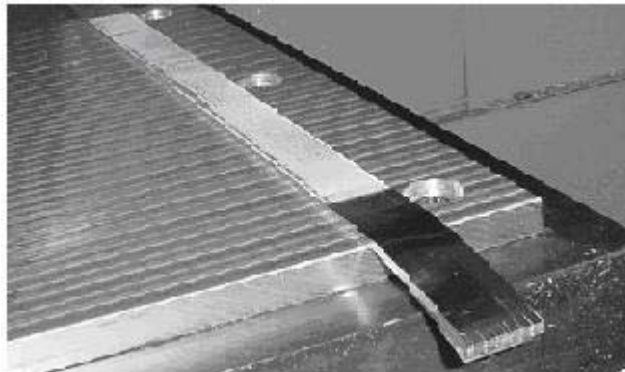


Figure 1.7 Clamping waste

The second step in the formation process is the Ultrasonic Consolidation of aluminum foils to form a solid bond with the previously laid layers or with the sacrificial anvil. Figure 1.8 shows the different components involved in the Ultrasonic Consolidation process. The direction of tacking process and the consolidating process is also shown in the figure.

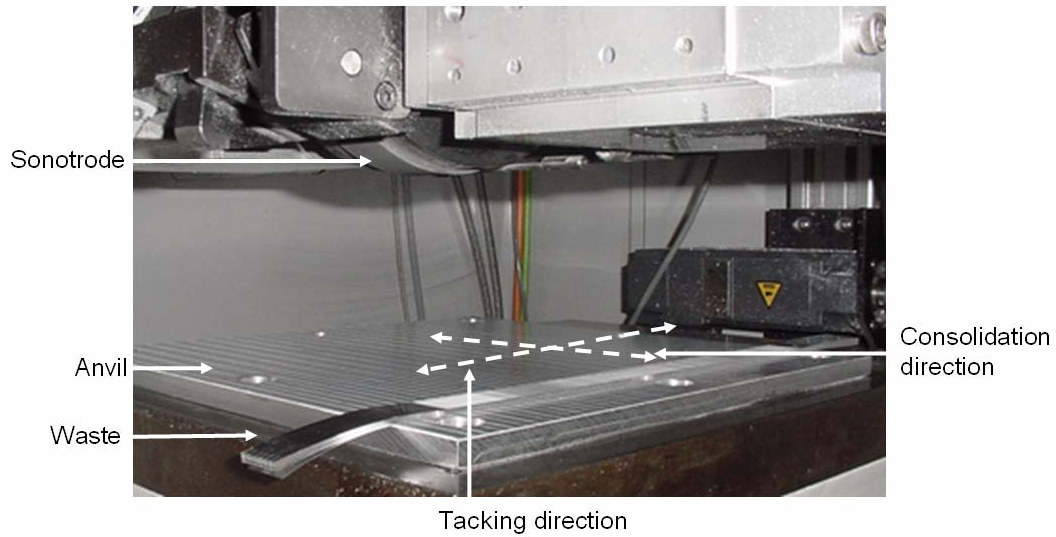


Figure 1.8 Ultrasonic Consolidation Process

The consolidation is effected by applying a vertical load on the aluminum foil by the consolidating head which is vibrating laterally at a frequency of 22 kHz^[22]. The ultrasonic vibration breaks the oxides formed on the surface of the aluminum foils. Due to the presence of the vertical load and lateral vibration, static and shearing stresses are developed causing the atoms to diffuse across the boundary forming a true metallic bond with the preceding layer. The process is schematically represented in Figure 1.9

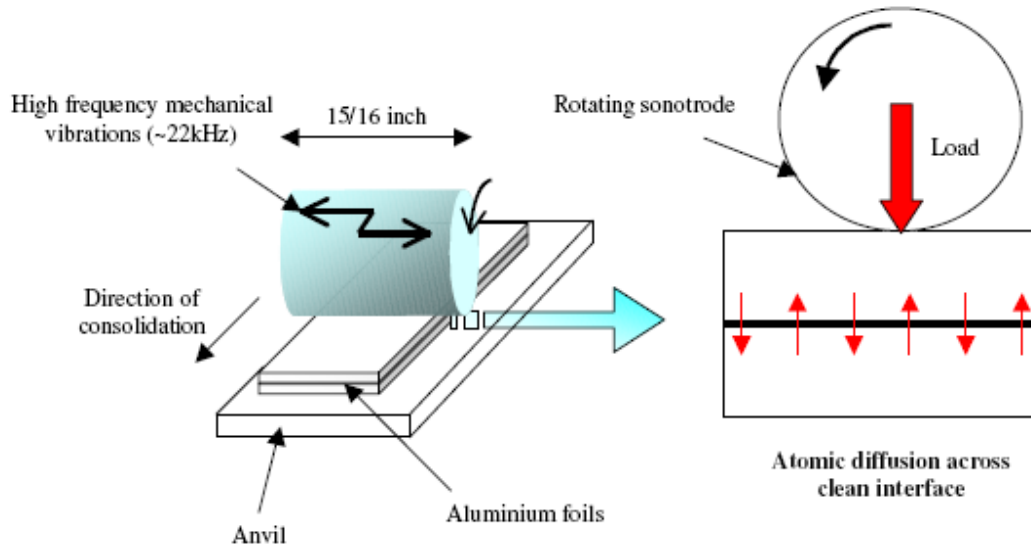


Figure 1.9 Ultrasonic Consolidation bond formation^[23]

After the consolidation process, the aluminum bands form the envelope of the product being manufactured. A milling process is used to form the detailed features of the artifact. The milling process can be activated for each layer of bands placed or for a series of layers. This cycle is repeated for each layer of the artifact to complete the 3D model of the artifact.

Figure 1.10(a) shows a cross section of a part being manufactured using the Ultrasonic Consolidation process. Based on the part dimensions and the band width, the bands are laid on the slice so that they completely cover the slice. Figure 1.10(b) shows the total area of the bands required to form the slice.

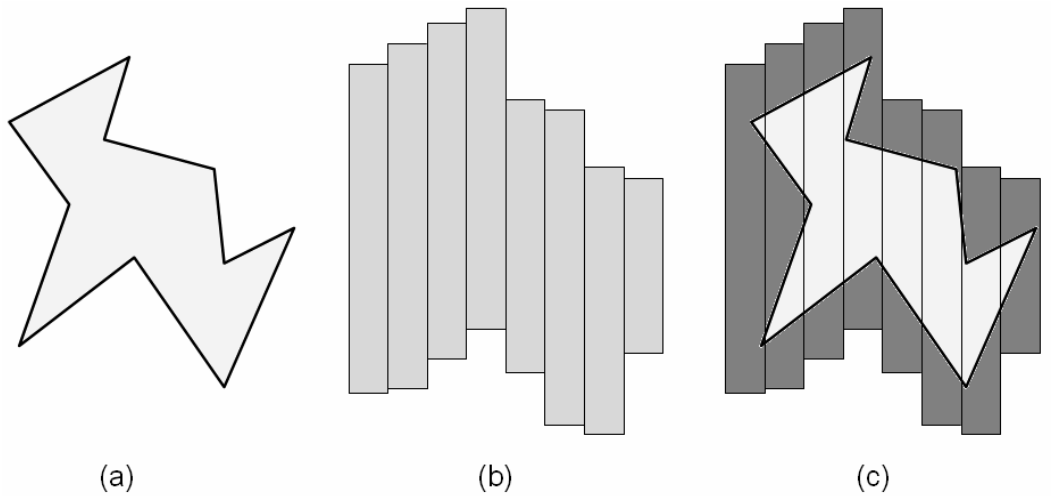


Figure 1.10 Part slice, aluminum bands and waste area

However it is noted that, on superposition of the part slice on the band grid, a significant area is wasted. Figure 1.10(c) shows the wasted area as the dark areas of the band grid. The useful portion of the band is enclosed by the part slice contour and is shown in a lighter shade.

1.1.5.1 Dependency of Waste Area on θ and δ

Figure 1.11 shows the coordinate system used in the Ultrasonic Consolidation process. The artifact is formed perpendicular to the slicing plane as shown in the figure. This direction is termed the z-axis or the build direction of the artifact. The slicing algorithm intersects an imaginary plane perpendicular to the z-axis to retrieve the corner points of the artifacts. These corner points lie in the same x-y plane.

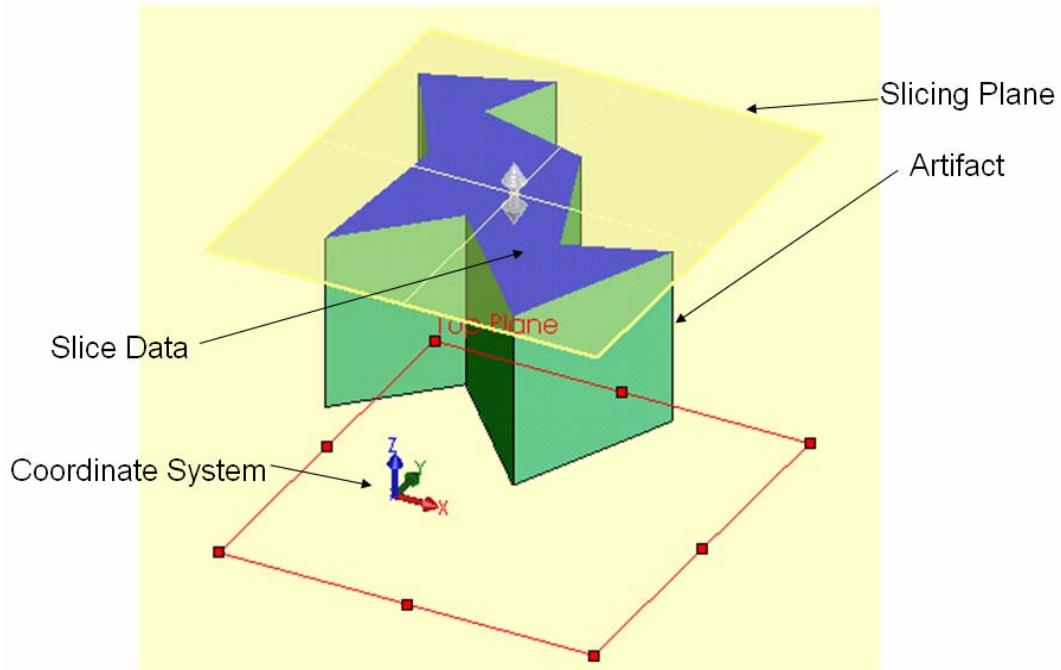


Figure 1.11 Coordinate System of the Ultrasonic Consolidation Process

For ascertaining the dependency of the waste area on the translation along x-axis (δ) and rotation about z-axis (θ) parameters, the following experiment is conducted. Complex slice data is placed on the band grid and the waste area is calculated as the difference between the total band area required and the slice area. The waste area is calculated for different values of δ and θ . The results of this experiment are shown in Figure 1.12. The total Number of Band (NoBs) required for placing the slice is also shown in the Figure 1.12

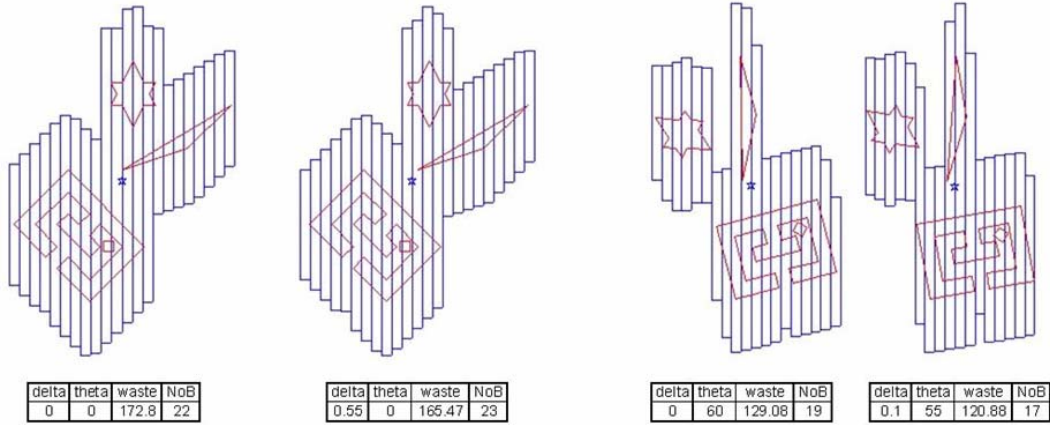


Figure 1.12 Comparison of waste area

It is seen from the comparative study that the waste area is a function of the parameters δ and θ . It is also noted from the figures that the NoBs required for the slice is also dependant on the choice of δ and θ .

1.1.5.2 Strength

Another issue that has been identified by research^[24], is the reduction of part strength beyond an aspect ratio of 1:1. It has been noted that as the height of the vertical stacking of a part increases beyond the foils width, the foils tend to spread out resulting in a reduction of part strength. This condition is shown in Figure 1.13.

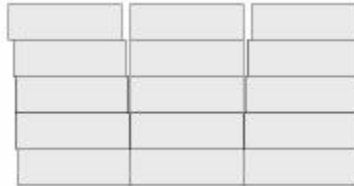


Figure 1.13 Reduction of part strength with increasing aspect ratio^[25]

However, this reduction in part strength can be countered by building a crisscross layout or an overlapping layout. This would maintain the part strength as desired as well as avoid the orthotropic behavior of the finished artifact which would ensue if the layers are laid out as in Figure 1.13.

1.1.5.3 Build Time

Another issue related to the issue of part strength is build time. It is desired that, due to the phenomenon of reduced strength with increasing number of bands, a minimum number of bands be used for the building of each slice. However, the optimizer may not converge to parameter values which would allow this. This is because, as far as the primary objective of waste reduction is concerned, reduction of NoBs would prove counterproductive if the clamping allowance is not considered. This is illustrated in Figure 1.14

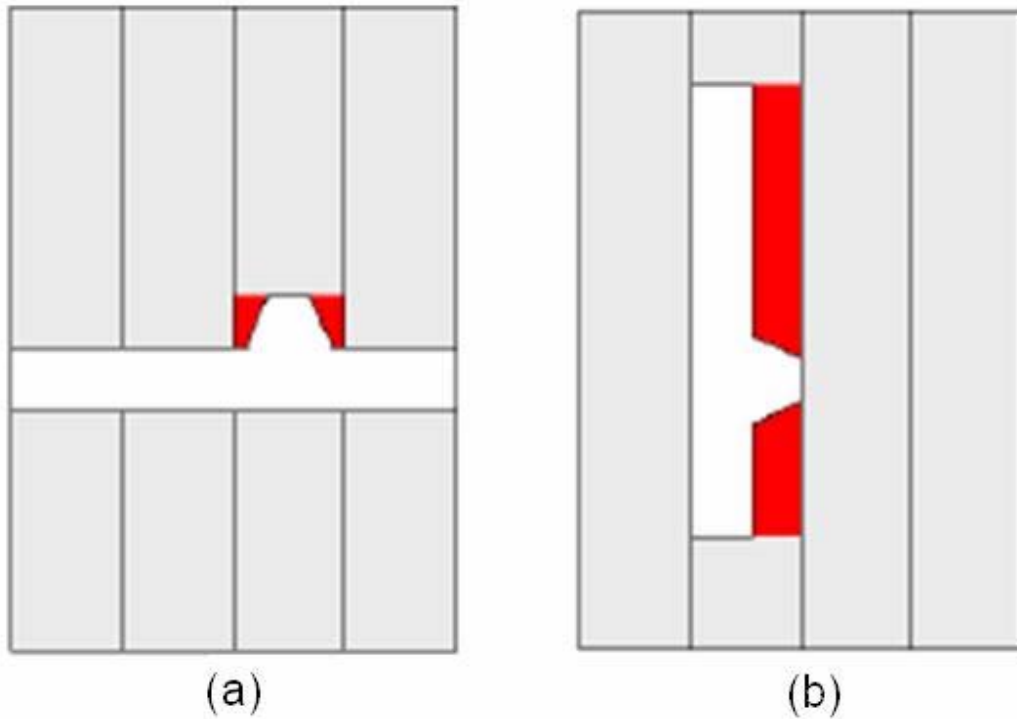


Figure 1.14 Compromise between build time/part strength and waste^[25]

Figure 1.14(a) shows the optimized layout for minimal waste formed. However, it is noted that to build the part, four bands are required. This would have negative impact on part strength. An alternate layout is shown in Figure 1.14(b). In this layout it can be seen that the waste area has increased as compared to the earlier layout. The advantage in the later layout can be appreciated if we consider the NoBs required for the building of the part. The later layout requires only one band for building the part, which considerably increases the part strength as compared to Figure 1.14(a).

1.2 Advantages of Rapid Manufacturing Methods

There are many advantages to using rapid manufacturing processes. The first and foremost is the geometric freedom afforded to the designer. With the advent of rapid manufacturing technology, the designer can develop products which were earlier considered to be infeasible for manufacture. This can be seen as a departure from the existing 'design for manufacture' to a 'manufacture to design' approach^[26]. A manufacture to design approach would open up new vistas to the designer, freeing him from many of the design constraints that exist with the use of conventional manufacturing methods. This is exemplified in the field of bionics which tries to imitate natural phenomena in the design of new products and technologies. Figure 1.15 shows a bionic structure that has been designed for structural application. However, as can be seen from Figure 1.15, the design cannot be manufactured using conventional manufacturing methods. It is logical to assume that this complex design idea was realizable only due to the advent of layered manufacturing technologies.

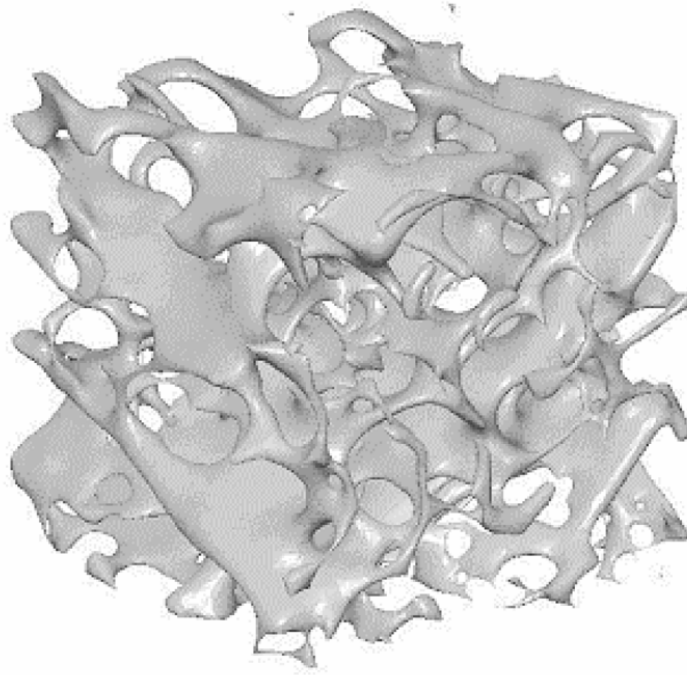


Figure 1.15 Bionic structure^[27]

The advantage of RM methods is further exemplified when we consider design solutions that are derived from topology optimization routines. Most of the time topology optimizers yield geometries which are not realizable using conventional manufacturing processes^[28]. These non realizable product geometries have to be approximated to manufacturable solutions. This would mean that the design which finally goes for the production run is a sub optimal design. Rapid manufacturing methods can be used in such situations to retain the advantages of the optimal design. The ability to manufacture any design intent developed by the designers increases the feasible design space which was earlier limited by the manufacturing feasibility domain. This is pictorially represented in Figure 1.16

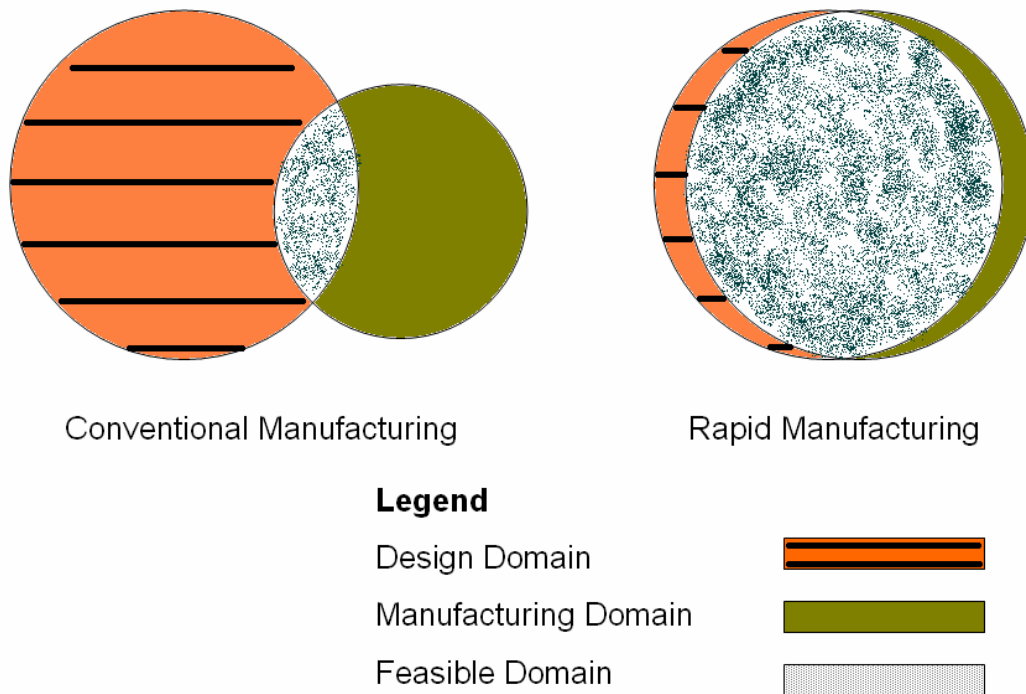


Figure 1.16 Feasible domains in Conventional and Rapid manufacturing

Studies ^[2] have shown that the cost of designing and realizing a product is directly proportional to the complexity of the product. However, this conclusion is arrived at by considering the cost of conventional manufacturing methods to develop the features in the product. This also includes the tools and fixtures that are required by the traditional manufacturing processes. Rapid manufacturing methods are capable of converting the design intent into tangible parts without using any special tooling. This decouples the cost of manufacturing from the product geometric complexity, which drastically reduces the manufacturing cost of the product. In other words the manufacturing cost is no longer dependant on the complexity of the part being manufactured

In addition to the advantages of design freedom and reduced cost, rapid manufacturing method form an integral part of concurrent engineering^[4]. The advantages of using concurrent engineering in design has been discussed by various researchers and a fair amount of literature has been generated in this field^[29, 30].

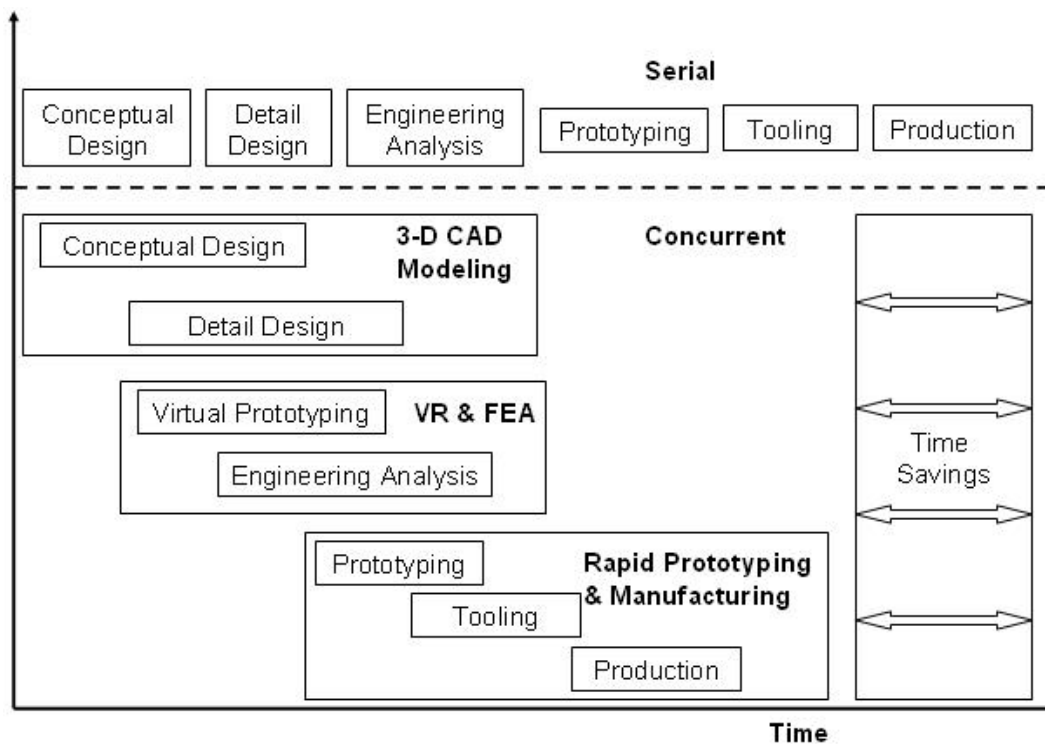


Figure 1.17 Concurrent Engineering and time saving^[4]

The advantage of using concurrent engineering techniques in engineering design and the importance of rapid prototyping/manufacturing methods is understood from Figure 1.17. It is further noticed from Figure 1.17 that the time savings can be further increased by collapsing the three boxes under the rapid prototyping and manufacturing section into a single box - rapid manufacturing.

Another advantage of using rapid manufacturing technology as a main stream manufacturing method is its capability to open new avenues that have enabled engineers to develop engineering solutions in realms which were earlier deemed as impossible^[31]. This has helped engineers realize multi material structures, embedded sensors, conformal cavity moulds and the like. Now, the capabilities of these processes are employed in a wide variety of fields like medical science, sports, consumer items, electronics and photonics^[32-35]

1.3 Closure

The various types of rapid manufacturing methods have been introduced to the reader and the advantages of using rapid manufacturing in design have been identified and discussed in this chapter. The process of UC was discussed in detail and its salient points were discussed. The dependence of the waste area and build time on the choice of δ and θ were also presented.

While the technology holds a lot of promise for the design engineer in terms of design freedom and time and cost savings, the existing technology is not devoid of problems. There are many issues that need to be addressed before the technology can replace the conventional manufacturing method. The major issues that affect the acceptance of the technology as a mainstream manufacturing method and the various efforts underway to achieve this acceptance are discussed in the next chapter.

CHAPTER 2

LITERATURE REVIEW

The previous chapter discussed the importance of rapid manufacturing as a new technology and how it can be used to the advantage of the design engineer to reduce the time taken and the cost of designing a new product or reengineering an existing product.

This chapter gives a brief overview of the relevant research efforts undertaken by researchers in industry and academia over the years to make the rapid manufacturing technology a mainstream manufacturing method. The first section of the chapter discusses the problems that have been identified in the fields of Rapid Prototyping and Rapid Manufacturing and how researchers have overcome these issues. The second section of the chapter gives an extensive review of the efforts to identify the research issues and those undertaken to improve the Ultrasonic Consolidation process. The chapter concludes by identifying areas where more research effort is required to improve the Ultrasonic Consolidation process

2.1 Research in Rapid Manufacturing/Prototyping

The previously discussed rapid manufacturing methods developed so far employ either a layered manufacturing method or an additive manufacturing method^[5],

while most of the conventional manufacturing methods use a single subtractive process or a combination of different subtractive processes to achieve the design detail. Due to the basic difference in the formation method of the artifact, many of the new manufacturing methods introduce new issues which have to be addressed and solved for the part to be manufactured.

Most of the issues that have been identified can be classified under the headings of

- Data representation (Mathematical)
- Material and
- Process^[10, 36]

For brevity considerations, only the issues related to process is discussed. Process related concerns can be addressed by varying the parameters of the manufacturing process. These concerns are further discussed in detail in the following sections.

2.1.1 Accuracy

Dimensional accuracy of the part is affected by the various conditions that exist during the manufacturing process. Depending on the shape of the part being manufactured, accuracy is affected by the shrinkage and warping of the product^[37]. This is mainly attributed to the unequal cooling or stress relief in the area of material formation^[38]. This defect is exacerbated if the part geometry has long overhangs.^[10, 39] as shown in Figure 2.1.

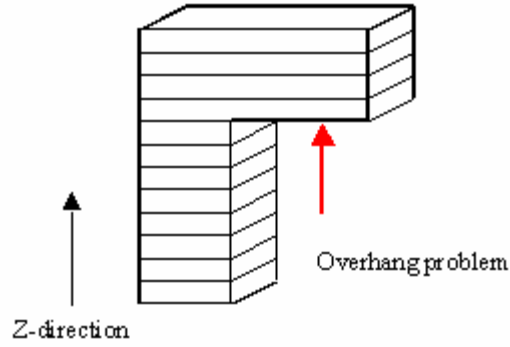


Figure 2.1 Overhang in layered manufacturing

Another condition that affects part geometry is the z-axis error. This error occurs mainly due to the variations in the process the layer thickness might change which affects the accuracy of the surfaces formed^[39, 40]. Figure 2.2 shows the effect of z-axis error. This variation in dimension can occur due to limitations of the machine used or due to the characteristics of the material used.



Figure 2.2 z-axis error^[40]

Various researchers have improved the accuracy of rapid manufacturing processes using different approaches which include use of materials which have minimal shrinkage characteristics^[41, 42] and by modifying the process so that the detrimental effects of shrinkage and warping are minimized^[43, 44].

2.1.2 Repeatability

For the rapid manufacturing technology to be accepted as a mainstream manufacturing method, the processes should be able to produce artifacts which are consistent with the design specification whenever a part is built. In other words the process should have repeatability. However, with the existing technology, the repeatability attained is inferior as compared to conventional manufacturing process^[37, 45].

For example the dimensional accuracy of products manufactured using FDM is affected by variable shrinking of the resin which is dependent on the ambient temperature and humidity. Due to this, it is seen that the environmental factors affect the repeatability of the parts being manufactured^[8].

2.1.3 Surface finish

A major factor which affects the acceptance of rapid manufacturing methods is the poor surface typically finish attained after the manufacturing run. Most of the time, the prototyped artifact has to be subjected to a secondary process which machines away the rough portions to attain the smooth surface finish required by the designer^[36].

The poor surface finish in can be attributed to a number of factors. Due to the method adopted for rapid manufacturing, namely, additive or layered, the product formed may have what is know as ‘stair step effect’^[46] as shown in Figure 2.3.

This is due to the discrete layer thickness and is affected by the choice of the build direction, the geometry of the shape being manufactured and the method used^[36, 46-48].



Figure 2.3 Stair Step Effect

Another aspect which affects the surface finish of the artifact is the area of contact made by the support structure with the part. At the end of the manufacturing process, the support structure has to be detached from the part to get the final artifact. The surface finish of the part is affected at areas from where support structure is detached from the artifact^[49]. The relative ease with which the support structure is detached from the artifact is dependant on the type of process used^[36].

Many researchers have tried different approaches to minimize the stair stepping effect and the use of support structures in the manufacture of artifacts. Adaptive slicing^[50, 51] has been used by researchers to reduce the stair stepping effect. The idea of optimal choice of z-direction (direction of build) has also been researched over the years^[47, 52, 53]. Novel ideas like multi-axis slicing based on decomposition of artifacts has also been developed^[54].

2.1.4 Part strength

Rapid manufacturing technology, being an additive fabrication technology, results in anisotropic material properties. Even if the raw material used for the building of the artifact is isotropic, due to the step by step addition of material, the finished artifact behaves as an orthotropic part^[46]. Due to this reason, the build direction of the part affects the mechanical properties of the finished artifact^[31].

Depending on the technology adopted for the fabrication of the artifact the part strength varies. For example, the strength of an artifact manufactured using Ultrasonic Consolidation and Selective Laser Sintering are different due to the basic difference in the formation process and the material used^[39]. This is because while Ultrasonic Consolidation process forms mechanical bond between layers at lower temperatures, Selective Laser Sintering forms the bonds at melting temperatures and this affects the mechanical properties of the artifact formed.

Depending on the material used for building the artifact, the strength varies. The strength attained by using stainless steel as raw material will be different from the strength achieved by using titanium alloy as raw material. Certainly, the strength variation exists because of the difference in mechanical properties of the raw materials used, but also due to the behavior of the material to consolidation forces and adhesion and cohesion properties^[39].

Calculation of the strength of a part produced using a rapid manufacturing method is not a trivial problem. The complexity arises due to the fact that inter layer interactions are not yet fully understood. However, previous research has tried to mathematically model the strength attained by a part manufactured using layered or additive manufacturing processes^[55, 56].

2.1.5 Performance

The performance of a rapid manufacturing process in economic terms is measured by the time taken for a standard part to be manufactured and the percentage of value retention of the raw material by the manufacturing process. The build time is positively affected by the part accuracy required and the path planning followed to convert the ‘hollow’ STL file into a ‘solid’ part. Furthermore, depending on the method used, the build time of a given artifact will vary.

Based on the type of manufacturing method used, the volume of support material that is required will vary. The build time is positively correlated to the volume of support material that needs to be built^[36]. The build time is also affected by the choice of build direction, since the same affects the total height of artifact, hence the number of layers that need to be laid and thus the time taken to produce the part^[36, 57].

Previous researchers have come up with algorithms which will reduce the time taken for the process completion based on varying constraints. The constraints on

the optimizer can be surface quality^[58], calculation speed^[59], warping^[60], part strength^[61] or bonding/cohesion characteristics^[62]. For a complete list of the various algorithms, the reader may refer to the available literature^[36].

Another major issue which affects the performance of the rapid manufacturing method is the waste generated during the formation process. Waste can be generated from primary operations like clamping allowances^[22] or support structures. These unwanted portions need to be removed to achieve the part design geometry. The building of support structures further affects the performance by increasing the time taken for the part to be completed.

The preceding discussion on the research issues identified with the development of rapid manufacturing is summarized in Figure 2.4 as a tree structure.

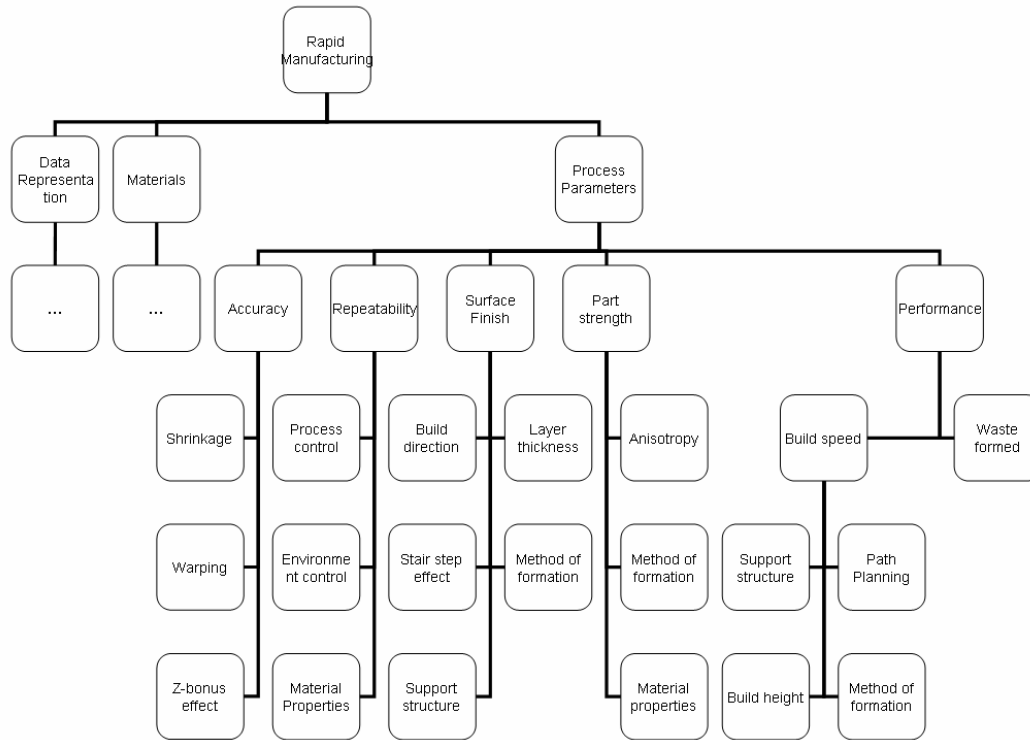


Figure 2.4 Rapid Manufacturing research issues

As mentioned earlier the research in the field of RM is broadly classified under the headings of data representation, materials and process parameters. The preceding discussion gave a brief overview of the research under the heading of process parameters.

2.2 Review of Research in Ultrasonic Consolidation

The previous section gave a broad overview of the concerns with the new manufacturing methods that are being addressed by various researchers for the technology to be accepted as a mainstream manufacturing method. In the following section, the relevant research efforts taken in the field of Ultrasonic

Consolidation specifically are discussed. While most of the issues highlighted in the previous section apply to the Ultrasonic Consolidation process, due to its unique combinational nature, a dedicated discussion section on the relevant research issues is warranted.

The research efforts in the field of Ultrasonic Consolidation can be grouped under the following headings

- Development of new applications
- Development of new materials
- Refinement of process variables

These research areas are discussed in detail in the following sections

2.2.1 New application development

Ultrasonic Consolidation has the unique capability of working directly with metals in a cold state. Since the consolidation does not occur at an elevated temperature, the technology can be adapted to novel areas of application. The technology has been adapted to varied fields of application including sensors, multi-materials, military, medical, and RFID. Sensors can be inserted between layers of bands which form a solid protection for the sensors. These sensor impregnated artifacts can be used in health monitoring systems of a larger system, for example, a military armored vehicle^[63, 64]. The Ultrasonic Consolidation process has been found capable of handling maintenance requirements of performance components in critical machinery like fighter jets^[65]. The Ultrasonic

Consolidation process has been tuned for use in the design of small satellites by researchers^[66]. The use of the technology in the field of medical applications has also been tested^[67]. Smart products can be manufactured using the Ultrasonic Consolidation process and used as surgical implants or micro-fluidic devices. Research efforts have identified the capability of the process to manufacture multi-material products^[68]. Such research has been further extended to enable the Ultrasonic Consolidation process to embed shape memory alloys in an aluminum matrix^[69].

2.2.2 New material development

Researchers have tried to develop new materials to be used with the Ultrasonic Consolidation process. Currently, the process uses mostly aluminum foils. The strength of the bond formed is a function of the process parameters namely, vibration amplitude, clamping load, temperature and consolidating speed. Materials like Aluminum 3003 and 6061 have been characterized for optimum parameters that would yield highest strength in the finished part^[23, 70]. The mechanical properties of the bond formed between aluminum and zinc has also required. The build time is also affected by the slicing thickness of the artifact being manufactured

rd<<rec-number>123</rec-number><ref-type name="Journal Article">17</ref-type><contributors><authors><author>Gunduz, Ibrahim E.</author><author>Ando, Teiichi</author><author>Shattuck, Emily</author><author>Wong, Peter Y.</author><author>Doumanidis, Charalabos C.</author></authors></contributors><titles><title>Enhanced diffusion and phase transformations during ultrasonic welding of zinc and aluminum</title><secondary-title>Scripta Materialia</secondary-title></titles><periodical><full-title>Scripta Materialia</full-title></periodical><pages>939-943</pages><volume>52</volume><number>9</number><keywords><keyword>High strain rate deformation</keyword><keyword>Excess vacancy</keyword><keyword>Enhanced

2.2.3 Process Refinements

The third main area of research in the field of Ultrasonic Consolidation is the study of the process itself. Research has shown that tweaking of process parameters affect the final part strength and accuracy.

2.2.3.1 Build Time

As has been discussed in Section 2.1.5, the time taken for the completion of a part is directly proportional to the number of layers that need to be stacked due to the layer by layer building of a part in Ultrasonic Consolidation. Researchers have tried to minimize the build time by developing algorithms which minimize the total height of the part in the build direction and the support volume required. The build time is also affected by the slicing thickness of the artifact being manufactured^[51, 73].

2.2.3.2 Strength

The strength of a part manufactured using the Ultrasonic Consolidation process has interested various researchers. A mathematical model of the interface formed between aluminum foils has been studied in the past^[74-76]. Previous research has also established that the part strength in the Ultrasonic Consolidation process, reduces considerably beyond a height to width ratio of 1:1^[24] which has led to the idea of forming brick structures and crisscross structures during the process itself.

2.2.3.3 Waste

The Ultrasonic Consolidation method is a unique process which combines additive and subtractive manufacturing. This creates a unique problem for Ultrasonic Consolidation - waste formation during the process.

The raw material currently used in the process costs around \$25 per pound when it is in the form of foils. However once the foil is consolidated and the unwanted areas of aluminum is removed the metal is considered as scrap aluminum since it cannot be used for further processing in the Ultrasonic Consolidation process. The scrap value of aluminum is 75 cents, which is a considerable reduction from the earlier \$25. This can turn into a significant loss if we consider the manufacturing of a complete artifact. The realization of the possible monetary saving by process refinement instigated the development of optimization algorithms for the Ultrasonic Consolidation process.

2.3 Problem Description And Objective

In the previous section, the unique problem of waste formation in Ultrasonic Consolidation process was explained. However it is seen from previous work done by Schwager and Galli^[22], that the waste formed is a function of the geometry of the part being manufactured and the relative orientation of the part layers with respect to the aluminum band grid. This presents an opportunity to explore ways of optimizing the layer placement across the aluminum bands in an effort to minimize the waste generated. Based on the understanding of the

Ultrasonic Consolidation process and the need for an automated process planning method the research objective is defined.

The problem is to develop an algorithm which optimally places the layers of the artifact across the aluminum bands so as to minimize the waste generated.

The rotation of the layer with respect to the centroid and translation of the layer across the aluminum bands are two variables which decide the total waste generated during the process. The consolidation forces required and the maximum achievable stack up of the aluminum layers are also considered for the optimization algorithm.

2.4 Existing Algorithm

The first attempt to optimize the Ultrasonic Consolidation process for waste minimization was done by Schwager and Galli^[22] in 2006. The problem was modularized into two sub-problems. The first problem was the orientation of the 3D part to minimize the support volume required and maximize the surface quality. This selection of the optimal z-direction was termed as the ‘3D problem’. Subsequent to the solution of the 3D problem, the individual layers were optimized to minimize the waste area formed during the band laying process. This sub problem was termed as the ‘2D problem’. The solution of the combined problem yielded the optimal orientation and layout of the part and layers

respectively. The optimization algorithm used an interactive solution technique, which made use of user input to solve the 3D problem. The orientation of the 3D part was left to the expertise of the user.

The solution of the 3-D problem yields a choice of z-direction which is used for the slicing of the 3-D part. This portion of the optimization problem was performed by a marching algorithm built into the CIDES slicing software^[77]. The output of the CIDES software is a point cloud which contains the contour points of the artifact for each layer. This point cloud forms the input to the 2-D problem. The contour points are read by the 2-D problem solver which was implemented in MATLAB. The contour points were placed onto a grid representing the aluminum foils. Based on the intersection of the contour point connecting lines with the grid, the total band area was calculated. The wasted area is calculated as the difference between the total area required and the slice area of the artifact. A gradient based optimizer was used to drive the waste area formed to a minimum value. The design variables used for the optimization run were the translation and the orientation of the slice data with respect to the grid. The output of the optimizer contained the translation value and the rotation angle from the original position. With this step the problem was solved for a given shape geometry. This process is pictorially represented in Figure 2.5

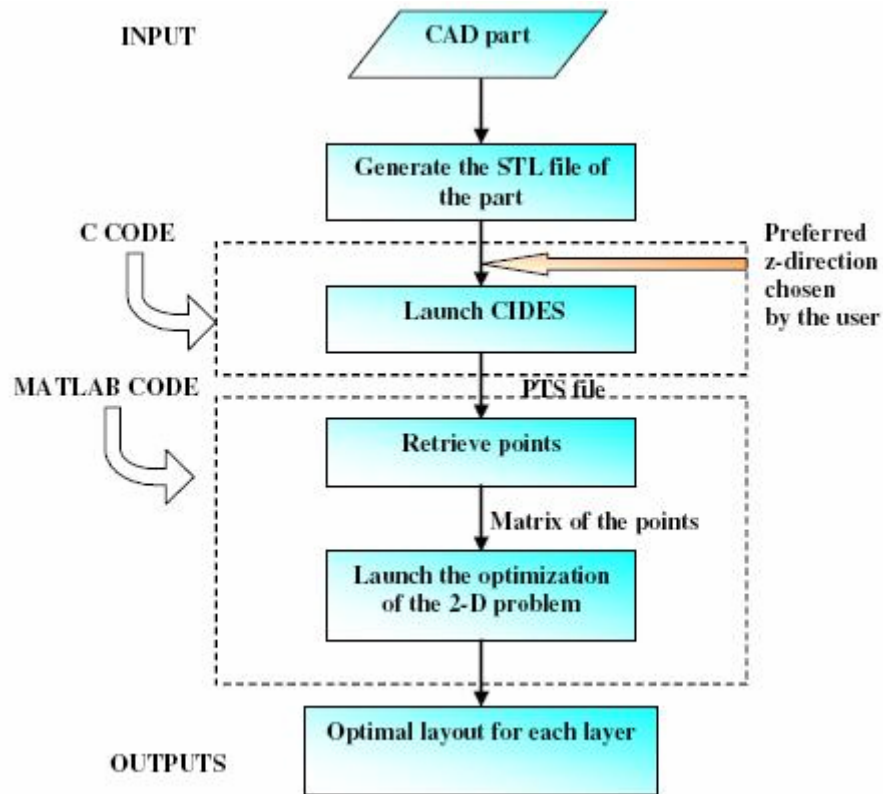


Figure 2.5 Optimization of UC process for waste reduction^[78]

This algorithm was developed by considerably reducing the calculation complexity and algorithmic complexity with assumptions on the input data. The algorithm approximated multiple loops, as shown in Figure 2.6, in a single slice to the convex hull of the slices. The convex hull approximation technique was also used for eliminating the non convexity of the input data. Furthermore, the algorithm does not consider the dependence of aspect ratio on part strength. Aspect ratio is defined as the ratio of the total height of the bonded foils to the width of a single metal foil. This is attributed to the fact that the algorithm was developed as an unconstrained optimization problem and can not handle multiple layer data at the same time. The algorithm was developed considering the

clamping allowance as fixed. However it is noted that the clamping allowance affects the waste area depending on the Number of Bands (NoB) required for the placement of the slice. Since this is dependant on the translation and rotation variable values, the clamping allowance cannot be considered as fixed as far as the optimization is concerned.

2.4.1 Multi Loop Slices

As discussed in the previously, past research efforts have approximated the input data to reduce the algorithmic and computational complexity of the problem by taking the convex hull of the slice data. Due to this approximation step, the output obtained from the optimizer might represent a suboptimal solution. For example, when slices having multiple loops are approximated into a single loop by the convex approximation step, an additional footprint is added to the slice data, which makes the area required by the slice higher, even though the actual part requires a lesser area as shown in Figure 2.6. This increases the number of bands required to cover the slice area. Since all calculations are based on this approximated data, the optimal point arrived at by the optimizer is a solution corresponding to the pseudo input data and not of the actual data set.

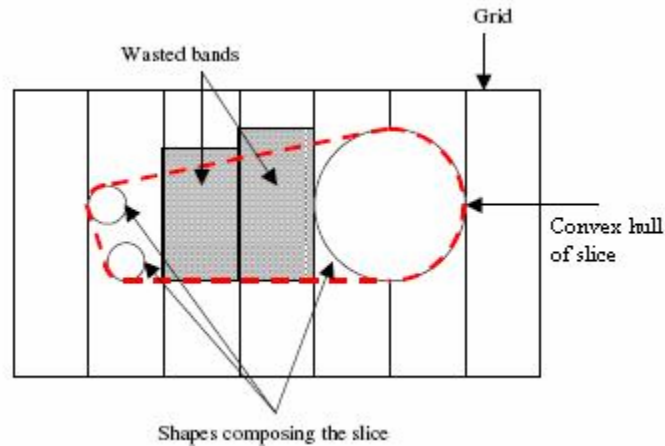


Figure 2.6 Addition of waste due to use of approximation^[78]

In Figure 2.7(a), a part slice comprised of four disjoint squares is shown. As is seen from the adjoining table, the waste area formed with the selected layout is 132 units. Figure 2.7(b) shows the approximation of the same input data, i.e. four disjoint squares. It is seen from the table for the same layout, the waste area has increased to 243 units. It is also seen that the NoBs has increased from 18 to 20. Since the NoBs is a direct measure of the build time required, any increase in the NoBs required will have negative impact on the build time.

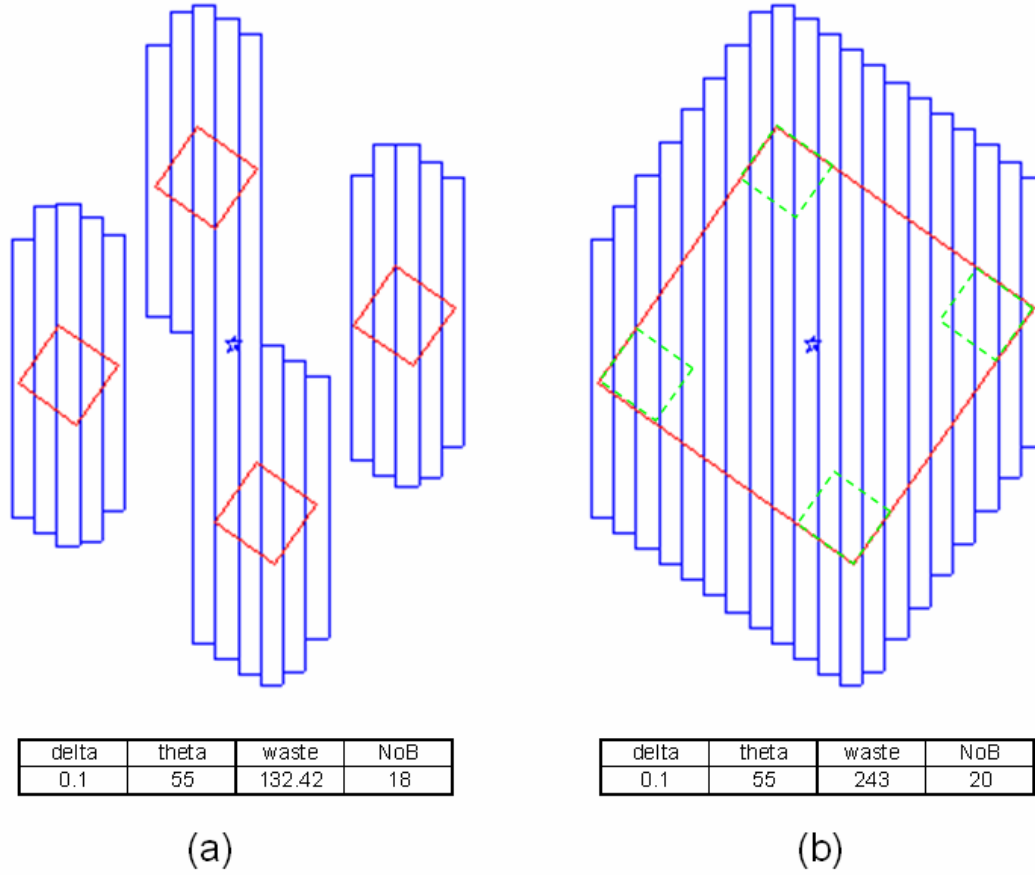


Figure 2.7 Comparison of waste area without and with approximation

2.4.2 Concave Data

In addition to the aforesaid issue which is not addressed by the existing algorithm, it is also seen that non convex slice data is converted to convex contours by a convex hull approximation. Figure 2.8(a) shows the actual non convex slice data and Figure 2.8(b) shows the conversion into convex slice data. This approximation also affects the optimization run and drives the optimizer to settle at a suboptimal solution.

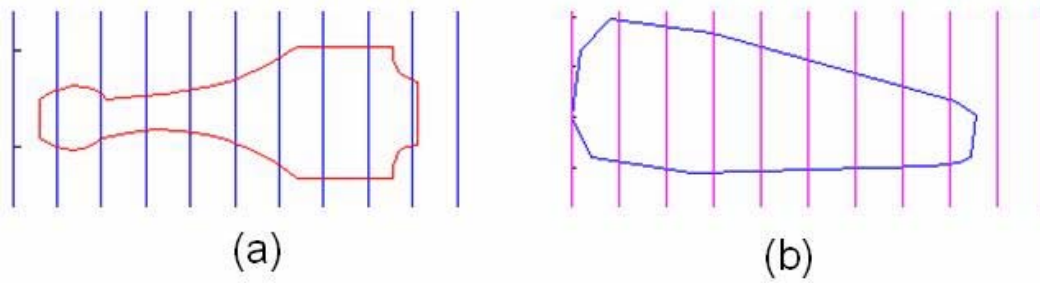


Figure 2.8 Conversion of concave data into convex data

In conclusion it is seen that the existing algorithm for Ultrasonic Consolidation process optimization has various drawbacks which prevent the adoption of the same on a commercial scale. This section has identified the issues which are negatively affecting the performance of the algorithm. This discussion has also put into perspective the future work that needs to be done to develop a new algorithm which can handle real slice data without approximations so that the solution attained by the optimizer is the true optimal solution and not a pseudo optimal solution.

2.5 Closure

This chapter has reviewed the relevant research work done in the past in the field of rapid manufacturing/prototyping and Ultrasonic Consolidation in particular. The various fields of research and the different approaches made by different researchers have been presented. It is seen from the discussion that an automated process planning for waste minimization has not yet been fully developed for the Ultrasonic Consolidation process. Published research has concentrated mainly on improving part strength by changing consolidation amplitude, consolidating

frequency and consolidation speed. The possibility of improving the part strength by changing the orientation has not been explored. A research in this direction promises gains in terms of waste reduction, increase of part strength and reduced process time. The next chapter will explore this possibility in detail and formulate the problem.

CHAPTER 3

RESEARCH ISSUES AND FORMULATION

The previous chapter analyzed the existing algorithm for various functional aspects. The discussion identified the dependency of the waste area formed on the translational and rotational parameters δ and θ . It also showed that the build time, which is a function of the NoBs, is directly related to the choice of δ and θ parameters. The chapter further analyzed the assumptions and approximations made in the previous algorithm. It also showed that the approximations made, though they reduced the algorithmic and computational complexity, can not give the actual optimal choice of θ and δ which minimize the waste for a given slice data. The need to consider the behavior of stacked and adjacent foils^[24] was also identified.

This chapter identifies the research issues and goals for this project. A mathematical formulation of the optimization problem is also presented

3.1 Research Issues

The preceding discussion has identified that research efforts should be directed to ascertaining the optimal choices of various optimization parameters so that the solution given by the optimizer is the true optimal for the given problem. Thus, it

can be deduced that continued research effort on the optimization of the Ultrasonic Consolidation process should incorporate the following functionalities.

1. Handle realistic CAD data
2. Handle multiple loops within one slice
3. Handle multiple layer data simultaneously
4. Build crisscross structures
5. Build overlap structures
6. Prevent vertical stacking
7. Reduced computational complexity
8. Reduce build time required
9. Handle non convex data
10. Use existing process capabilities
11. Use previous research efforts
12. Open up new vistas for future research efforts

The following sub functions are also identified which have to be addressed as a prerequisite to the achieving the above mentioned functionalities.

1. Develop efficient file structure
2. Establish global coordinate system for multi layer referencing
3. Establish accurate search bounds
4. Establish optimal optimization algorithm
5. Ascertain need for sampling prior to optimization run
6. Establish optimal sampling method

With the aforesaid desirable capabilities of the new algorithm, the scope and the objective of this project is defined as

‘To develop a generic algorithm which can operate on sliced CAD data and present to the user an optimized orientation for the metal bands which

- *Reduces waste area*
- *Increases part strength and*
- *Reduces processing time*

in the Ultrasonic Consolidation process.’

An initial assessment of the research objective and the optimization problem indicates that the problem can be formalized into a single objective optimization problem with constraints and search bounds. Based on this assumption, a mathematical model for the problem has been developed and is presented in the next section. A validation of this assumption is presented in a subsequent chapter.

3.2 Mathematical Formulation

The mathematical formulation of the optimization problem is stated below. The objective function is minimizing the waste area which is defined as the difference (Figure 1.10(c)) between the total area of the bands required to place the slice (Figure 1.10(b)) and the actual foot print of the slice as shown by the white area contained by the contour in Figure 1.10(a). The constraining equation for building

part strength is also formulated. To increase the part strength, a brick structure or crisscross structure approach is adopted. This is achieved by constraining the search space for subsequent layers based on the optimized configuration of the previous layer

$$\begin{aligned}
& \min \quad \text{waste area} = f(\delta_i, \theta_i) \\
& \quad \delta_i, \theta_i \quad i = 1, \dots, n \\
& \text{subject to } |\delta_i - \delta_{i-1}| \geq 0.1 * \text{bandwidth} \\
& \quad |\theta_i - \theta_{i-1}| \geq 10^\circ \quad i = 2, \dots, n \\
& \quad |\theta_i - 180^\circ - \theta_{i-1}| \geq 10^\circ \\
& \quad 0^\circ \leq \theta_i \leq 360^\circ \\
& \quad 0 \leq \delta_i \leq \text{bandwidth} \\
& \text{where } \text{bandwidth} = 0.9375 \\
& \quad n = \text{number of layers}
\end{aligned}$$

Equation 3.1 Problem Formulation

The objective function is a measure of the waste area formed for each slice. It can be noted from the constraints in Equation 3.1 that the strength of the bond formed is not analytically computed. The constraints are developed based on the assumption that the strength of the part is increased by using the crisscross and brick structure. This assumption is made due to two reasons. First, a complete

mathematical model of the interface physics has not been developed by researchers. This aspect was discussed in Section 2.1.4. Second, using an analytical solver to compute the part strength would not be economically viable due to the prohibitive computational expenses.

The optimization step formulated in Equation 3.1 is executed for each slice of the artifact. Once a slice is optimized for waste, the optimized design variable values are passed to the next optimization cycle as fixed parameters which are then used in the constraints evaluations for subsequent optimization cycles. This ensures the formation of brick structures or crisscross structures by the metal foils. The build time is reduced by reducing the NoBs. This is achieved by penalizing the objective function for every band added to make the artifact. This drives the optimizer to converge to a solution which has a lesser number of bands.

In addition to this direct reduction of build time, an indirect reduction of build time is also effected by the reduction of waste area. This is because any waste area formed has to be milled away by a milling head. So a reduction in the waste area reduces the build time of the artifact indirectly.

3.3 Closure

This chapter identified the research issues that need to be considered for the development of the new algorithm for automation of the Ultrasonic Consolidation process planning step. The chapter also formalized the problem into a constrained

optimization problem. This discussion formed the basis for developing the research procedure which is presented in the next chapter.

CHAPTER 4

RESEARCH PROCEDURE AND STEPS

The discussion in the previous chapter identified the research issues that need to be considered for the development of the new algorithm and formally defined the optimization problem. This chapter describes the development of a logical framework and the steps involved to arrive at the solution of the problem.

The algorithm is intended to work on any valid binary or ASCII STL file. The first step in the process is visualization of the STL data of the part so that the user can choose the build direction. This choice of z direction is not automated since it was considered out of scope and was dealt with by a former student. This research focuses on the waste reduction and increased part strength by altering slice parameters. A marching algorithm implemented in CIDES software is used for the visualization and the slicing of the STL data. The algorithm intersects an imaginary slicing plane with all the facets of the triangles of the STL files and returns the intersection points forming the point cloud which is saved as a PTS file^[25, 78]. The marching algorithm progresses from one triangle to an adjacent triangle of the STL file. This enables the easy extraction of the slice data from the point cloud. The slice data is read from the PTS file by the algorithm developed in MATLAB and is preprocessed for the optimization run.

A gradient based optimizer is used for the optimization. The converged values of the design variables are supplied as fixed parameters for the optimization of the next layer. To form a brick structure or crisscross structure, constraints are built into the optimization loop which restricts the feasible design space. After optimization of each slice, the original and optimized configurations are presented to the user along with the waste savings achieved and the build time. A flowchart representation of the steps for solving the problem is shown in Figure 4.1

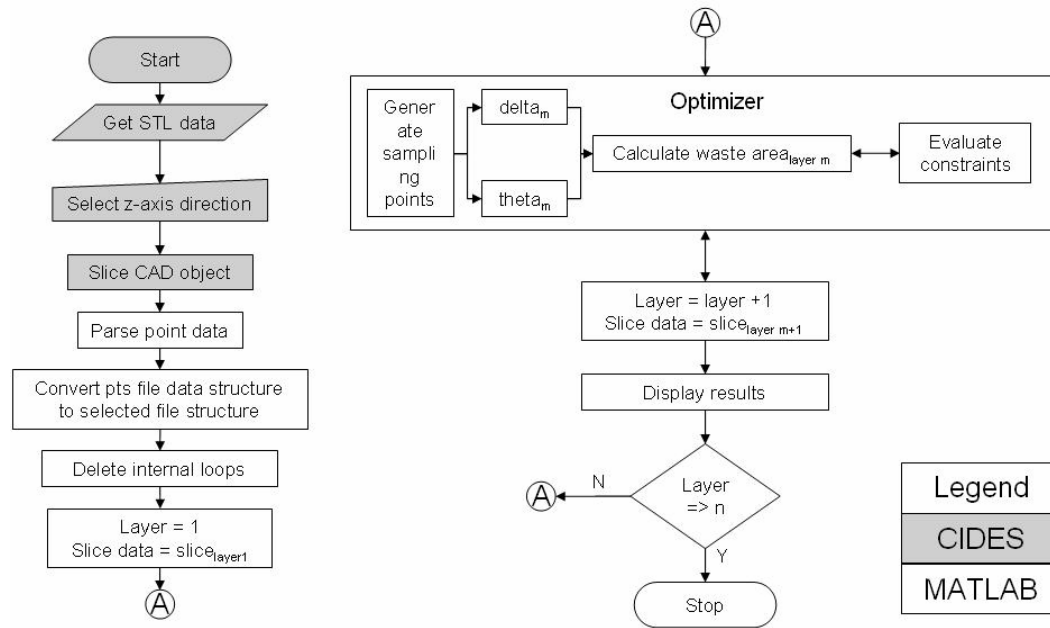


Figure 4.1 Problem solution approach and flowchart

A detailed discussion of the finer aspects of the algorithm is presented next

4.1 Band area calculation

The band area is estimated by computing the intersection points of the slice with the metal band grid. The minimum and maximum intersection points of a band in

the grid gives the length required for that band if the clamping allowance is zero. The clamping length is added to the maximum intersection point and subtracted from the minimum intersection point to get the actual length of band required. The calculation steps involved is listed below

1. The first step in the process is to identify all the intersections that the artifact makes with the band grid. This is shown in Figure 4.2(a).
2. In the second step the maximum and minimum intersection points for each band are identified as shown in Figure 4.2(b).
3. In the third step the maximum and minimum intersection points calculated in the previous step are compared to the contour end points to determine the minimum band length required. This is shown in Figure 4.2(c).
4. From the points calculated in step three, an envelope is formed which represents the minimum band area required for the slice to be placed. It should be noted that the area enclosed by the envelope is the band area required if the clamping allowance is zero (Figure 4.2(d)).
5. The clamping allowance is added to the maximum and minimum points to get the actual band length required to form the part slice as shown in Figure 4.2(e).
6. Band area is calculated as the product of the total band length required and the band width. Figure 4.2(f) shows the final band area required for building the part slice.

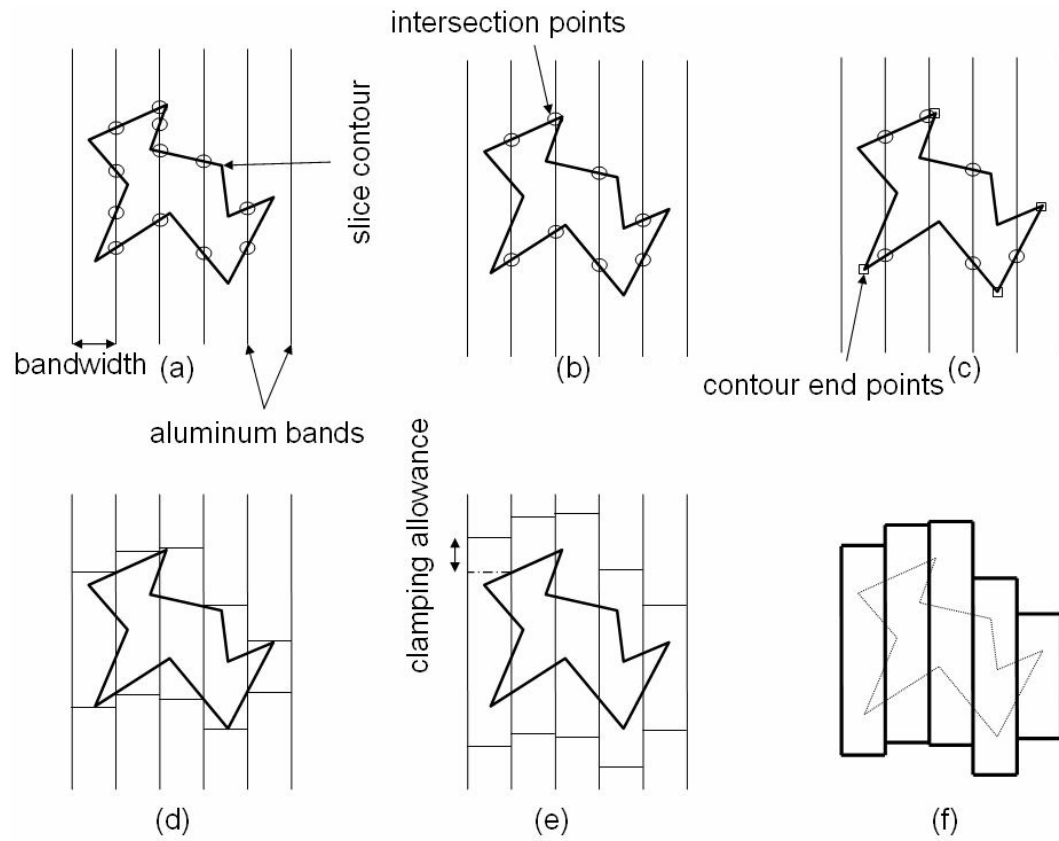


Figure 4.2 Calculation of band area required

The area enclosed by the contours in the slice (Figure 4.3(b)) is subtracted from the required band area (Figure 4.3(a) or Figure 4.2(f)) to calculate the waste area (Figure 4.3(c))

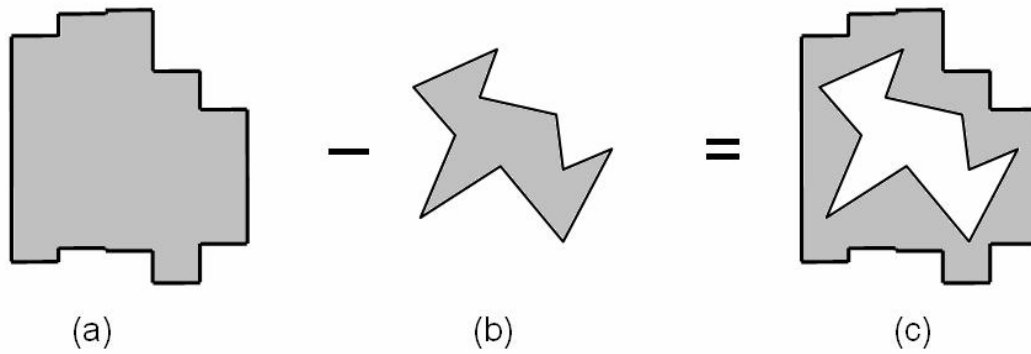


Figure 4.3 Calculation of waste area

4.2 Ability to handle multiple loops in the same slice

The earlier implementation of the algorithm approximates multiple loop data into a single loop. However this has a detrimental effect on the waste area formed since metal bands might be placed between loops where material is not actually needed for building the artifact. This condition was demonstrated in Section 2.4.1.

Rapid manufacturing can be employed for building of complex geometry also. An example of the typical complexity is shown in Figure 4.4.



Figure 4.4 Brain Gear

The figure shows a brain gear whose slices are shown in Figure 4.5. It is seen that multiple loops are found within the slice.

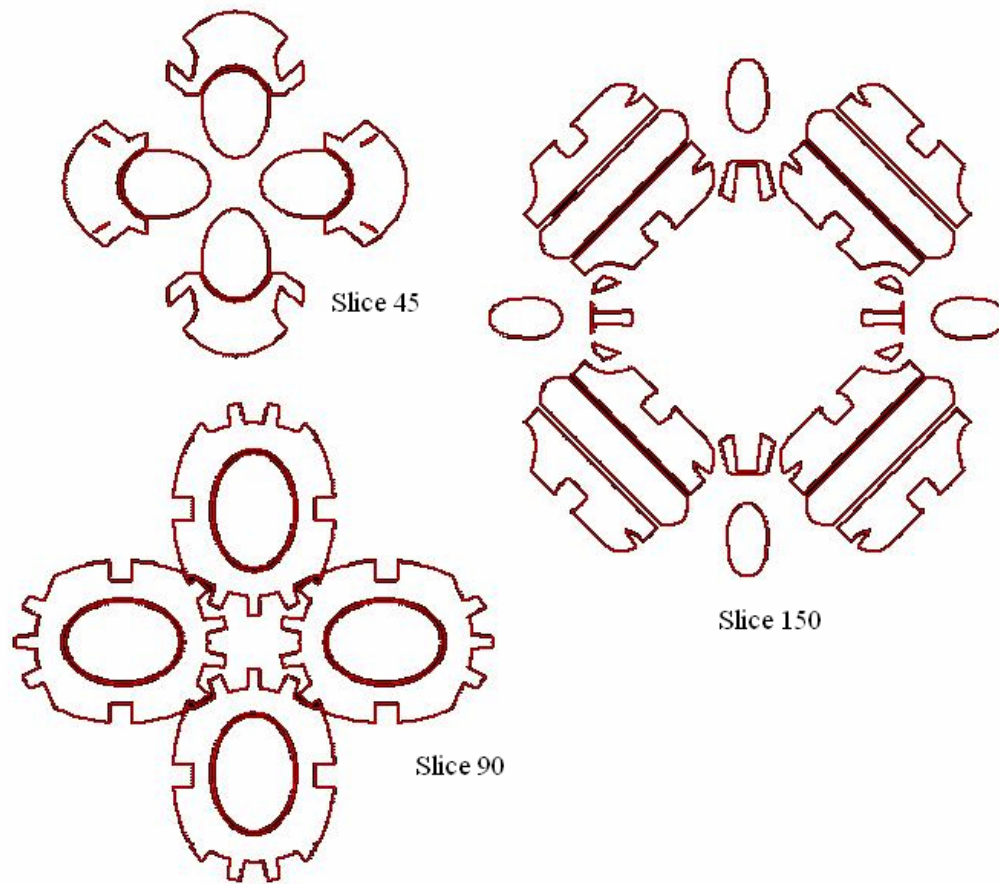


Figure 4.5 Brain gear slices

A comparison of the existing and proposed algorithm is shown in Figure 4.6. It is noted that, in spite of giving the same input to both the algorithms, the output of the algorithm vary. As is seen from Figure 4.6(a) the input data was approximated to a single loop by the former algorithm. However, the algorithm developed in this work is designed to retain the original data as received from the slicing module - CIDES as shown in Figure 4.6(b).

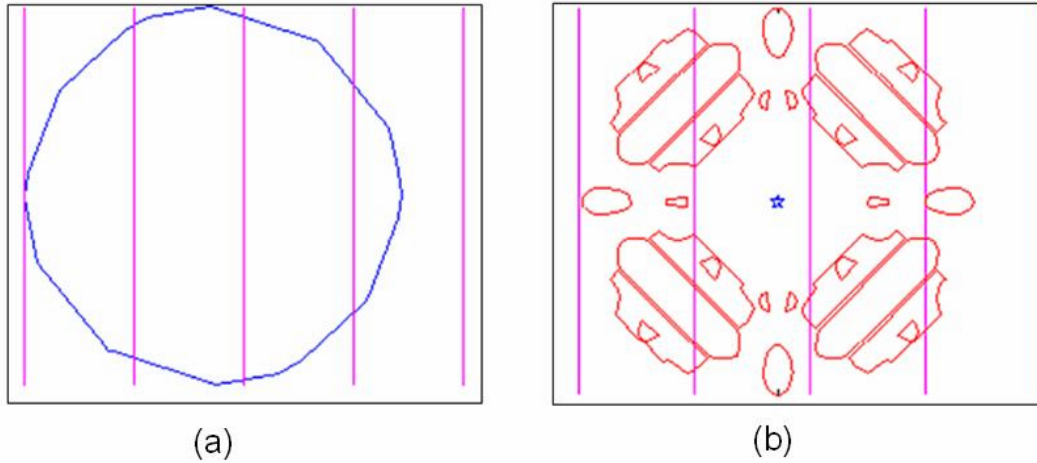


Figure 4.6 Ability to handle multiple loops

4.3 Ability to handle non convex objects

The new algorithm is developed with the ability to handle non convex objects also. The earlier algorithm approximated the point cloud to the convex hull, adding pseudo material areas as shown in Figure 4.7(a) that needs to be machined away in the subsequent milling step, which increases waste formed as well as build time. Figure 4.7(b) shows the data handling capability of the new algorithm which retains all the information of the part to be manufactured

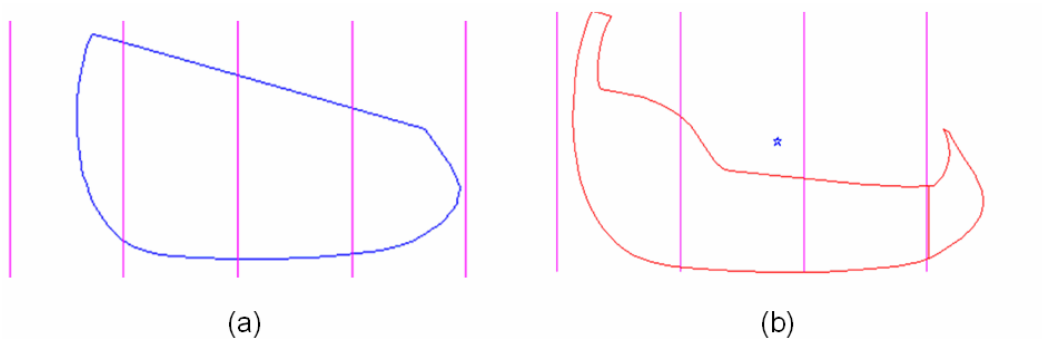


Figure 4.7 Ability to handle non convex objects

4.4 Constraint handling

The strength of the part is dependent on the overlap of bands of subsequent layers. If the optimizer converges to the same δ and θ values for consecutive layers the part strength is affected. To circumvent this problem, constraints are introduced on the search space which ensures that the final part has a crisscross and brick structure. Figure 4.8(a) shows an example in which the earlier algorithm converged to the same design variable values causing a vertical stack up, reducing the part strength. However, the proposed algorithm has capabilities to prevent the stack up by limiting the search space to bounds that ensures crisscross structure or brick structure. In Figure 4.8(b) below, the output of a constrained algorithm is shown. It is seen that the optimal δ and θ values for consecutive layers are different. The degree to which the consecutive layer optimal parameter values vary can be controlled by the changing the constraining equation.

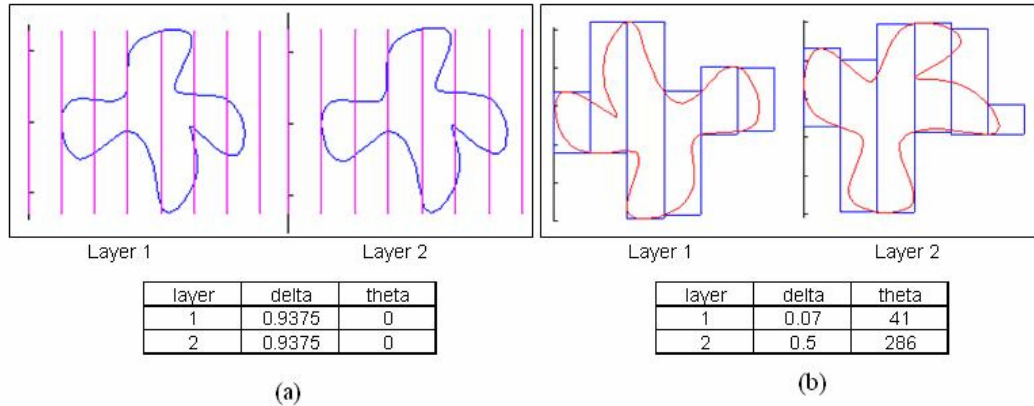


Figure 4.8 Optimization for part strength

Figure 4.9 and Figure 4.11 shows the pictorial representation of the constraints built into the optimization problem.

4.4.1 Angular Constraint

To achieve a crisscross structure of the aluminum bands, the angular constraints as shown in Equation 4.1 are employed.

$$\begin{cases} |\theta_i - \theta_{i-1}| \geq 10^\circ & i = 2..n \\ |\theta_i - 180 - \theta_{i-1}| \geq 10^\circ \end{cases}$$

Equation 4.1 Angular Constraints

The angular constraints ensure that no two consecutive layers converge to θ values which are within a specified angle to each other. Figure 4.9 shows the infeasible θ values for layer_{n+1} when the optimal value of θ for layer_n is given. In this example a deviation angle of 10° is used.

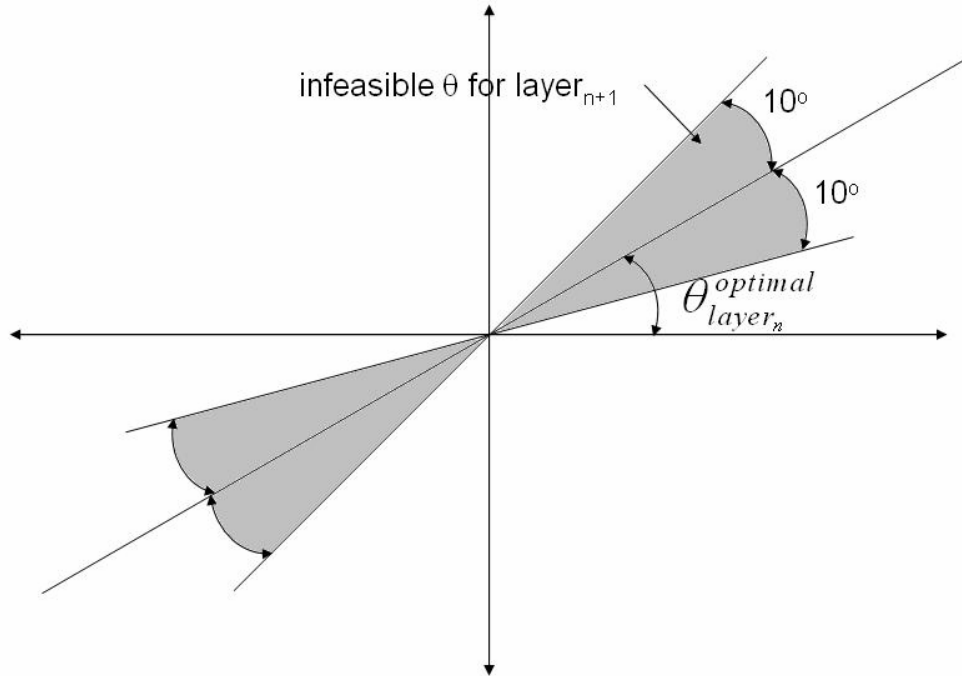


Figure 4.9 Angle constraint

The aforesaid implementation of the constraining function results in the formation of a crisscross structure of aluminum bands as shown in Figure 4.10

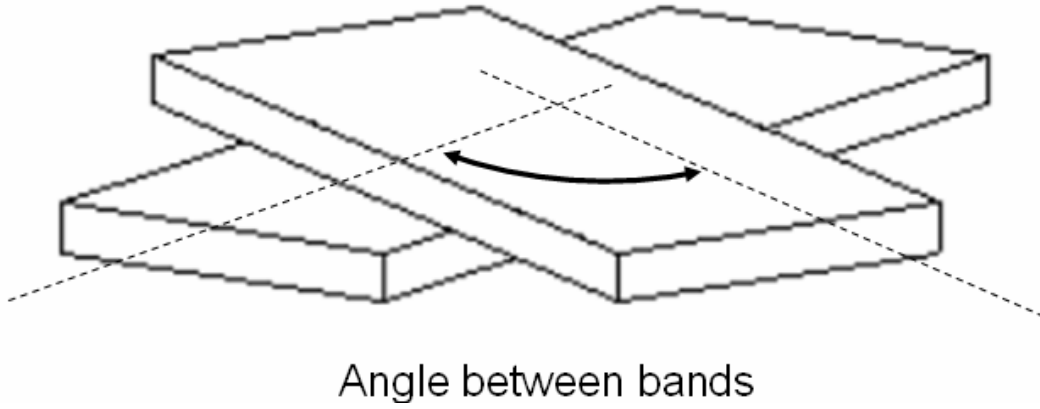


Figure 4.10 Aluminum bands in crisscross structure^[22]

4.4.2 Translational Constraint

The second aspect of building in strength by varying layout is forming a brick layout with the aluminum foils. To form the brick layout, the constraining equation added is shown in shown in Equation 4.2

$$\left| \delta_i - \delta_{i-1} \right| \geq 0.1 * \text{bandwidth}$$

Equation 4.2 Translation Constraint

The translational constraint ensures that two consecutive layers converge to δ values which are within a specified overlap percentage of each other. Figure 4.11 shows the infeasible δ values for layer_{n+1} when the optimal value of δ for layer_n is given. In this example an overlap percentage of 10 % is used.

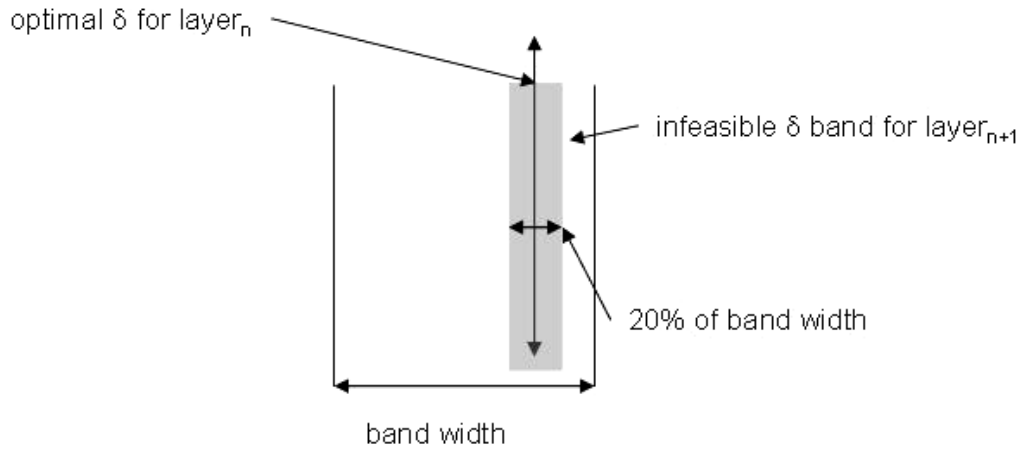


Figure 4.11 Translation constraint

The aforesaid implementation of the constraining function results in the formation of a brick structure of aluminum bands as shown in Figure 4.12

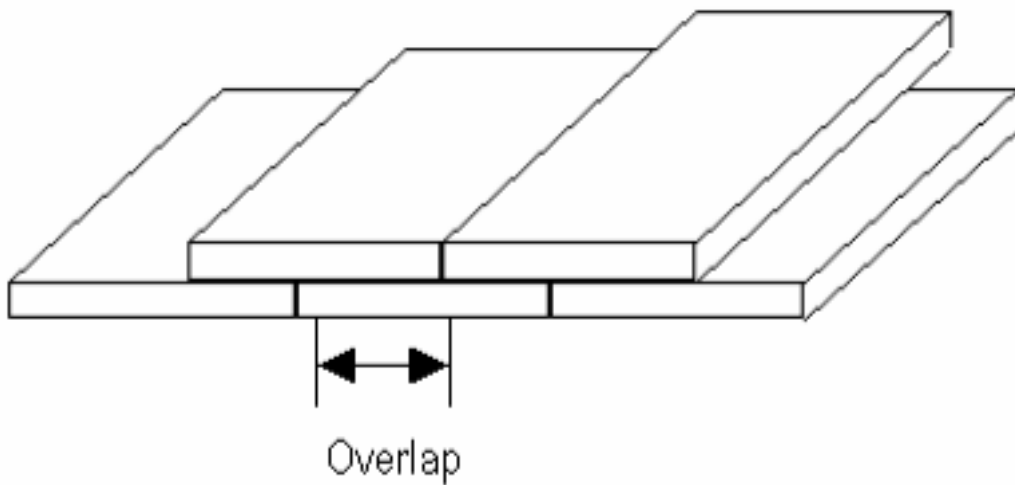


Figure 4.12 Aluminum foils in brick structure^[22]

4.5 Reduced computational complexity

For any optimization problem, the most important factor affecting the performance of the algorithm is the time taken for a single function evaluation.

This is due to the fact that the objective function evaluator is called many times for a single iteration and, based on the complexity of the optimization problem, the number of iterations required for convergence also increases^[79]. Furthermore, since the optimization is done for each slice of the part, the total time required to complete the total optimization will be high. Rigorous code optimization was done to minimize the time taken for the function evaluation. Two such modifications are discussed below.

4.5.1 Intersection calculation

The core of the algorithm is the calculation of the intersection points of the contour with the band grid as explained in Section 4.1. Most of the line intersection algorithms parametrically represent the line connecting two points, and find the intersection point using matrix methods (Figure 4.13(a)). However matrix manipulation including finding inverse of a matrix is computationally expensive and substantially reduces the performance of the algorithm. Other line intersection algorithms use information of direction of lines, the order of lines, or dot product methods. The reader may refer to literature available for an extensive list of line intersection algorithms available^[80-84].

These algorithms had been developed for the general case of any two lines intersecting. However, in the current problem, one set of lines were always vertical. This facilitates the development of different methods for the calculation of the intersection points. For the purpose of reducing the computational cost of

calculating the intersection points the algorithm was modified. The modified algorithm considered a pair of points to be the end points of a right triangle such that the band grid divides the triangle into similar triangles as shown in Figure 4.13(b). After this modification is done, the intersecting points are calculated by principle of symmetric triangles as given in Equation 4.3.

$$y = y_1 + \frac{x_3 - x_1}{x_2 - x_1} y_2$$

Equation 4.3 Calculation of intersection point

However it can be noted from Equation 4.3 that the equality degenerates when $x_2 = x_1$ which makes the denominator zero. This situation arises when the contour line is parallel to the band grid. However, if the contour line is parallel to the band grid, there will be no intersections between the contour line and the band grid. By comparing the value of x_2 and x_1 , this condition is detected and the algorithm skips to the next pair of points.

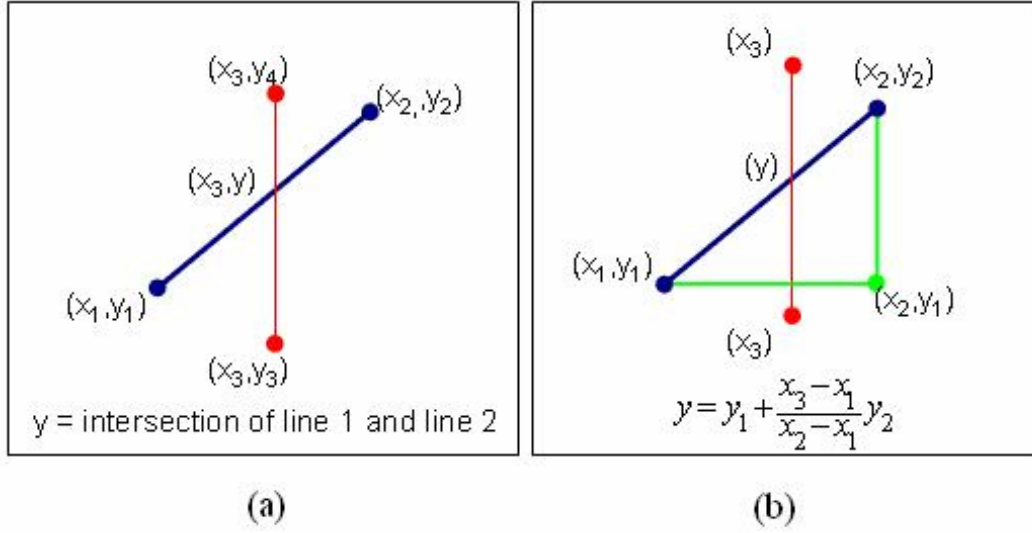


Figure 4.13 Modified intersection point calculation

4.5.2 Elimination of internal loops

As explained in section 4.1, the waste area is determined by the maximum and minimum intersection points with the band. The intersections made by the internal loops with the band grid do not contribute to the calculation of waste area. This motivates the elimination of internal loops. As explained in Section 4.5.1, the core of the algorithm is the calculation of the intersection of the contour lines with the band grid. By eliminating the internal loops, the number of intersection calculations goes down drastically. This reduces the time taken by the optimizer for convergence since the objective function evaluator has to parse through a lesser number of point pairs. The following figure shows the representation of the point cloud before (Figure 4.14(a)) and after (Figure 4.14(b)) the internal loop elimination routine.

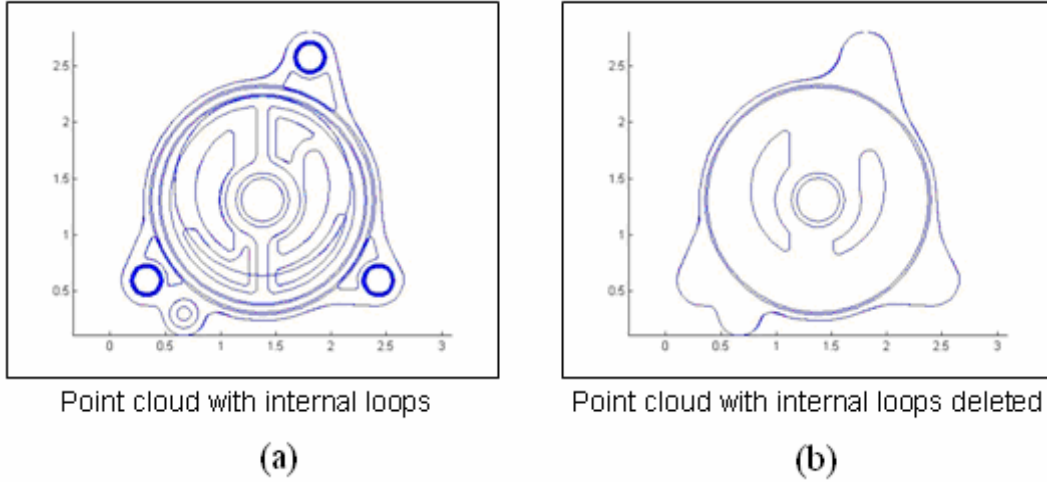


Figure 4.14 Modified algorithm for eliminating internal loops

The elimination of internal loops is achieved in multiple steps. The first step in the process is the formation of closed contours from the point cloud so that they form a loop which can be checked whether it is contained within another loop (Figure 4.15(a, b)). Once a closed contour is formed, the individual points that form the contour points are checked to see whether they within or outside a second loop formed by another set of contour points. Once the points lying within the second loop are identified, they are compared with the parent set of points to see whether all the points are enclosed by the second loop. If some of the points are inside the loop and some are outside, the loop is retained for further processing (Figure 4.15(c)). If it is found that all the points are within the second loop, the points are flagged for deletion (Figure 4.15(d)). The deletion is done only after the pair wise checking is completed for all the loops in the slice (Figure 4.15(e)). This is done to ensure data integrity even after point deletion.

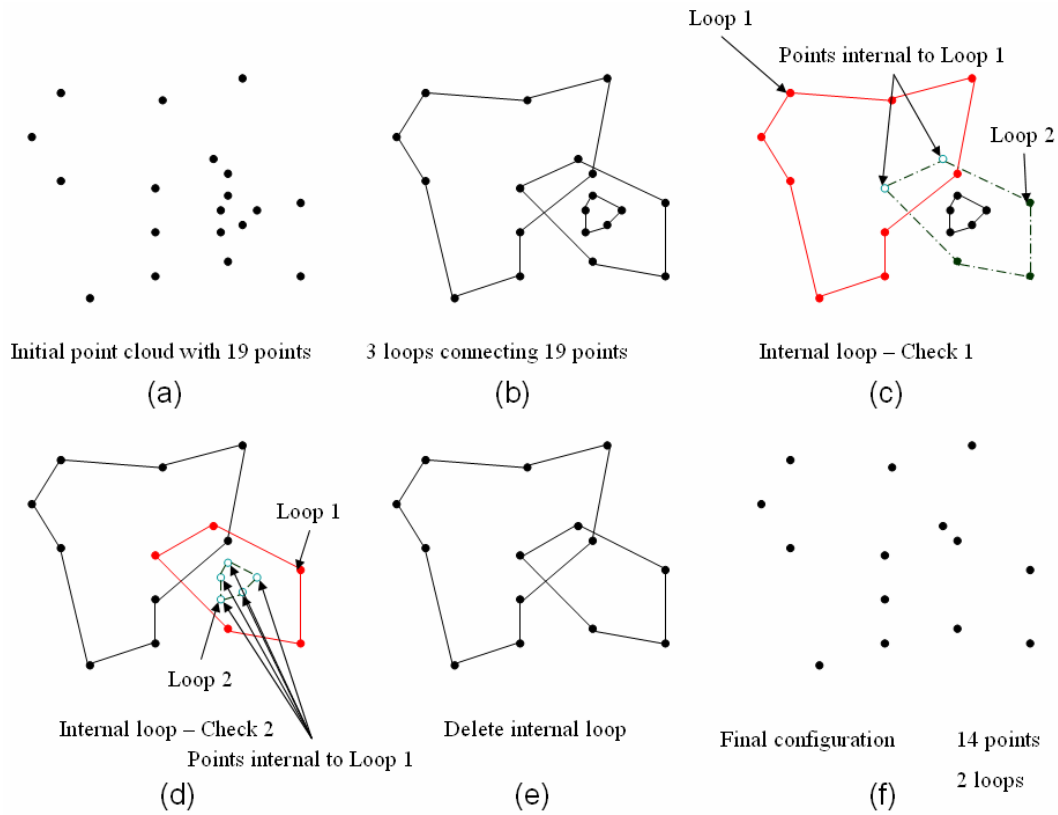


Figure 4.15 Elimination of internal loops

It can be seen in comparison (Figure 4.15(a, f)) that after this preprocessing the complexity of the input data reduces considerably. In the example shown it is seen that the number of points is reduced from 19 to 14 and the number of loops reduced from three to two.

4.6 Ability to Reduce Build Time Required

It was illustrated in Section 1.1.5.3 that the build time of the Ultrasonic Consolidation process is directly related to the NoBs required for placing a slice. NoBs also affect the strength of the part. A higher number of bands would

decrease the part strength and increase the build time. The proposed algorithm ensures a reduction of NoBs to reduce build time and improve part strength.

Figure 4.16(a&b) shows two artifacts that are used for comparison of the previous algorithm and the newly implemented algorithm. Figure 4.16(c&e) represent the optimal layout achieved by the existing algorithm. It is to be noted here that the clamping allowance was considered as fixed and not used in the calculation of waste area in the previous algorithm^[22, 85]. This drives the optimizer to a more ‘horizontal’ layout as shown in figure.

However, in the proposed algorithm, the clamping allowance is considered for calculation of waste area. Due to the addition of wasted band length of two times the clamping allowance for every band laid, the solution gets penalized heavily for every extra band it lays. This drives the optimizer to converge to a more ‘vertical’ layout of the slice as shown in Figure 4.16(d&f). Depending on the shape of the artifact being placed, the change of layout from horizontal to vertical reduces the NoB. This is seen from comparing the NoBs required for placing the slices for the example artifacts. There was reduction of 44% in the first example and 83% in the second example. However, this value can be as low as 0% depending on the shape of the artifact. Such a condition will arise when shape is more round than long as is the case of the examples shown.

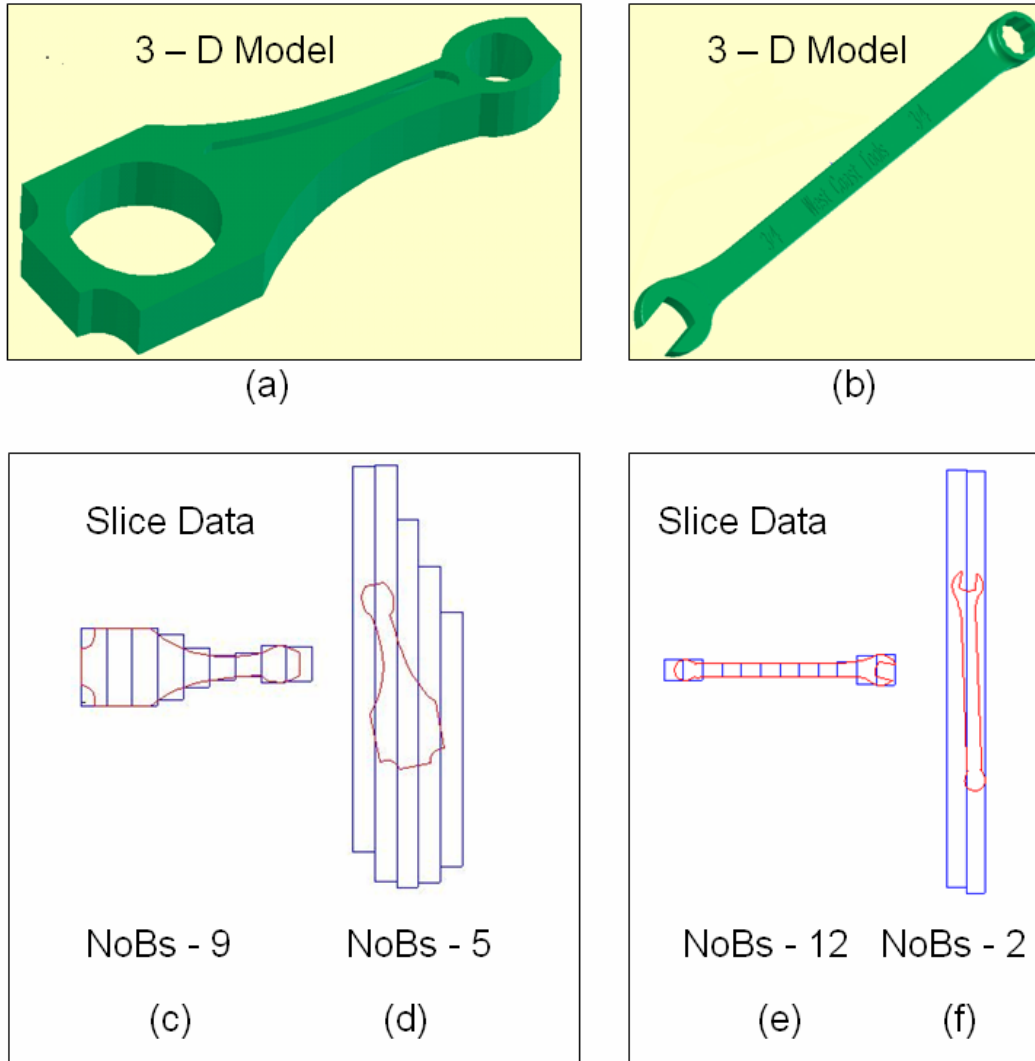


Figure 4.16 NoB Reduction

4.7 Modified File Structure for Efficient Processing

A major issue that needs to be addressed is the data handling capability and the file structure employed by the algorithm for internal calculations. Since the former algorithm dealt with only one loop per slice, the file structure used did not have provision to differentiate between multiple loops within the same slice.

However, since the proposed algorithm needs the capability of handling multiple loops within the same slice as explained in Section 4.2, a new file structure needs to be developed to accommodate the improved functionality.

The existing algorithm was developed in MATLAB and employed an all numerical file structure as shown in Figure 4.17(b). Figure 4.17(a) shows the file structure of the output file generated by CIDES software. The z-axis value is extracted from the output file and stored in the 3rd column of the internal file structure, while the individual x-y coordinate values are stored as the 1st and the 2nd columns. Slices are differentiated from each other using a keyword native to MATLAB, ‘NaN’, which is recognized as a special numerical character. Since all the data is represented as numbers, the entire data can be represented in a numerical matrix.

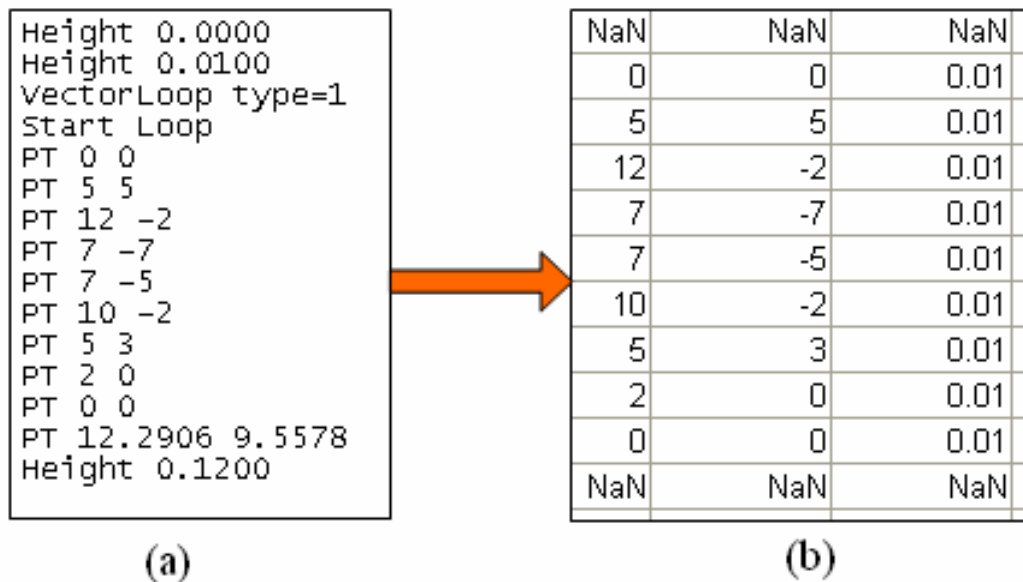


Figure 4.17 Existing File Structure

Various trials were conducted to develop a practical file structure for the new algorithm. Since the existing algorithm had an efficient file structure which enabled fast portability of data between subroutines, it was decided to improve on the existing file structure. The additional information that was required for the new algorithm was loop identifiers. It is proposed to use the keyword 'Inf' to differentiate slice data and 'NaN' to differentiate loop data. This ensures the easy portability of the existing algorithm to the new implementation. It also ensures that the numerical matrix format used by the earlier algorithm is retained which reduces the access time for extracting values from the matrix as and when required.

Figure 4.18 shows an example of the proposed file structure. As is seen, the slices are differentiated from each other by 'Inf' and each loop within the same slice are separated from each other by 'NaN'. It is seen from the internal file structure shown in Figure 4.18 that the 3rd column which represents the height of the slice is repeated for every coordinate point. Since the z-coordinate value does not contribute to the optimization calculation, the 3rd column is deleted which further reduces the data to an Nx2 matrix. The z-coordinate values are reintroduced into the matrix to expand the same into an Nx3 matrix after the optimization run.

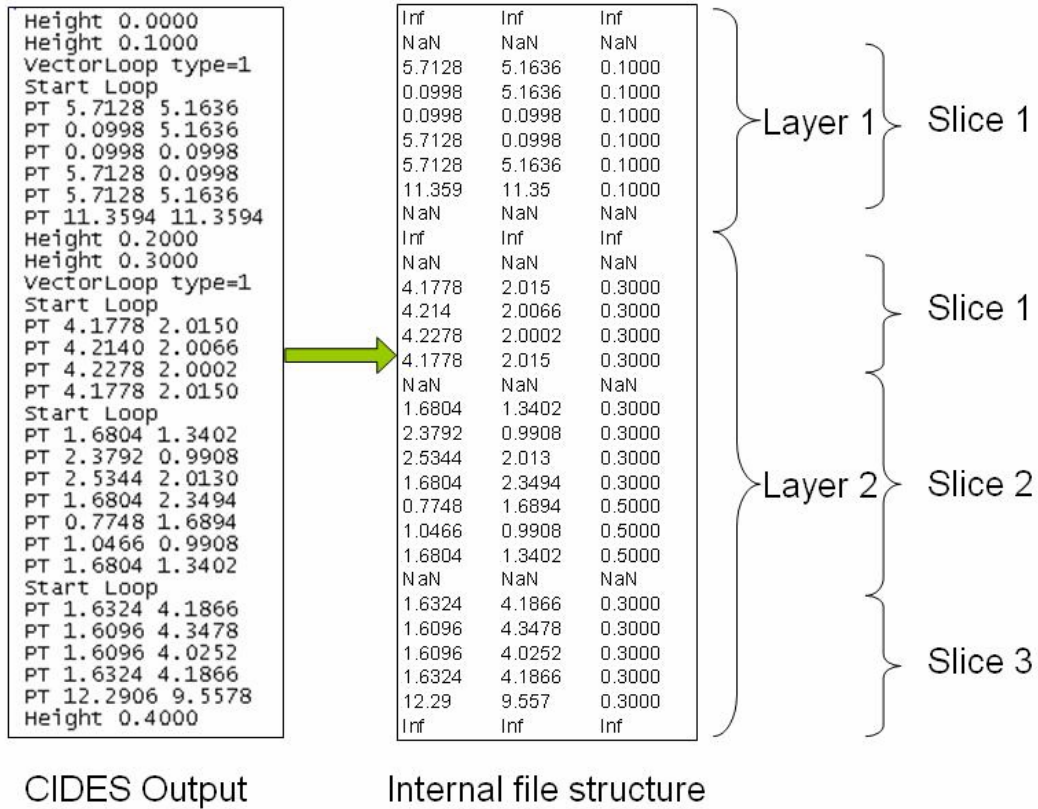


Figure 4.18 Proposed File Structure

4.8 Global Coordinate System

In Section 4.4 the need for constraint handling and its advantages were discussed. However for efficient implementation of the constraint handler, the referencing system used for extracting data from different slices had to be revisited and redesigned. The former implementation of the algorithm specified a coordinate system for the bands based on the slice data. In the earlier implementation, the centroid of the slice was identified and aligned with the origin of the slice coordinate system. After this, the furthest point of the slice from the centroid was aligned with the x-axis of the coordinate system. The angle of rotation required to

achieve this was applied to all the contour points of the slice so that the entire slice was rotated about the centroid. The extreme point of the slice from the centroid formed the origin of the band grid coordinate system. This is shown in Figure 4.19(a-c). However, this creates unique coordinates systems for each slice being built. Due to this issue, the ‘structural integrity’ of the part is affected and additional calculations have to be done to recreate the artifact. This creates problems when referencing across slices as shown in Figure 4.19(c).

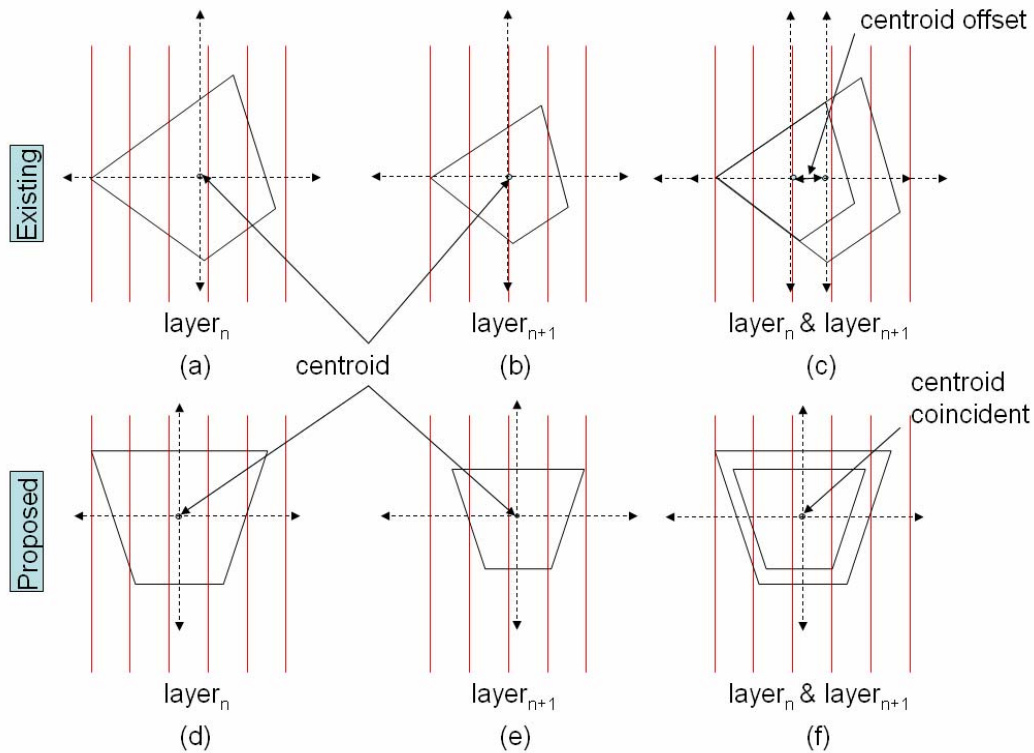


Figure 4.19 Global Coordinate System

In the newly implemented algorithm, a global coordinate system with origin at the geometrical centre of the work table is used to reference all slices and all band grids. This is shown in Figure 4.19(d-f). The midpoint of each slice is calculated

and aligned with the global coordinate system. The band grid is already placed on the global coordinate system and no referencing is needed to the slice data. This ensures that the slices are built maintaining the ‘structural integrity’.

4.9 Search Bounds

A major factor which affects the output of the algorithm is the search bound used for the optimization algorithm. It can be deduced from the description of the problem that, the waste area repeats itself for every translation step above the band width and every angle above 360° . However, the problem needs to be studied thoroughly for this assumption to be validated.

4.9.1 Slice data with no axis of symmetry

Figure 4.20(a) shows a slice data geometry with no axis of symmetry. Figure 4.20(b) shows the distribution of waste area as a function of θ when θ is varied in the range $[0^\circ - 360^\circ]$. A probe of the graph reveals the waste at $\theta = 62^\circ$ and $\theta = 242^\circ (180 + 62)$ have the same value of 662.3 sq. units as shown in the figure. It is noted that the waste area is symmetrical about the 180° , after which it gets repeated. This experiment invalidates the initial assumption of $[0^\circ - 360^\circ]$ as the search bound limits.

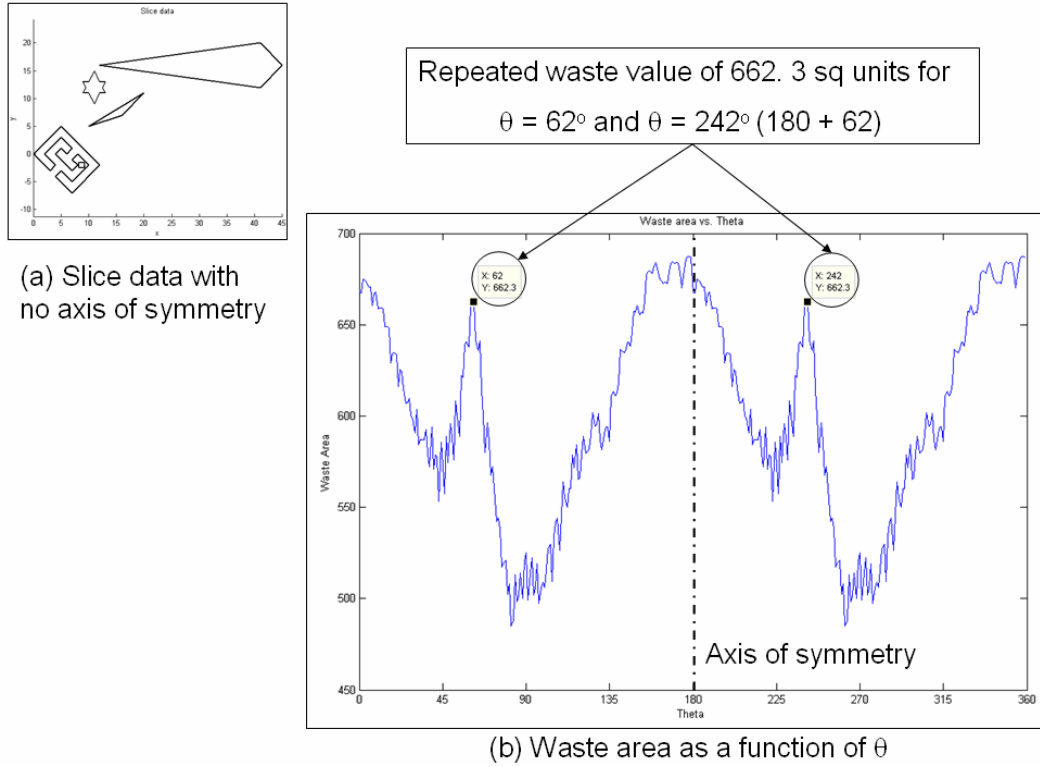
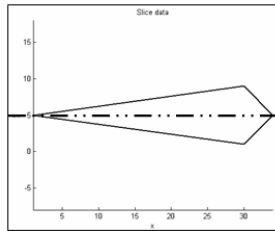


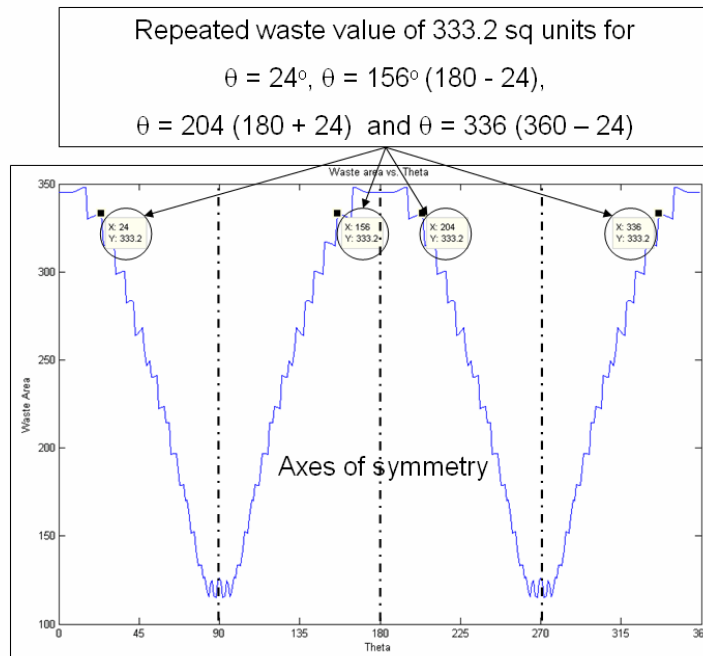
Figure 4.20 Validation of search bounds

4.9.2 Slice data with Multiple axes of symmetry

The previous experiment is further extended by using slice data which has one axis of symmetry as shown in Figure 4.21(a). It is seen from the plot of waste area vs. θ (Figure 4.21(b)), that there are three axes of symmetry, as shown by the dotted lines. This divides the search space into four similar subspaces which reduces the search bounds to $[0^\circ - 90^\circ]$. In another experiment, slice data with four axes of symmetry is chosen for ascertaining the search bounds (Figure 4.22(a)). It is seen from Figure 4.22(b) that the waste area plot as a function of θ is divided into eight subsections which reduces the search bounds to $[0^\circ - 45^\circ]$.

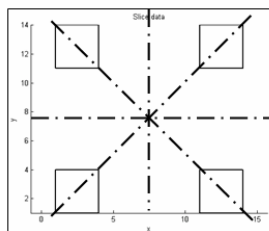


(a) Slice data with one axis of symmetry

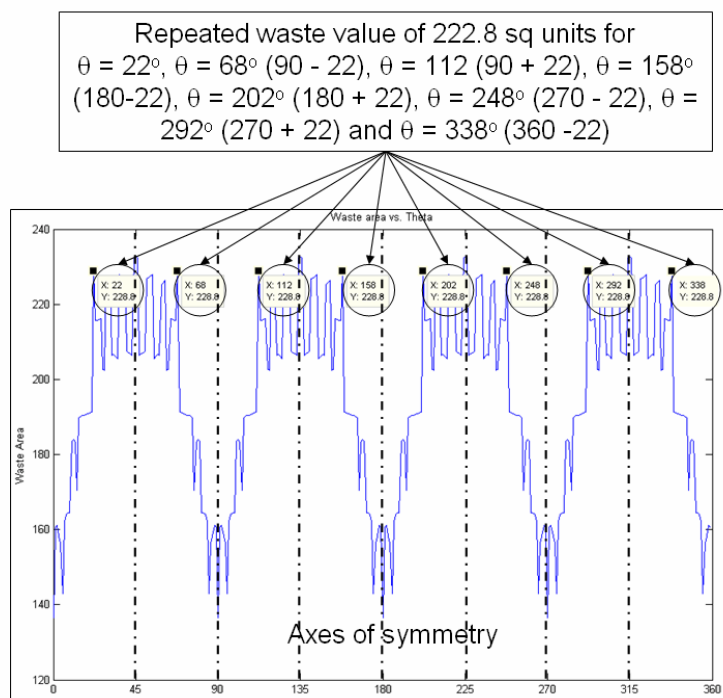


(b) Waste area as a function of θ

Figure 4.21 Waste area for slice data with multiple axes of symmetry



(a) Slice data with multiple axes of symmetry



(b) Waste area as a function of θ

Figure 4.22 Waste area for slice data with one axis of symmetry

It can be concluded from these results that the search bound for this optimization problem is $[0^\circ - 180^\circ]$ for general slice geometry. If the symmetry conditions of the slice geometry are known beforehand, the search bounds can be reduced to $[0^\circ - 90^\circ]$ or $[0^\circ - 45^\circ]$ as the case maybe.

4.10 Closure

This chapter has discussed the various research issues that were identified in Section 3.1. The steps involved in the resolution of the research issues were discussed in detail including the procedure followed. It was seen from Section 4.9 that the search bound that is to be used for the optimization problem can be reduced from $[0^\circ - 360^\circ]$ to $[0^\circ - 180^\circ]$ for any general shape. It was also identified that, depending on the symmetry of the slice data, the search bounds can be reduced to $[0^\circ - 45^\circ]$ or even less. Based on this new learning the problem formulation is restated as shown in Equation 4.4.

$$\begin{aligned}
& \min \quad \text{waste area} = f(\delta_i, \theta_i) \\
& \quad \delta_i, \theta_i \quad i=1, \dots, n \\
& \text{subject to} \quad |\delta_i - \delta_{i-1}| \geq 0.1 * \text{bandwidth} \\
& \quad |\theta_i - \theta_{i-1}| \geq 10^\circ \quad i=2, \dots, n \\
& \quad 0^\circ \leq \theta_i \leq 180^\circ \\
& \quad 0 \leq \delta_i \leq \text{bandwidth} \\
& \text{where bandwidth} = 0.9375 \\
& \quad n = \text{number of layers}
\end{aligned}$$

Equation 4.4 Modified Problem formulation

It is noted that, in addition to the reduction of search bound for one variable, i.e. θ , the number of constraints has also been reduced to one. This is because the algorithm no longer has to deal with angles above 180° which make the alignment anti-parallel resulting in reduced part strength.

In the next chapter the implementation and the results obtained from the aforementioned algorithm are presented and discussed.

CHAPTER 5

IMPLEMENTATION

In the previous chapter the various facets of problem and the different steps involved in the solution process were discussed in detail. In the current chapter the implementation of the previously discussed algorithm will be presented.

5.1 Program Architecture

As discussed in Section 2.4 and shown in Figure 4.1, the whole problem has been modularized into two parts. Part one involves the selection of the build direction and the slicing of the artifact. The first part was implemented in the CIDES algorithm. The program was modified to generate the PTS file which contained the x-y coordinates of the point cloud of individual slices^[22]. The second part involves the identification of the optimal layout and orientation of the aluminum foils for the individual slices of the artifact for minimizing the waste formed. The optimization sub problem was solved using the MATLAB implementation of the algorithm. The program architecture of the optimization algorithm is shown in Figure 5.1.

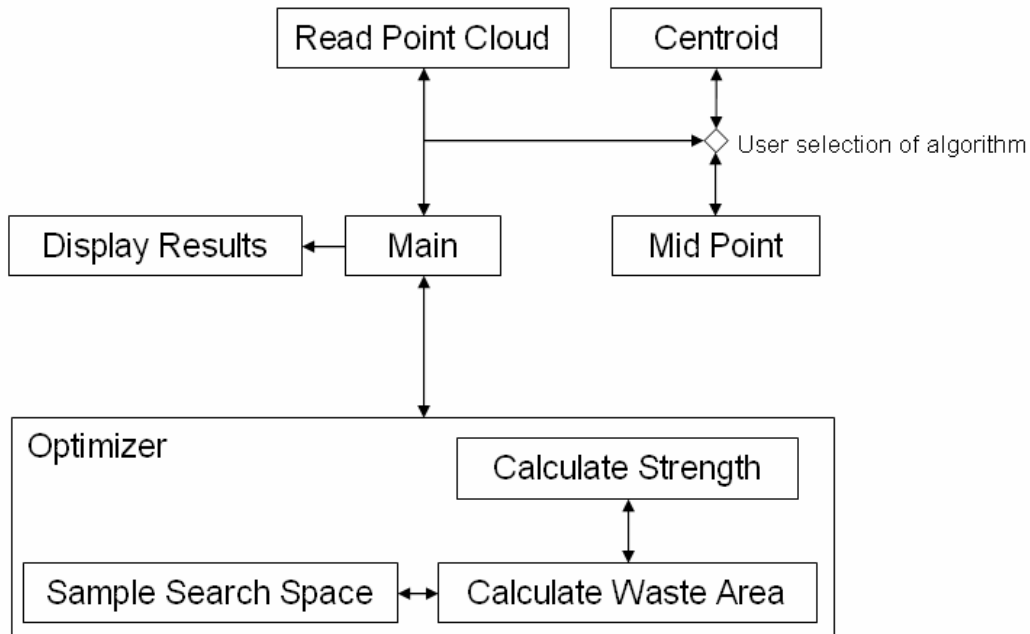


Figure 5.1 Program Architecture

As is seen from the figure, the program had seven sub programs which deals with the various aspects of the problem. The ‘main’ program calls a subprogram which reads in the point cloud and preprocesses it before the data is fed further down the program. The preprocessing is done based on the selection made by the user on the method to be used for positioning the artifact on the work table viz. centroid method or midpoint method. The preprocessed data is transferred for the optimizer which calculates an optimal choice for θ and δ values based on the waste area formed and the part strength calculated empirically. These optimized θ and δ values are used to generate the final display of the optimized layout in comparison with original layout. This data is also used for calculating the percentage reduction in waste area and build time.

A discussion of the sub programs used for the solution of the problem is discussed next. Flowcharts of the major sub programs are also presented.

5.2 Preprocessor

The preprocessor sub function takes care of the issue identified in Section 4.5.2, namely the elimination of internal loops. It also converts the ASCII input file data into matrix data format for easy processing. The sub function parses the ASCII file and encloses the slice data within ‘Infs’ and loop data within ‘NaNs’ as discussed in Section 4.7. Once the data is converted to native MATLAB format the complexity of the input data is reduced by elimination of internal loops.

A pair of loops is identified and a check is initiated to establish whether Loop 1 encloses Loop 2 completely or not. If the condition evaluates to be true all the points in that loop is flagged for subsequent deletion. A third loop is identified and the same check is initiated with Loop 1. The algorithm has a complexity of $\Theta(N^2)$. Once a pair wise comparison of all the loops is completed, the earlier identified loops are deleted. Figure 5.2 shows this process in a flowchart representation. After the deletion of the internal loops the matrix is transferred back to the main function for further processing.

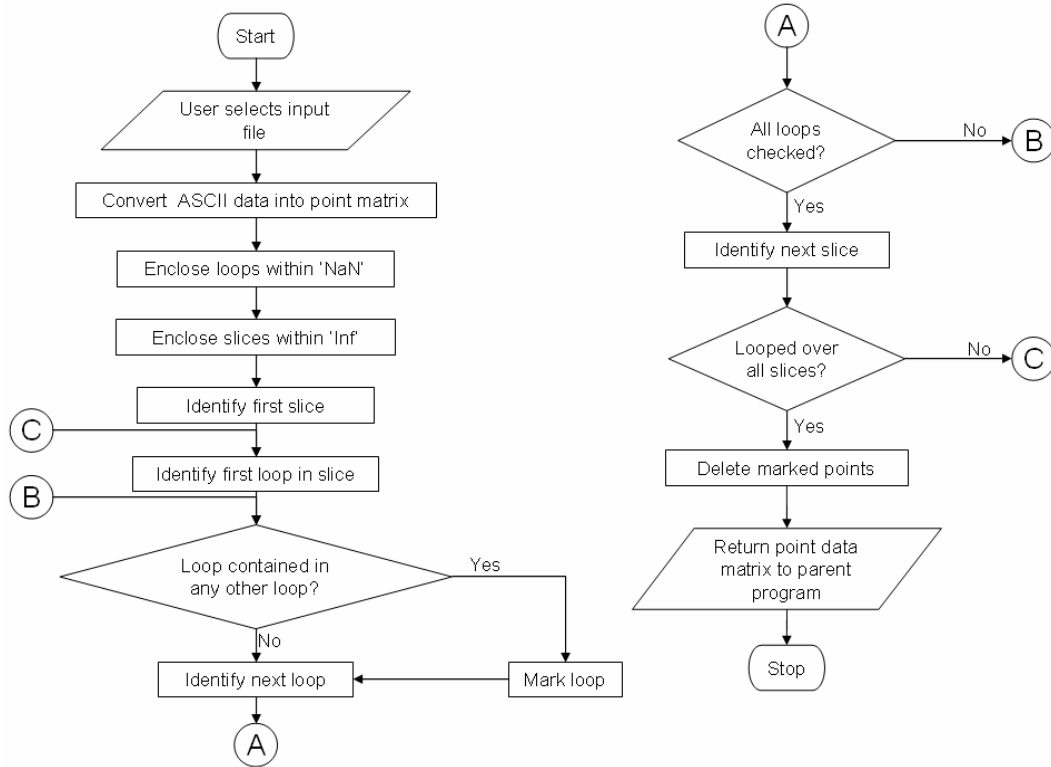


Figure 5.2 Preprocessor flowchart

5.3 Objective Function

The objective function evaluator contains the waste area calculation sub routine. The program starts by accepting the values of δ and θ from the parent program. The slice area is also transferred into this sub routine. Based on the θ values the slice data is rotated about the centroid or the midpoint of the artifact slice data. After the rotation the slice data is translated by the δ parameter. This gives the final orientation and layout of the artifact for that optimization step. Based on the orientation of the slice data, the table grid is reduced to band grid which contains just enough number of bands to cover the entire slice data.

After the placement of the slice data on the band grid, the algorithm parses through the point data in pairs so that it covers all the contour lines of the slice data. For every pair of point selected, a line is formed connecting the two points. This line is checked for possible intersection with the band grid and the intersection points are saved in a matrix. The algorithm moves to the next pair of points till it completes the all data points in the given slice. After collecting all the intersections made by the contour lines with the band grid, the algorithm parses all the intersection points stored for each of the band in the band grid. The maximum and the minimum intersection point for each band are saved. These saved points are compared with the maximum and the minimum contour points of each slice and the maximum and the minimum in this comparison is saved for the calculation of the band area. The clamping allowance is added to the maximum abscissa value and subtracted from the minimum abscissa value to get the final band length required. This process is repeated for every band of the band grid and added to the band length. The final band length is multiplied by the band width to get the band area. The slice area which was passed from the parent program is subtracted from the calculated band area to get the waste area which is passed back to the calling function. The entire process is pictorially represented in Figure 5.3.

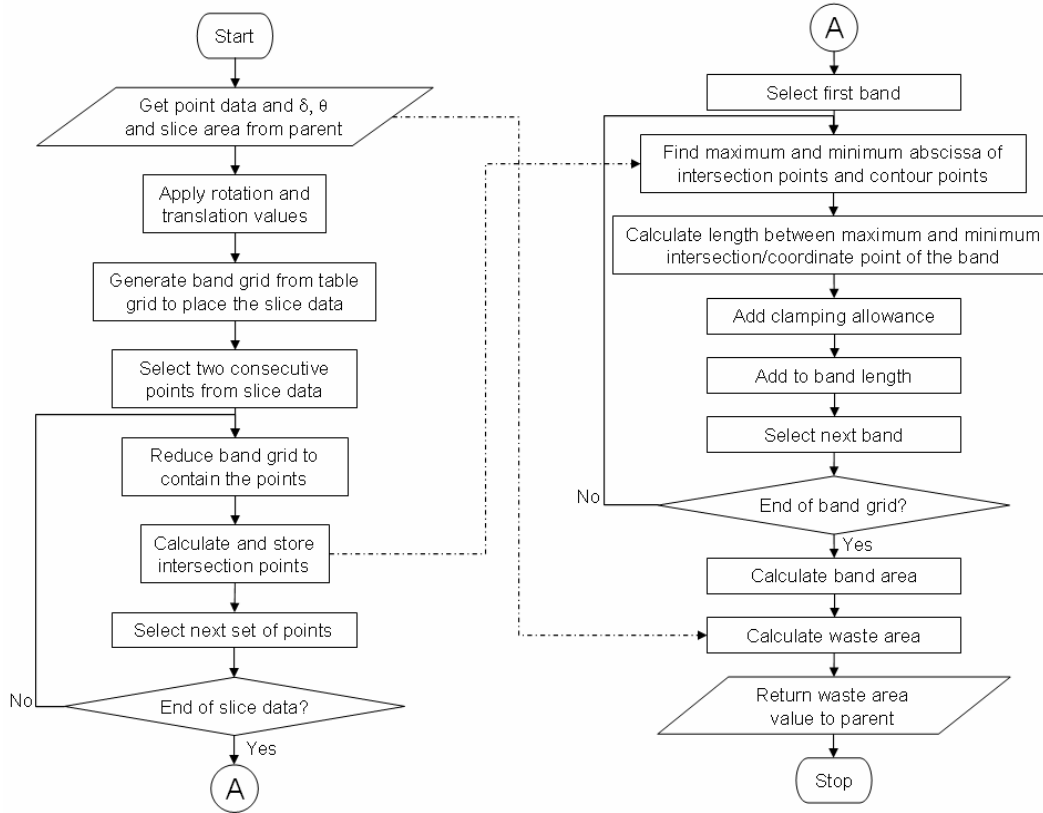


Figure 5.3 Objective function flowchart

5.4 Constraint Evaluator

The constraint evaluator function contains the implementation of the algorithm discussed in Sections 4.4. The constraint evaluator sub function ensures the layouts of the metal foils are such that it forms crisscross and brick structures. The program receives the optimal θ and δ values of the previous slice optimized and the current θ and δ value of the slice being optimized. Based on these four values the overlap percentage and the crossover angle is calculated. These values are passed back to the parent function which is the optimizer, which modifies the

values of the θ and δ based on the values received from the constraint evaluator.

The pictorial representation of the algorithm is shown in Figure 5.4.

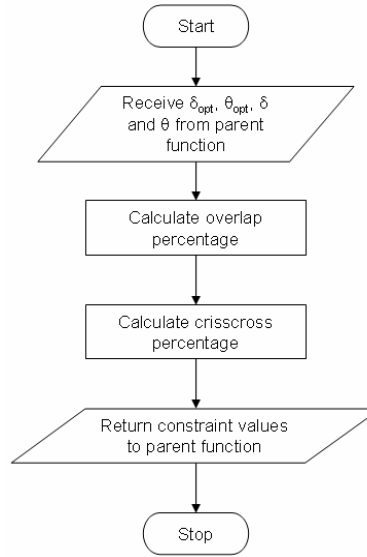


Figure 5.4 Constraint evaluator flowchart

The algorithm is tested using sample slice data as shown in Figure 5.5.

5.5 Search Space Sampler

The objective function evaluator discussed in Section 5.3 is run on a sample slice data (Figure 5.5) with δ values varied uniformly in the range of $[0 - \text{bandwidth}]$ and θ values varied in the range $[0^\circ - 180^\circ]$. Each of the search bands are divided into 50 equal parts, which yields a 50x50 grid. Waste area corresponding to these 2500 grid points are calculated and plotted as shown in Figure 5.6. The figure shows the Response Surface Model (RSM) of the slice data show in Figure 5.5.

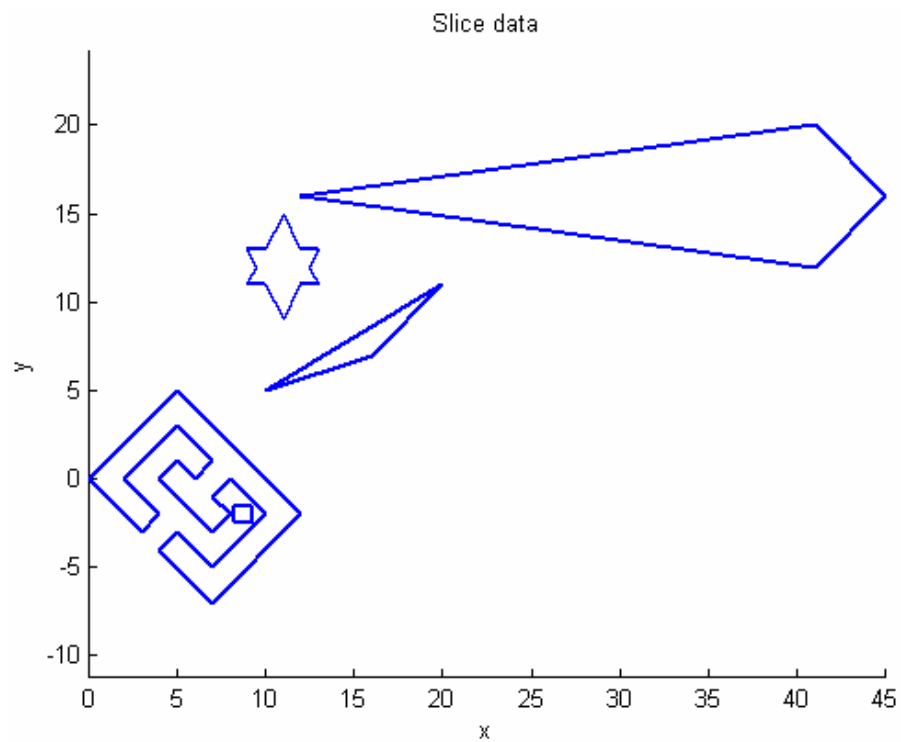


Figure 5.5 Sample slice data

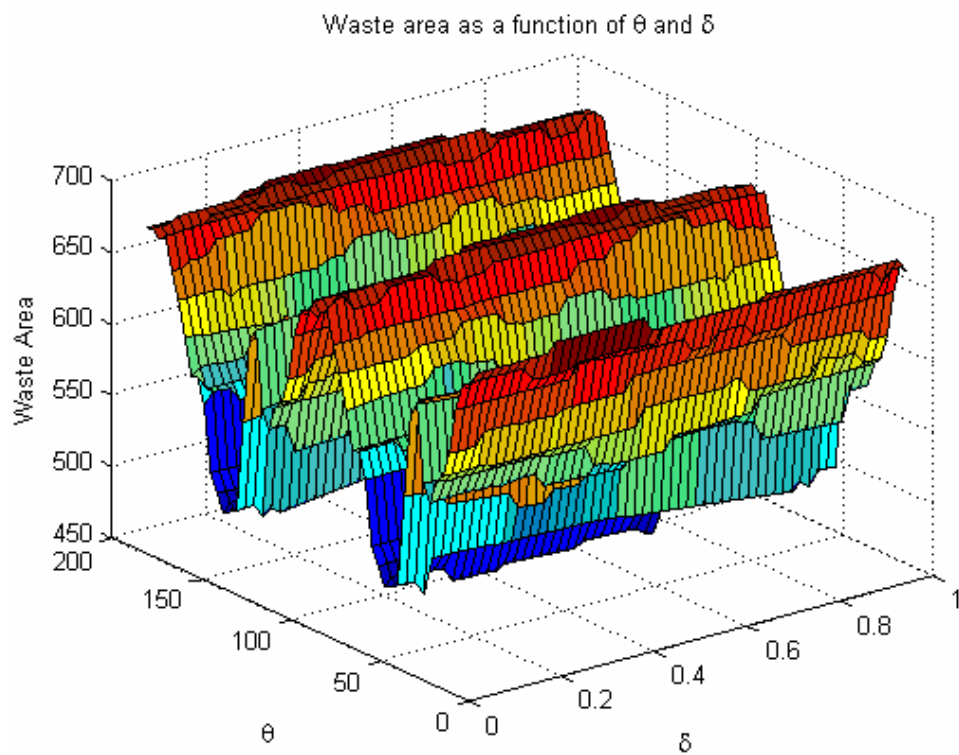


Figure 5.6 Waste area as a function of θ and δ

It is noticed from the above plot that as the δ and θ values are changed, the waste area forms a complex surface with multiple local optimal points. This might result in premature convergence during the optimization run. To circumvent this problem the search space is sampled at a number of points for the calculation of the waste area. The point corresponding to the least waste area value is used as the starting point of the optimization run. This concept of optimal sampling point selection is shown in Figure 5.7.

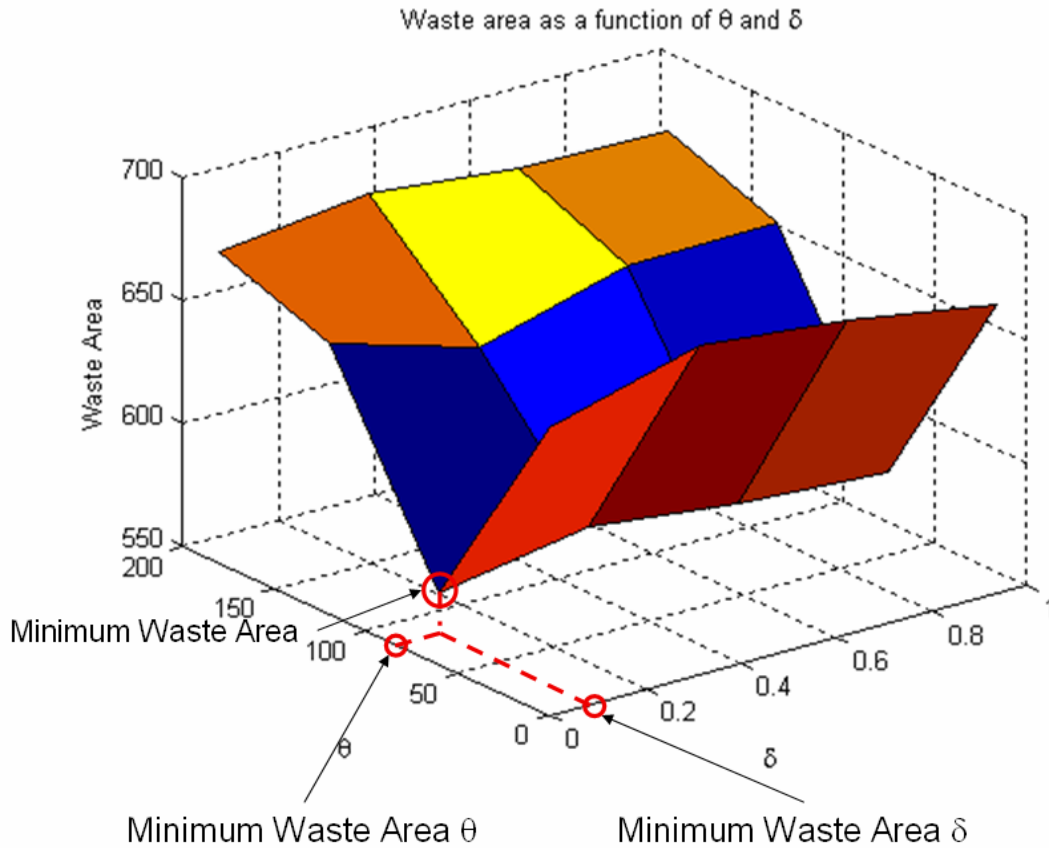
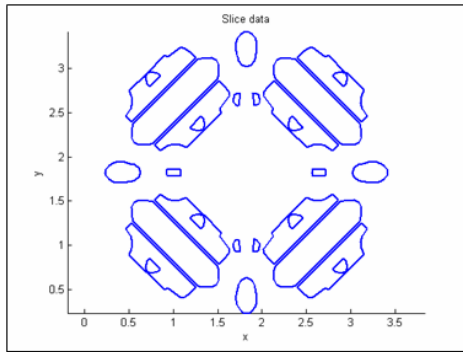


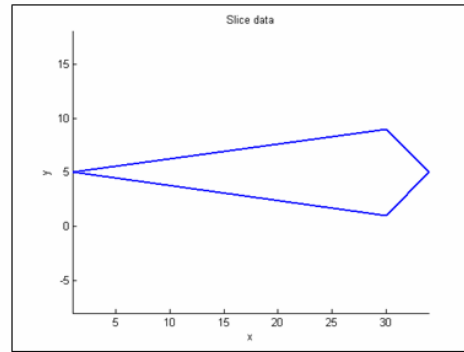
Figure 5.7 Starting point selection by sampling

However, the selection of the sampling process has to be done judiciously. This is because, depending on the symmetry conditions of the slice data, the RSM will

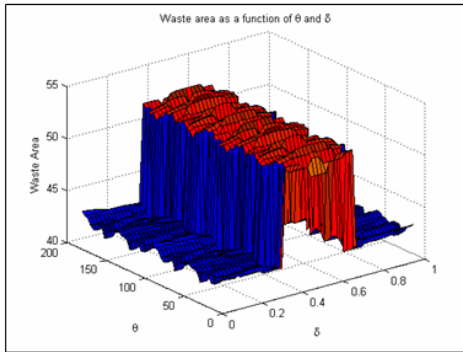
exhibit corresponding regularity. Figure 5.8(a) shows a slice data which has rotational symmetry. It is noticed from its RSM (Figure 5.8(c)) that the waste area do not change with θ values. However, large changes are noticed as we move along the δ axis. On the other hand Figure 5.8(b) shows slice data which has translational symmetry and Figure 5.8(d) shows the corresponding RSM. It is noted from this figure that the waste area is largely influenced by θ and weakly influenced by the δ value.



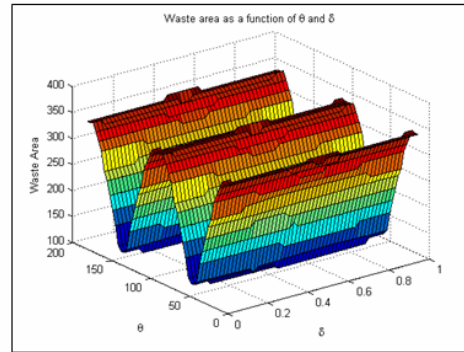
Slice Data with Rotational Symmetry
(a)



Slice Data with Translational Symmetry
(b)



RSM of slice data with rotational symmetry
(c)



RSM of slice data with translational symmetry
(d)

Figure 5.8 Need for robust sampling

The preceding discussion highlighted the effects of part symmetry on RSM. It can be deduced from the discussion that, the sampling of the search space should be

done such that the points are spread out within the search bounds so that similar points are avoided. A uniform sampling of the search space as shown in Figure 5.9(a) results in sampling of points, which might not yield additional advantage as compared to the increased computational expense of creating a higher resolution RSM. However sampling method based on random distribution like Latin Hyper Square method, as shown in Figure 5.9(b), will ensure that the search bounds are covered and at the same time ensure that additional information is gained with every extra point that is sampled.

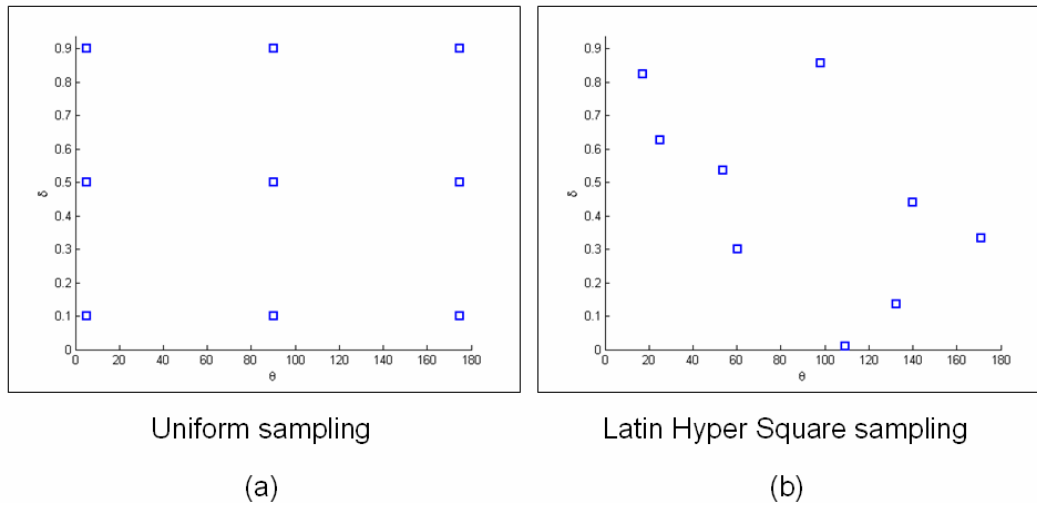


Figure 5.9 Comparison of Sampling Methods

The issues discussed have been solved by the implementing the search space sampler algorithm. The search space algorithm receives the total number of points at which the search bounds have to be sampled. Based on this number a Latin Hyper Square (LHS) up to the required depth is formed by the algorithm. However, the values will be the LHS sampling points of a unit square. To get

LHS sampling points of the search bound, the unit square points are scaled to the maximum search bound values, i.e. 180° and bandwidth. The waste area corresponding to the sample points are calculated using the objective function evaluator discussed in Section 5.3. The waste areas at the sampling points are compared and the δ and θ value which correspond to the minimum waste area is transferred back to the calling function. A pictorial representation of the algorithm is shown in Figure 5.10.

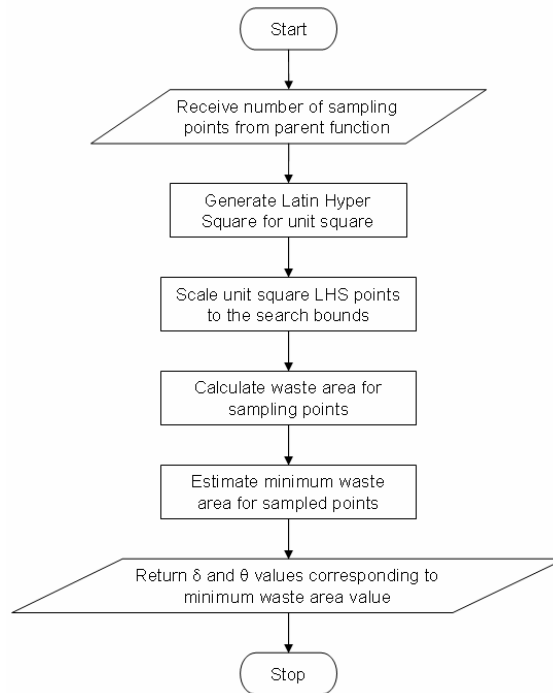


Figure 5.10 Sampling flowchart

5.6 Closure

This chapter dealt with the details of the implementation of the algorithm. Research issues that were identified in the previous sections were revisited and the algorithm adapted to address the issues that were identified during the

implementation phase. The program architecture of the program with detailed discussion of the working of the individual sub functions was also presented. The robustness and accuracy of the implemented algorithm was checked by conducting validation trials which is discussed in the next chapter.

CHAPTER 6

RESULTS

This chapter discusses the results obtained from the implementation of the algorithm. Key metrics for test cases are identified based on the major research issues discussed in the previous section. The test cases are used for the validation of the algorithm. A discussion on the trials conducted with two types of optimizers, viz. gradient based and genetic algorithm is presented. The advantages and drawbacks of each of the algorithms as applied to the current problem is discussed and conclusion drawn.

6.1 Test Case Metrics and Test Shapes

Section 3.1 identified the various research issues that need to be considered for the development of the new algorithm. It is imperative that these research issues be considered for developing metrics for selecting the test cases which is used for validating the algorithm. The metrics that have been developed for the selection of test cases is listed below.

1. Multiple loops within one slice
2. Multiple layer data
3. Non convex data

Based on these metrics a number of test shapes have been selected for validating the algorithm as shown in Figure 6.1. It can be noted from the figure that all the test cases selected have multiple loops within the same slice, have multiple layers and also include slice data which are non convex in nature.




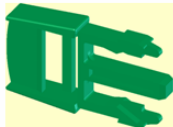
Sl No.	Part	Multiple Loops	Multiple Layers	Non Convex Data
1		✓	✓	✓
2		✓	✓	✓
3		✓	✓	✓
4		✓	✓	✓

Figure 6.1 Test shapes for validation

Since the shapes satisfy all the metrics identified for test cases, the shapes can be considered as ideal test shapes for the validation of the algorithm.

6.2 Validation of algorithm

A gradient based optimization algorithm is used for the optimization of these test shapes. The optimization results obtained from these test shapes are presented in Figure 6.2(a-d). The figure shows the different test shapes and a randomly

selected slice of each test shape. The original position of the slice as well as the optimized position of the slice is shown in the figures. The δ and θ values that need to be applied to transform the original layout to the optimized layout is displayed in bold figures. The percentage saving achieved in the waste area formed and the build time is represented by the histogram.

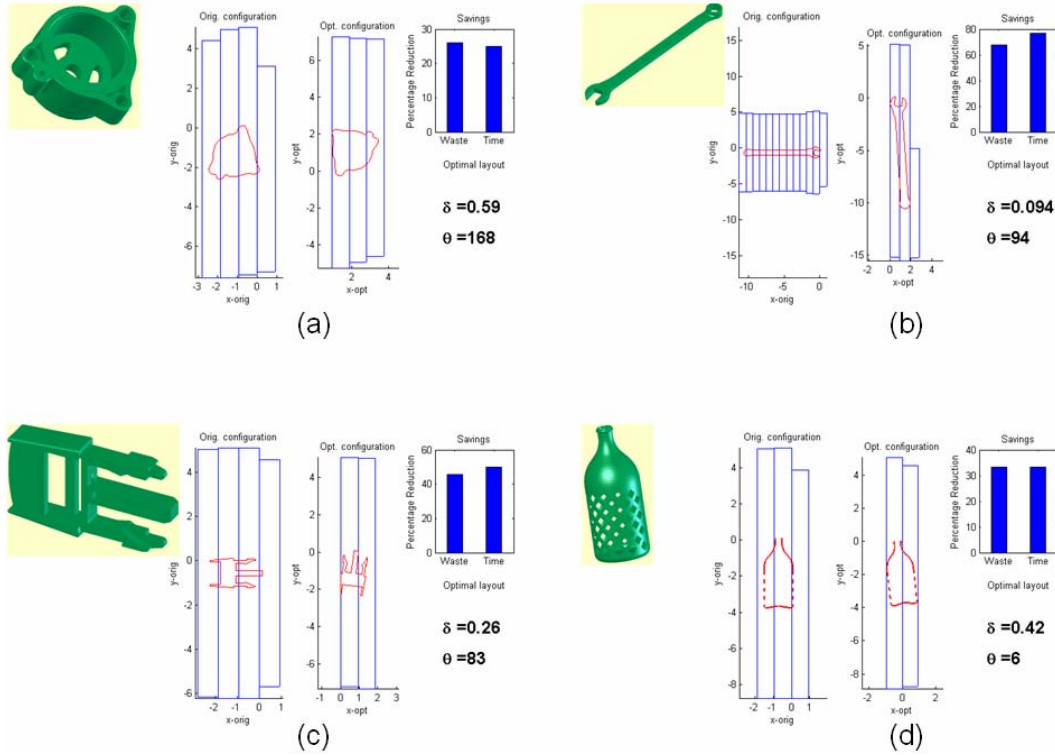


Figure 6.2 Optimization results of test cases

It is seen that the algorithm is capable of handling multiple loops (Figure 6.2(d)) and non convex data (Figure 6.2(c)). It is also noted from the figure that the algorithm reduces the process time by reducing the NoBs required for building the artifact. The reduction of NoB can be seen in optimization runs on all the test cases. This also validates the assumption that the problem can be formulated as a single objective optimization problem as discussed in section 3.1

The ability of the algorithm to handle multiple slices simultaneously is exemplified by formation of crisscross and overlap of metal foils. Figure 6.3 shows the optimal values of δ and θ returned by a gradient based optimizer with test case 4 as input. It is seen consecutive θ values differ from each other by at least 10° . Similarly the δ values are seen to vary from δ value of neighboring δ values by at least 10%. This is due to the constraint built into the optimizer. This result in the formation of crisscross and overlap structure which exemplifies the ability of the algorithm to handle multiple slice data simultaneously.

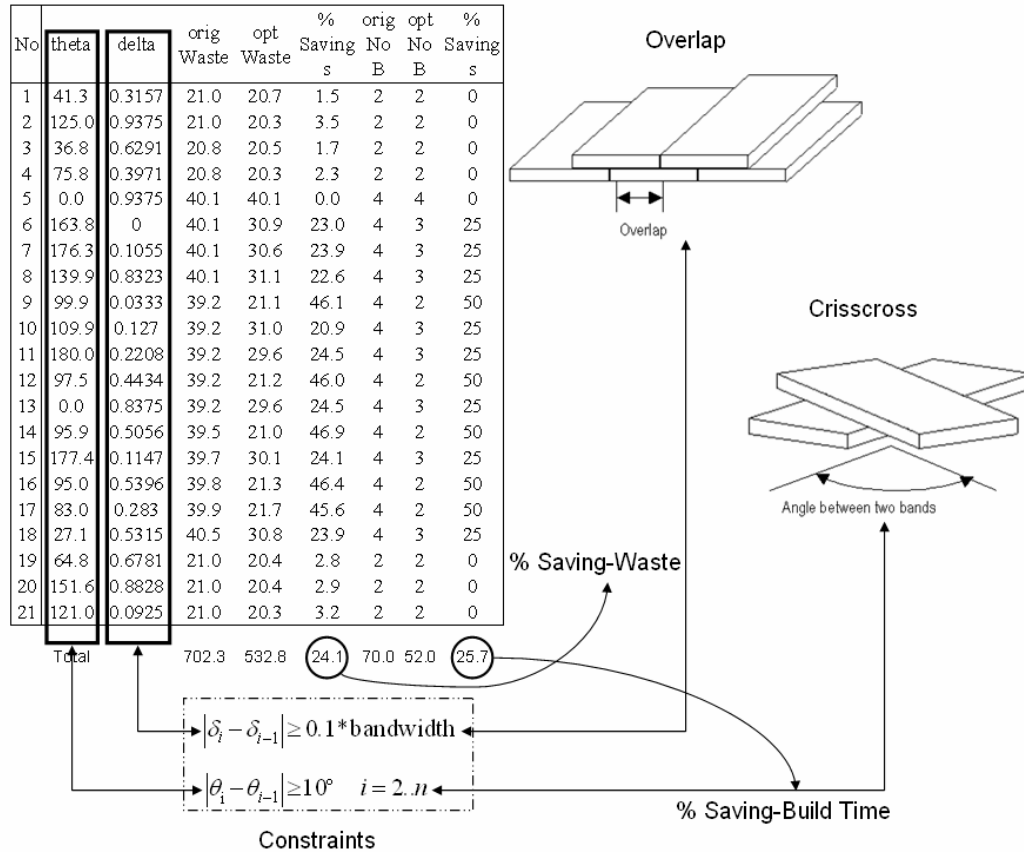


Figure 6.3 Formation of crisscross and overlap structure

A comparison study of the waste area formed and build-time before and after optimization is also seen from Figure 6.3. It is seen that a waste saving of approximately 25% and a build-time reduction (by means of NoB reduction) of 25% has been achieved.

6.3 Choice of Optimizer

One of the important aspects that affect the quality of the solutions obtained is the type of optimizer used. Depending on the complexity of the problem and the choice of the optimizer, the quality of the solution obtained varies. Section 5.5 discussed the complexity of the RSM obtained from a sample slice data. Figure 5.6 showed that the RSM of complex models can be highly non unimodal which can result in premature convergence of gradient based optimizers. This is illustrated in the following discussion.

The artifact shown in Figure 6.4 was used as the input data for the optimization using Nelder – Mead simplex algorithm and NSGA II. The artifact is chosen since it meets all the conditions that were identified as requirements for test cases in Section 6.1. The objective function of this optimization trial is to minimize the overall waste generated during the process.

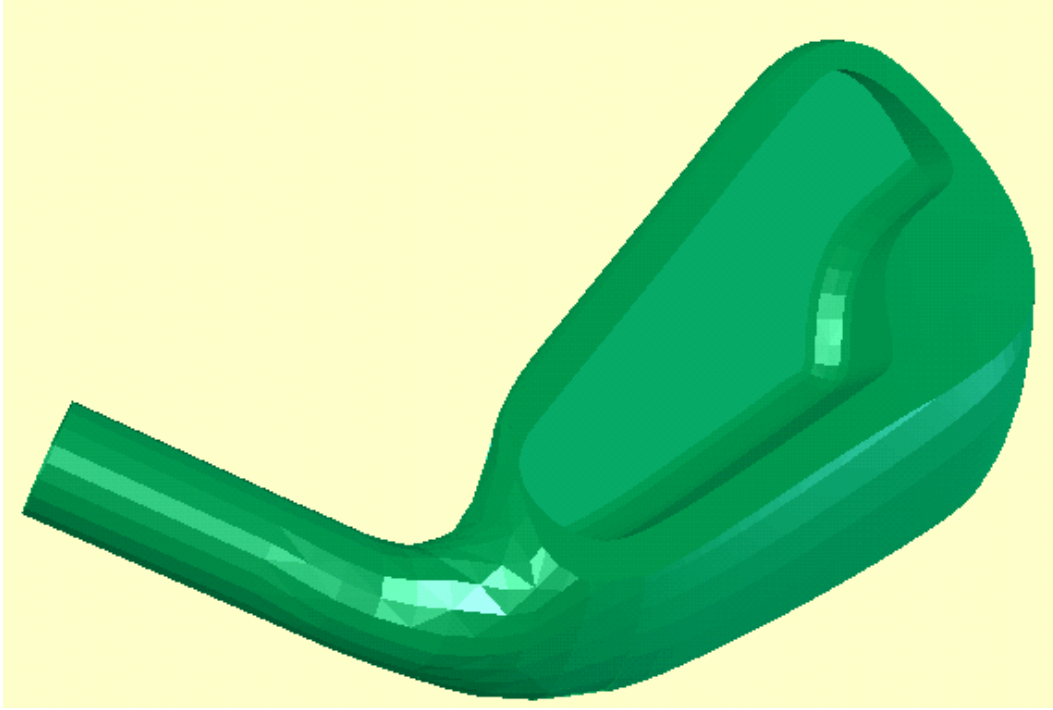


Figure 6.4 STL file of club

This optimization problem has two design variables for every layer of the artifact and constraint functions are evaluated for all slices simultaneously. The mathematical formulation is shown in Equation 6.1

$$\begin{aligned}
& \min \quad \text{waste area} = \sum_{i=1..n} f(\delta_i, \theta_i) \\
& \quad \delta_i, \theta_i \quad i=1, \dots, n \\
& \text{subject to} \quad |\delta_i - \delta_{i-1}| \geq 0.1 * \text{bandwidth} \\
& \quad |\theta_i - \theta_{i-1}| \geq 10^\circ \quad i=2, \dots, n \\
& \quad 0^\circ \leq \theta_i \leq 180^\circ \\
& \quad 0 \leq \delta_i \leq \text{bandwidth} \\
& \text{where bandwidth} = 0.9375 \\
& \quad n = \text{number of layers}
\end{aligned}$$

Equation 6.1 Mathematical formulation of all in one optimization

The results obtained from the optimization run using simplex algorithm is shown in Figure 6.5. It is seen from the graph that the optimizer was able to reduce the waste area by 26.7% from an initial value of 204.61 sq.inches to 149.966 sq.inches

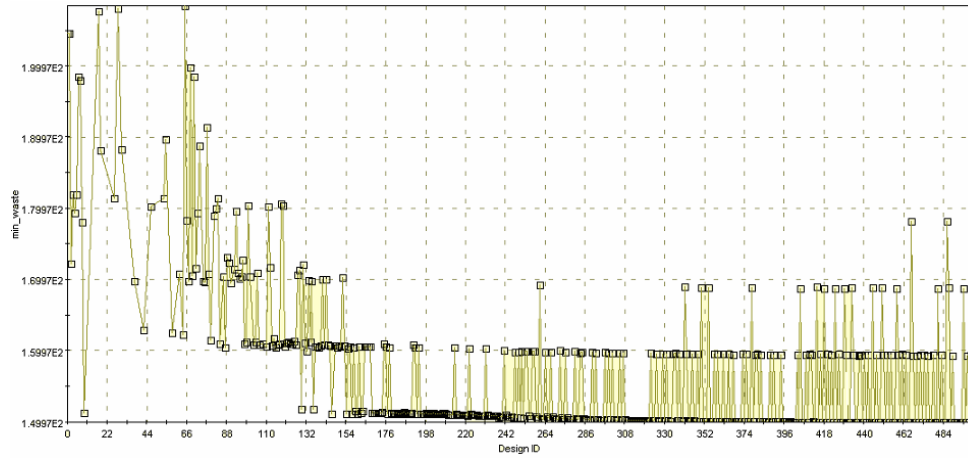


Figure 6.5 Waste area history using Simplex algorithm

A second optimization was conducted using the same input data with NSGA II as the optimizer. It was noticed that the objective function value reduced to 131.49in^2 from the starting value of 204.61in^2 . This corresponds to a saving of 35.7%. In comparison with the output obtained from the simplex algorithm, the output from the GA algorithm is an improvement of 9%. Figure 6.6 shows the optimization history.

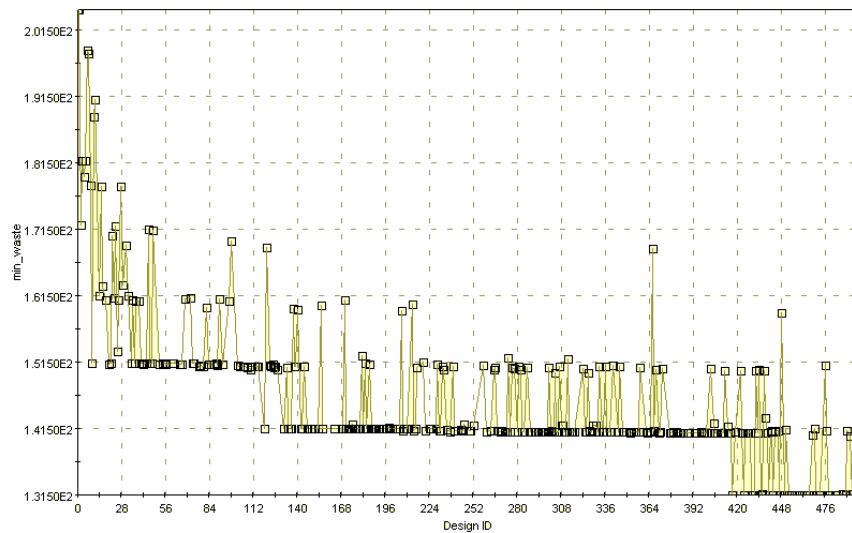


Figure 6.6 Waste area history using NSGA II algorithm

It is significant to note that the improvement of 9% is achieved with the same number of function evaluations. For the Simplex trial the maximum number of function evaluations was limited to 500 and for the GA trial, a population of 10 was allowed to evolve for 50 generations.

It was also seen that, from a different experiment, the objective function value reduced to 121.6915in^2 , a reduction of 40.52%, when the number of generations were increased to 1000. The convergence history is shown in Figure 6.7.

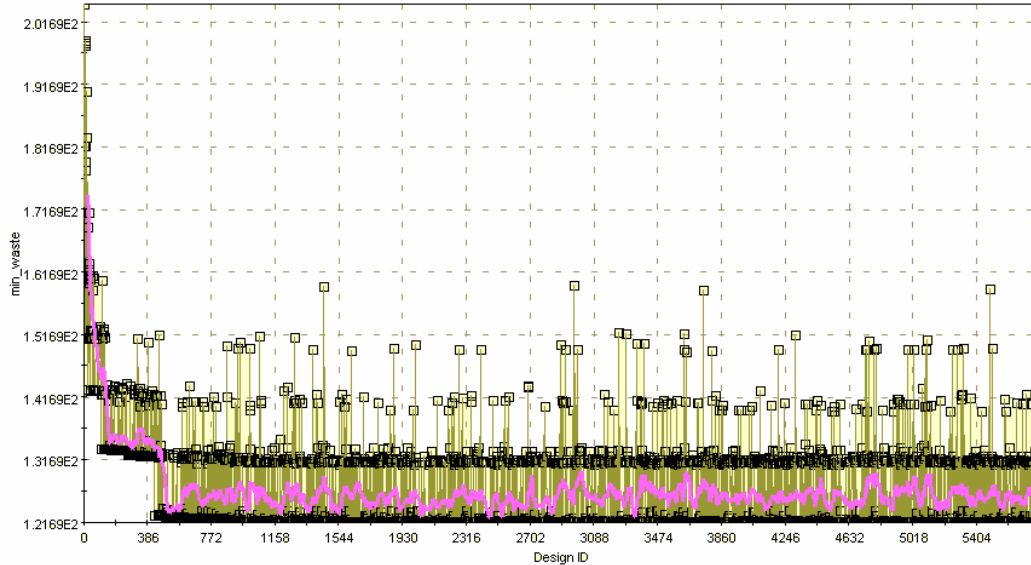


Figure 6.7 Waste area history using NSGA II algorithm-1000 generations

In conclusion it can be seen that the choice of the algorithm needs to be done based on the availability of computational resources. Satisfactory results were obtained by use of deterministic algorithms. Trials have proved that evolutionary algorithms can yield better results. However, the computational cost is higher as compared to deterministic algorithms. It is suggested to use evolutionary

algorithms for artifacts which are highly non convex and have no axis of symmetry.

6.4 Benchmarking

A comparison study of the earlier algorithm and the new algorithm was done. One of the test shapes identified in Section 6.1 was used for this trial. The same test shape was used as input for both algorithms and the results are shown in Figure 6.8.

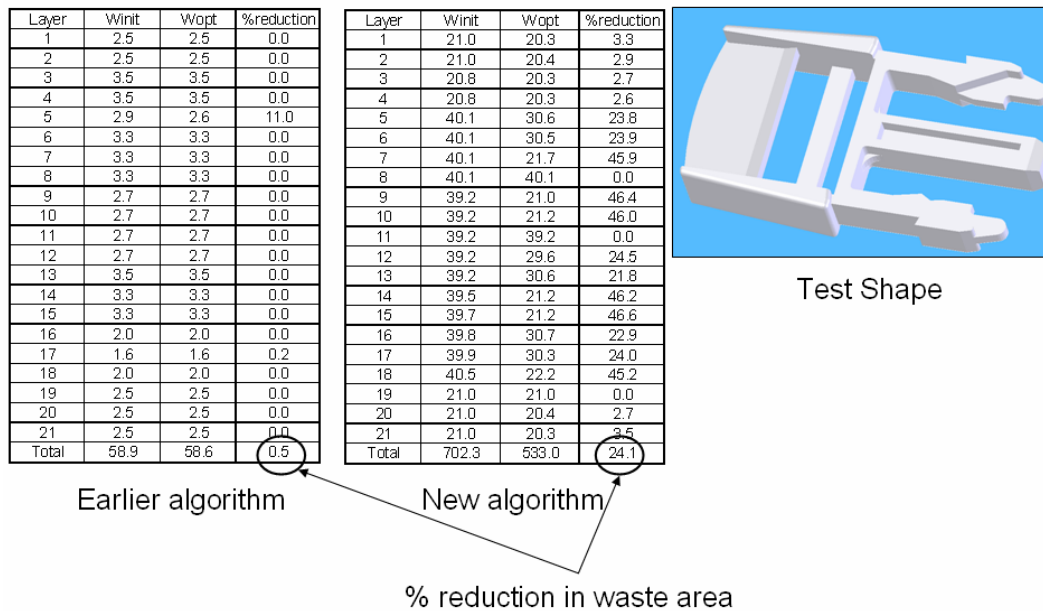


Figure 6.8 Comparison of existing and new algorithm

As is seen from the table, the earlier implementation of the algorithm considers the clamping allowance as fixed area. The percentage saving achieved in the earlier implementation of the algorithm is 0.5%. The new algorithm was able to

reduce the waste area by 24.1%. This saving is achieved with constraints on design variables to increase the part strength. It is also observed from the test results that a saving of approximately 25% of metal bands and an equal percentage of build time reduction by way of NoB reduction can be achieved by the optimization algorithm.

6.5 Closure

The chapter identified key metrics for selecting test cases and the same were applied to validate the algorithm. The chapter also presented a detailed discussion of the performance of the algorithm based on the waste and build time reduction achieved. The results revealed the capability of the algorithm to reduce the waste area formed as well as the build time using a single objective minimization approach. The various aspects which affect the optimality of the solutions were also discussed. Trials were also conducted to ascertain the type of optimizer to be used for different input conditions.

CHAPTER 7

CONCLUSIONS AND FUTURE WORK

The previous chapter discussed the results obtained from the newly implemented algorithm. It also discussed the validation of the algorithm. This chapter will conclude the work by highlighting the salient points of the research work and identifies possible future works in the field.

7.1 Conclusion

The objective of this research work was to develop an algorithm that would optimally place metal foils in an Ultrasonic Consolidation process to minimize the waste formed and build time at the same time increase the part strength. The algorithm was developed to enable processing of real world complex data including non convex part geometries.

The problem was solved by modularizing the problem into two subsections. The first section was solved using the existing CIDES software which is used to generate the vertex points of the part once the user selects the z-direction. The vertex points generated by the CIDES software are used as the input to the optimization sub problem. Based on the user selected options, the optimization is completed to minimize the waste area formed. Secondary objective functions of reducing build time and increasing the part strength has also been achieved.

Majority of the future works identified in previous literature^[22, 25, 78] related to this work were considered and implemented in the new algorithm. This includes the ability of the algorithm to build crisscross and overlapping structures to improve the part strength and to reduce the anisotropic nature of the finished artifact. The clamping allowance has also been taken into consideration for optimization in the new algorithm.

7.2 Future Work

The choice of z-axis for the slicing is important for efficient building of the artifact. As has been discussed in Section 2.1, the accuracy, build time and the support volume required is determined by the choice of z-axis. In the current research work, the choice of z-axis direction was left to the user. However, the automation of this process promises increased savings in terms of waste area formed and the build time required.

The problem can be formulated as a bi-level optimization problem with inclination of the artifact with the primary axes- α , β and γ as the design variables for the first level of optimization (Figure 7.1).

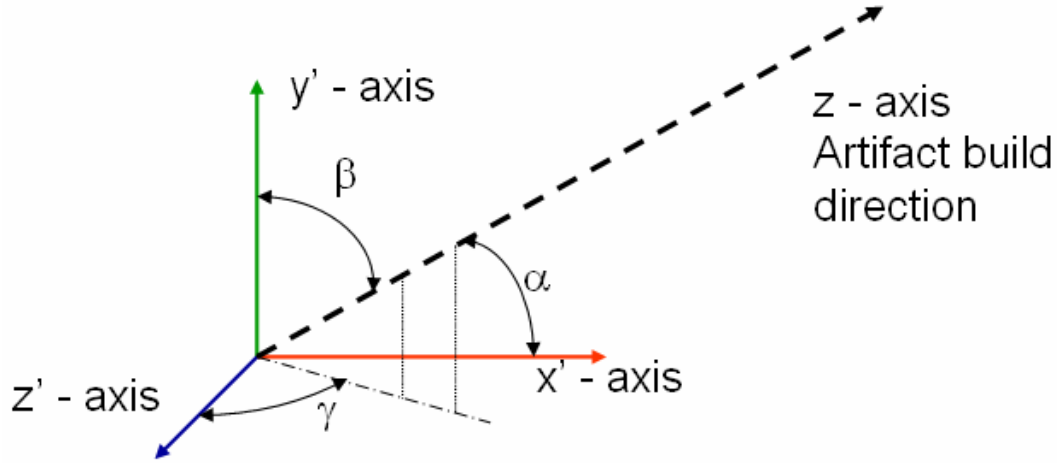


Figure 7.1 Choice of z-axis

The optimized value of α , β and γ can be used for the slicing of the artifact and the output of the slicing algorithm can be used as input for the second level of optimization. Based on the waste volume formed the α , β and γ values can be perturbed by the primary optimizer to generate a new slicing direction. The process is continued till a global optimal of waste area is achieved. The problem can also be formulated as a multi-objective problem at the primary level. The objectives of minimizing support volume, maximizing part accuracy and decreasing support volume can be used. The design variables which correspond to the trade of value of the all the objectives is used for the slicing and the algorithm proceeds as explained earlier.

However, it is imperative that the slicing algorithm and the optimization algorithm are developed in the same platform for easy data handling and improved performance of the algorithm.

Another possible area of future work is the development of mathematical model for analyzing the strength of the bonds formed. In the current work, the increase of strength has been achieved by forming crisscross and brick structures. The development of a mathematical model will ensure the adequate part strength is achieved by the overlap and the crisscross structures.

Future work could improve on the functionality of the algorithm by generating G-code required for the machining. This would avoid the need of multiple software for the formation process.

Another possible research avenue is the adaptive optimization of the slice layers. It can be noted from the test shape identified in the earlier section that the cross section of the artifact does not change for every layer. However, the current implementation tries to optimize each layer irrespective of the geometry of the previous layer. The new algorithm could do adaptive optimization based on changes of the part geometry as the algorithm steps through each slice data. If the slice data is found similar to the previous slice data, the algorithm could skip the optimization of the current layer by applying the optimal θ and δ values calculated for the previous layer. However, care has to be taken that vertical stacking is avoided by limiting the number of layers for which optimization is skipped.

REFERENCES

1. Pahl, G and W Beitz, *Engineering Design: A Systematic Approach*. 2nd ed. 1995: Springer.
2. Bashir, Hamdi A and Vince Thomson, *Estimating Effort and Time for Design Projects*, in *Canadian Society of Value Analysis Conference*. 2001.
3. Simon, Herbert A, *The Sciences of the Artificial*. 3 ed. 1996, Massachusetts: The MIT Press.
4. Pham, DT and SS Dimov, *Rapid Manufacturing: The technologies and applications of rapid prototyping and rapid tooling*. 2001: Springer.
5. Hopkinson, N, RJM Hague, and PM Dickens, *Rapid Manufacturing An Industrial Revolution for the Digital Age*. 2006: John Wiley & Sons.
6. McMath, Ian, *Getting real [Rapid Manufacturing]*, in *Engineering & Technology*. 2006. p. 40-43.
7. Hilton, PD and PF Jacobs, *Rapid Tooling: Technologies and Industrial Applications*. 2000.
8. Jacobs, Paul F, *Stereolithography & Other RP&M Technologies: From Rapid Prototyping to Rapid Tooling*. 1995, Michigan: Society of Manufacturing Engineers.
9. Grenda, Ed. *Rapid Manufacturing Directory*. 2006 [cited 2007 February 19]; Available from: http://home.att.net/~castleisland/odd1_lks.htm.
10. Yan, Xue and P. Gu, *A review of rapid prototyping technologies and systems*. *Computer-Aided Design*, 1996. **28**(4): p. 307-318.
11. Grenda, Ed. *Fused Deposition Modeling*. 2006 [cited 2007 February 20]; Available from: <http://home.att.net/~castleisland/fdm.htm>.
12. Walters, William A. *Rapid Prototyping Using FDM: A Fast, Precise, Safe Technology*. in *Solid Freeform Fabrication Proceedings*. 1992. Austin, TX.
13. Systems, MCAE. *3D Printers*. 2007 [cited 2007 February 20]; Available from: <http://www.mcae.cz/katalog.php?lang=cs&id=106&>.

14. Arptech. *How SLS (Selective Laser Sintering) process works*. 2007 [cited 2007 February 20]; Available from: <http://www.arptech.com.au/sls-help.htm>.
15. Beaman, JJ, John W Barlow, DL Bourell, RH Crawford, HL Marcus, and KP McAlea, *Solid Freeform Fabrication: A New Direction in Manufacturing*. 1 ed. 1997, Massachusetts: Kluwer Academic Publishers.
16. Sandia-Corporation. *Laser Engineered Net Shaping™*. 2005 [cited 2007 March 01]; Available from: <http://www.sandia.gov/mst/technologies/net-shaping.html>.
17. Grenda, Ed. *Laser Engineered Net Shaping TM*. 2006 9/1/06 [cited 2007 March 01]; 3c:[Available from: <http://home.att.net/~castleisland/lens.htm>.
18. Wohlers, Terry. *New Developments and Trends in Rapid and High-Performance Tooling*. 2002 [cited 2007 March 02]; Available from: <http://www.wohlersassociates.com/EuroMold-2002-paper.html>.
19. Lindhe, Ulf and Ola Harrysson, *Rapid Manufacturing with Electron Beam Melting (EBM) – A manufacturing revolution?* 2003: Michigan.
20. Wikipedia. *Electron Beam Melting*. 2007 February 27 07 [cited 2007 March 02]; Available from: http://en.wikipedia.org/wiki/Electron_Beam_Melting.
21. Synergeering-Group. *EBM - Electron Beam Melting*. [cited 2007 March 02]; Available from: <http://www.synergeering.com/ebm.php>.
22. Schwager, M Manuel, Julien Galli, and Georges M Fadel, *Optimal slicing for ultrasonic consolidation*, in *TMCE*. 2006, Rotterdam: Slovenia.
23. Kong, C. Y., R. C. Soar, and P. M. Dickens, *Optimum process parameters for ultrasonic consolidation of 3003 aluminium*. *Journal of Materials Processing Technology*, 2004. **146**(2): p. 181-187.
24. Robinson, CJ, Chunbo Zhang, Janaki GD Ram, Erik J Siggard, Brent Stucker, and Leijun Li. *Maximum height to width ratio of freestanding structures build using ultrasonic consolidation*. in *Solid Freeform Fabrication Symposium*. 2006. Austin, TX.
25. Schwager, Manuel M, *Optimal Slicing for Ultrasonic Consolidation - Thesis*, in *Mechanical Engineering*. 2005, Swiss Federal Institute of Technology Zurich. p. 87.

26. Campbell, RI, RJM Hague, B Sener, and PW Wormald, *The potential for the bespoke industrial engineer*. The Design Journal, 2003. **6**(3): p. 24-34.
27. Das, Suman, Scott J. Hollister, Colleen Flanagan, Adebisi Adewunmi, Karlin Bark, Cindy Chen, Krishnan Ramaswamy, Daniel Rose and, and Erwin Widjaja, *Freeform fabrication of Nylon-6 tissue engineering scaffolds*. Rapid Prototyping Journal, 2003. **9**(1): p. 43-49.
28. Ngim, D. B., J. S. Liu, and R. C. Soar, *Design optimization for manufacturability of axisymmetric continuum structures using metamorphic development*. International Journal of Solids and Structures, 2007. **44**(2): p. 685-704.
29. Biren, Prasad, *Concurrent engineering fundamentals*. 1996: Prentice Hall
30. Salomone, Thomas A, *What Every Engineer Should Know about Concurrent Engineering* 1995: CRC.
31. Dutta, D, BP Fritz, D Rosen, and W Lee, *Layered Manufacturing: Current Status and Future Trends*. Journal of Computing and Information Science in Engineering, 2001. **1**(1): p. 60-71.
32. Pohl, Haiko, Frank Petzoldt, and Peter Gosger, *New features in three dimensional printing of metal powders*. Powder Metallurgy, 2001: p. 309-312.
33. Song, Yuhua, Yongnian Yan, Renji Zhang, Da Xu, and Feng Wang, *Manufacture of the die of an automobile deck part based on rapid prototyping and rapid tooling technology*. Journal of Materials Processing Technology, 2002. **120**: p. 237-238.
34. Chandra, A, J Watson, JE Rowson, J Holland, RA Harris, and DJ Williams, *Application of rapid manufacturing techniques in support of maxillofacial treatment: evidence of the requirements of clinical applications*. Proceedings of the I MECH E Part B Journal of Engineering Manufacture,, 2005. **B6**: p. 469-476.
35. Berce, P, H Chezan, and N Balc, *The application of Rapid Prototyping Technologies for manufacturing the custom implants*, in *ESAFORM Conference*. 2005: Cluj-Napoca, Romania.
36. Kulkarni, Prashant , Anne Marsan, and Debasish Dutta, *A review of process planning techniques in layered manufacturing*. Rapid Prototyping Journal, 2000. **6**(1): p. 18-35.

37. West, A. P., S. P. Sambu, and D. W. Rosen, *A process planning method for improving build performance in stereolithography*. Computer-Aided Design, 2001. **33**(1): p. 65-79.
38. Agarwala, Mukesh K, Vikram R Jamalabad, Noshir A Langrana, Ahmad Safari, Philip J Whalen, and Stephen C Danforth, *Structural quality of parts processed by fused deposition*. Rapid Prototyping Journal, 1996. **2**(4): p. 4-19.
39. Castillo, Laura, *Study about the rapid manufacturing of complex parts of stainless steel and titanium*. 2005.
40. Arni, Ramakrishna and SK Gupta *Manufacturability Analysis of Flatness Tolerances in Solid Freeform Fabrication*. Journal of Mechanical Design, 2001. **123**(1): p. 148-156.
41. Iwanaga, S, F Kurihara, M Ohkawa, and K Igarashi, *Influence of material characterization on dimensional stability*, in *Third International Conference on Rapid Prototyping*. 1992.
42. Comb, JW, WR Priedeman, and PW Turley. *Layered manufacturing control parameters and material selection criteria*. in *Manufacturing Science and Engineering*. 1994. Chicago, IL.
43. Crump, SS. *The extrusion process of fused deposition modeling*. in *Third International Conference on Rapid Prototyping*. 1992.
44. Bourell, DL, RH Crawford, HL Marcus, JJ Beaman, and JW Barlow. *Selective laser sintering of metals*. in *Manufacturing Science and Engineering*. 1994. Chicago, IL.
45. Jacobs, Paul F, *Rapid Prototyping & Manufacturing, Fundamentals of Stereolithography*. 1 ed. 1993, New York: McGraw-Hill.
46. Thomson, David and Richard H Crawford. *Optimizing Part Quality with Orientation*. in *SFF Symposium Proceedings*. 1995. Austin, TX.
47. Masood, S. H. and W. Rattanawong, *A Generic Part Orientation System Based on Volumetric Error in Rapid Prototyping*. The International Journal of Advanced Manufacturing Technology, 2002. **V19**(3): p. 209-216.
48. Tata, Kamesh and Georges M Fadel. *Feature Extraction from Tessellated and Sliced Data in Layered Manufacturing*. in *Solid Freeform Fabrication Symposium*. 1996. Texas, Austin.

49. Majhi, Jayanth, Ravi Janardan, Michiel Smid, and Prosenjit Gupta, *On some geometric optimization problems in layered manufacturing*. Computational Geometry, 1999. **12**: p. 219-239.
50. Akula, Sreenathbabu and K. P. Karunakaran, *Hybrid adaptive layer manufacturing: An Intelligent art of direct metal rapid tooling process*. Robotics and Computer-Integrated Manufacturing, 2006. **22**(2): p. 113-123.
51. Ma, Weiyin and Peiren He, *An adaptive slicing and selective hatching strategy for layered manufacturing*. Journal of Materials Processing Technology, 1999. **89-90**: p. 191-197.
52. Pandey, P. M., N. Venkata Reddy, and S. G. Dhande, *Part deposition orientation studies in layered manufacturing*. Journal of Materials Processing Technology, 2007. **185**(1-3): p. 125-131.
53. Thrimurthulu, K., Pulak M. Pandey, and N. Venkata Reddy, *Optimum part deposition orientation in fused deposition modeling*. International Journal of Machine Tools and Manufacture, 2004. **44**(6): p. 585-594.
54. Singh, Prabhjot and Debasish Dutta, *Multi-Direction Slicing for Layered Manufacturing*. Journal of Computing and Information Science in Engineering 2001. **1**(2): p. 129-142.
55. Tsai, Stephen W and Edward M Wu, *A General Theory of Strength for Anisotropic Materials*. Journal of Composite Materials, 1971. **5**(58): p. 58-80.
56. Lee, C. S., S. G. Kim, H. J. Kim, and S. H. Ahn, *Measurement of anisotropic compressive strength of rapid prototyping parts*. Journal of Materials Processing Technology. **In Press, Corrected Proof**.
57. Kirschman, Chuck, *Automated Support Structure Design For Stereolithographic Parts - Thesis*, in *Mechanical Engineering*. 1991, Clemson: Clemson.
58. Ganesan, M and GM Fadel. *Hollowing rapid prototyping parts using offsetting techniques*. in *Proceedings of the 5th International Conference on Rapid Prototyping*. 1994. Dayton.
59. Rock, Stephen J and Michael J Wozny. *Utilizing Topological Information to Increase Scan Vector Generation Efficiency*. in *Solid Freeform Fabrication Symposium Proceedings*. 1991. Texas, Austin.

60. Bugada, Gabriel, Miguel Cervera, Guillermo Lombera, and Eugenio Onate, *Numerical analysis of stereolithography processes using the finite element method*. Rapid Prototyping Journal 1995. **1**(2): p. 13-23.
61. Cheah, C. M., J. Y. H. Fuh, A. Y. C. Nee, L. Lu, Y. S. Choo, and T. Miyazawa, *Characteristics of photopolymeric material used in rapid prototypes Part II. Mechanical properties at post-cured state*. Journal of Materials Processing Technology, 1997. **67**(1-3): p. 46-49.
62. Yardimci, M Atif and Selçuk Güçeri, *Conceptual framework for the thermal process modelling of fused deposition*. Rapid Prototyping Journal, 1996. **2**(2): p. 26-31.
63. Sensormag. *Solidica Awarded \$1.6M to Advance Smart Armor Technology*. 2007 [cited 2007 February 26]; Available from: <http://www.sensormag.com/sensors/article/articleDetail.jsp?id=400406&ref=25>.
64. Kong, C. Y. and R. C. Soar, *Fabrication of metal-matrix composites and adaptive composites using ultrasonic consolidation process*. Materials Science and Engineering: A, 2005. **412**(1-2): p. 12-18.
65. Johnson, Ken. *Ultrasonic Consolidation of Titanium Alloys for High Performance Military Aircraft Damage Repair*. 2005 12/16/2005 [cited 2007 February 26]; Available from: http://ctmaideas.ncms.org/ideas/project_detail.asp?Project_ID=36.
66. George, J and B Stucker, *Fabrication of lightweight structural panels through ultrasonic consolidation*. Virtual and Physical Prototyping, 2006. **1**(4): p. 227-241.
67. Solidica. *Smart Devices*. 2006 [cited 2007 February 26]; Available from: http://www.solidica.com/smart_devices1.htm.
68. Solidica. *Advanced Materials*. 2006 [cited 2007 February 26]; Available from: http://www.solidica.com/advanced_materials1.htm.
69. Kong, C. Y., R. C. Soar, and P. M. Dickens, *Ultrasonic consolidation for embedding SMA fibres within aluminium matrices*. Composite Structures, 2004. **66**(1-4): p. 421-427.
70. Kong, C. Y., R. C. Soar, and P. M. Dickens, *Characterisation of aluminium alloy 6061 for the ultrasonic consolidation process*. Materials Science and Engineering A, 2003. **363**(1-2): p. 99-106.

71. Gunduz, Ibrahim E., Teiichi Ando, Emily Shattuck, Peter Y. Wong, and Charalabos C. Doumanidis, *Enhanced diffusion and phase transformations during ultrasonic welding of zinc and aluminum*. Scripta Materialia, 2005. **52**(9): p. 939-943.
72. Matsuoka, Shin-ichi, *Ultrasonic welding of ceramics/metals using inserts*. Journal of Materials Processing Technology, 1998. **75**(1-3): p. 259-265.
73. Frank, Dietmar and Georges Fadel, *Expert system-based selection of the preferred direction of build for rapid prototyping processes*. Journal of Intelligent Manufacturing, 1995. **6**(5): p. 339-345.
74. Gao, Yuan and Charalabos Doumanidis, *Mechanical Analysis of Ultrasonic Bonding for Rapid Prototyping*. Journal of Manufacturing Science and Engineering, 2002. **124**: p. 426-434.
75. Kong, CY, RC Soar, and PM Dickens, *A model for weld strength in ultrasonically consolidated components*. Journal of Mechanical Engineering and Science, 2004. **219**(C): p. 83-91.
76. Gao, Yuan and Charalabos Doumanidis, *Mechanical Modeling of Ultrasonic Welding*. Journal of Welding Research, 2004. **83**(44): p. 140S-146S.
77. Tata, Kamesh, *Efficient Slicing and Realization of Tessellated Objects for Layered Manufacturing*, in *Mechanical Engineering*. 1995, Clemson University: Clemson.
78. Galli, Julien, *Optimal Slicing for Ultrasonic Consolidation - Thesis*, in *Mechanical Engineering*. 2005, Ecole Nationale Supérieure d'Arts et Métiers: Paris. p. 92.
79. Onwubiko, Chinyere, *Introduction to Engineering Design Optimization*. 1st ed. 1999: Prentice Hall.
80. Mortenson, Micheal E, *Geometric Modelling*. 1985, New York: John Wiley and Sons.
81. Dewey, Bruce R, *Computer graphics for engineers*. 1988, New York: Harper & Row,.
82. Egerton, PA and WS Hall, *Computer graphics : mathematical first steps*. 1998 London ; New York: Prentice Hall.
83. Spoelder, Hans JW and FOns H Ullings, *Graphics Gems*, ed. A.S. Glassner. 1990 Boston Academic Press.

84. Boissonnat, JD and M Yvinec, *Algorithmic Geometry*. 1995, Cambridge: Cambridge University Press. 519.
85. Rexavier, Raji and GM Fadel, *Optimal Placement of Foils in UC Process for Waste Minimization and Part Strength Maximization*, in *Rapid Manufacturing Conference*. 2007: Loughborough University.